

APPLIED
COMPUTATIONAL
ELECTROMAGNETICS
SOCIETY
JOURNAL
AND
NEWSLETTER

March 1999
Vol. 14 No. 1

ISSN 1054-4887 - JOURNAL
ISSN 1056-9170 - NEWSLETTER

AQU99-06-1137

GENERAL PURPOSE AND SCOPE. The Applied Computational Electromagnetics Society Journal hereinafter known as the **ACES Journal** is devoted to the exchange of information in computational electromagnetics, to the advancement of the state-of-the-art, and to the promotion of related technical activities. A primary objective of the information exchange is the elimination of the need to "re-invent the wheel" to solve a previously-solved computational problem in electrical engineering, physics, or related fields of study. The technical activities promoted by this publication include code validation, performance analysis, and input/output standardization; code or technique optimization and error minimization; innovations in solution technique or in data input/output; identification of new applications for electromagnetics modeling codes and techniques; integration of computational electromagnetics techniques with new computer architectures; and correlation of computational parameters with physical mechanisms.

SUBMISSIONS. The **ACES Journal** welcomes original, previously unpublished papers, relating to **applied computational electromagnetics**.

Typical papers will represent the computational electromagnetics aspects of research in electrical engineering, physics, or related disciplines. However, papers which represent research in **applied computational electromagnetics** itself are equally acceptable.

Contributions may be sent to the Editors-in-Chief, Dr. Ahmed Kishk or Dr. Allen Glisson

Department of EE

University of Mississippi

University, MS, 38677 USA

Phone: 601-232-5385 (Ahmed)

Phone: 601-232-5353 (Allen)

Fax: 601-232-7231

email:ahmed@olemiss.edu

email:aglisson@mail.olemiss.edu. See "Information for Authors" on inside of back cover.

SUBSCRIPTIONS. All members of the Applied Computational Electromagnetics Society (**ACES**) who have paid their subscription fees are entitled to receive the **ACES Journal** with a minimum of three issues per calendar year.

Visit us on line at: www.emclab.umn.edu/aces, and <http://aces.ee.olemiss.edu>

Back issues, when available, are \$15.00 each. Subscriptions to **ACES**, orders for back issues of the **ACES Journal** and changes of addresses should be sent to:

Dr. Richard W. Adler

ACES Executive Officer

ECE Department, Code ECAB

Naval Postgraduate School

833 Dyer Road, Room 437

Monterey, CA 93943-5121 USA

Allow four week's advance notice for change of address. Claims for missing issues will not be honored because of insufficient notice or address change or loss in mail unless the secretary is notified within 60 days for USA and Canadian subscribers or 90 days for subscribers in other countries, from the last day of the month of publication. For information regarding reprints of individual papers or other materials, see "Information for Authors".

LIABILITY. Neither ACES or the **ACES Journal** editors are responsible for any consequence of misinformation or claims, express or implied, in any published material in an **ACES Journal** issue. This also applies to advertising, for which only camera-ready copies are accepted. Authors are responsible for information contained in their papers. If any material submitted for publication includes material which has already been published elsewhere, it is the author's responsibility to obtain written permission to reproduce such material.

APPLIED
COMPUTATIONAL
ELECTROMAGNETICS
SOCIETY
Journal

March 1999
Vol. 14 No. 1

ISSN 1054-4887

19990311 007

The ACES Journal is abstracted in INSPEC, in Engineering Index, and in DTIC.

The second, third, fourth, and fifth illustrations on the front cover have been obtained from Lawrence Livermore National laboratory.

The first illustration on the front cover has been obtained from FLUX2D software, CEDRAT S.S. France, MAGSOFT Corporation, New York.

DISTRIBUTION STATEMENT A
Approved for Public Release
Distribution Unlimited

DTIC QUALITY INSPECTED 2

AQ499-06-1137

THE APPLIED COMPUTATIONAL ELECTROMAGNETICS SOCIETY

JOURNAL EDITORS

EDITOR-IN-CHIEF/ACES

W. Perry Wheless, Jr.
University of Alabama, EE Dept.
PO Box 870286
Tuscaloosa, AL 35487-0286 USA

EDITOR-IN-CHIEF, EMERITUS

Duncan C. Baker
EE Dept. U of Pretoria,
0002 Pretoria, SOUTH AFRICA

MANAGING EDITOR

Richard W. Adler
833 Dyer Rd. Room 437, EC/AB
NPS, Monterey, CA 93943-5121, USA

Ruediger Anders

Applied EM Engineering
Roswell, GA, USA

Brian A. Austin

University of Liverpool
Liverpool, UK

Joao Bastos

University Fed De Santa Catarina
Florianopolis, BRAZIL

John Beggs

Mississippi State University
Mississippi State, MS, USA

Fulvio Bessi

Ingegneria dei Sistemi S.p.A.
Pisa, ITALY

John R. Bowler

University of Surrey
Surrey, UK

John Brauer

Ansoft Corporation
Milwaukee, WI, USA

Tony Fleming

Telecom Australia.
Clayton, Victoria, AUSTRALIA

Pat Foster

Microwave & Antenna Systems
Gt. Malvern, Worc. UK

Gregory R. Haack

DSTO
Salisbury, SA, AUSTRALIA

Christian Hafner

Swiss Federal Inst. of Technology
Zurich, SWITZERLAND

CO-EDITOR-IN-CHIEF/JOURNAL

Ahmed Kishk
University of Mississippi, EE Dept.
University, MS 38677 USA

EDITOR-IN-CHIEF, EMERITUS

Robert M. Bevensee
Box 812
Alamo, CA, 94507-0516 USA

Kueichien C. Hill

Wright Laboratory
Wright-Patterson AFB, OH, USA

Todd H. Hubing

University of Missouri-Rolla
Rolla, MO, USA

Nathan Ida

The University of Akron
Akron, OH, USA

Andrzej Krawczyk

Institute of Electrical Engineering
Warszawa, POLAND

Peter Krylstedt

National Defence Research Est.
Sundbyberg, SWEDEN

Stanley Kubina

Concordia University
Montreal, Quebec, CANADA

Ronald Marhefka

Ohio State University
Columbus, OH, USA

Gerard Meunier

NPG/ENSIEG
St. Martin-d'Heres Cedex, FRANCE

Edmund K. Miller

LASL
Santa Fe, NM, USA

Giorgio Molinari

University of Genova
Genova, ITALY

Frederick A. Molinet

Societe Mothesim
Plessis-Robinson, FRANCE

Gerrit Mur

Technische Universiteit Delft
Delft, NETHERLANDS

CO-EDITOR-IN-CHIEF/JOURNAL

Allen Glisson
University of Mississippi, EE Dept.
University, MS 38677 USA

EDITOR-IN-CHIEF, EMERITUS

David E. Stein
USAF Scientific Advisory Board
Washington, DC 20330 USA

Krishna Naishadham

Wright State University
Dayton, OH, USA

Antonio Orlandi

University of L'Aquila
L'Aquila, ITALY

Giuseppe Pelosi

University of Florence
Florence, ITALY

Andrew F. Peterson

Georgia Institute of Technology
Atlanta, GA, USA

Kurt Richter

Technical University of Graz, IGTE
Graz, AUSTRIA

Harold A. Sabbagh

Sabbagh Associates
Bloomington, IN, USA

Neil R.S. Simons

Communications Research Center
Ottawa, Ontario, CANADA

Norio Takahashi

Okayama University
Tsushima, JAPAN

Yoshiki Uchikawa

Nagoya University
Nagoya, JAPAN

Jean-Claude Verite

Electricite de France
Clamart, Cedex, FRANCE

THE APPLIED COMPUTATIONAL ELECTROMAGNETICS SOCIETY

Vol. 14 No. 1

March 1999

TABLE OF CONTENTS

"A User-Friendly Computer Code for Radiated Emission and Susceptibility Analysis of Printed Circuit Boards"	
J. Carlsson and P-S. Kildal	1
"A Sparse Iterative Method (SIM) for Method of Moments Calculations"	
A.P.C. Fourie, D.C. Nitch and A.R. Clark	9
"Radiation from 3D Sources in the Presence of 2D Composite Objects of Arbitrary Cross-Sectional Shape"	
A.A. Kishk, P. Slattman and P-S. Kildal	17

© 1999, The Applied Computational Electromagnetics Society

A User-friendly Computer Code for Radiated Emission and Susceptibility Analysis of Printed Circuit Boards

Jan Carlsson¹ and Per-Simon Kildal²

¹ Swedish National Testing and Research Institute, Borås, Sweden

² Chalmers University of Technology (CTH), Gothenburg, Sweden

Abstract - A user-friendly computer code, PCB-MoM, that is intended to be used in EMC applications for predicting radiated emission and susceptibility of printed circuit boards (PCB) is presented. The formulation is based on an electric field integral equation (EFIE) expressed in the frequency domain. The EFIE is solved by the method of moments using two-dimensional pulse basis functions and one-dimensional pulse test functions. In order to incorporate dielectric material in the substrate a spectral domain formulation is used. The code has been validated by comparison with previously published results and results obtained by other methods and codes.

I. Introduction

Knowledge of emission and susceptibility of printed circuit boards is important in order to control the electromagnetic compatibility of an electronic device. The main advantage of computation compared with measurements, is that the former can be done already during the design phase of the device. Thereby, a costly redesign due to a failure in passing an EMC test can be avoided. Still, it is important to realise that computation is not a substitute to EMC tests, but rather a complement. As a complement the computation can give us insight into different coupling phenomena etc. on the circuit board, which can be very difficult to understand through measurements. It is also very easy by computation to test different methods for reducing the radiated emission or increasing the susceptibility level. As an example, the re-routing of the clock signals on a printed circuit board in order to reduce the radiated emission, can hardly be done by experiments.

The purpose of this paper is to present a user-friendly computer program called PCB-MoM that can be used for analysing planar conducting structures, such as PCB, regarding radiated emission and susceptibility as well as crosstalk. The formulation used by the program is based on an electric field integral equation (EFIE) expressed in the frequency domain. In order to solve the EFIE the method of moments [1] is used. The formulation and choice of basis and test functions is based on that in [2]. The dielectric material in-between the structure and the

ground plane is taken into account by a spectral domain technique similar to the one presented in [3]. The spectral domain approach is speeded up by making use of asymptotic extraction, as explained in [4]. The circuit board is treated as a grounded single layer structure. The approach is readily extended to a multilayer structure of arbitrary number of layers by means of the G1DMULT algorithm presented in [5].

II. Theory for conducting plane surfaces in homogenous region

Referring to Fig. 1, we know that the incident field, \mathbf{E}^{inc} , will induce a surface current on the conducting structure and that the surface current in turn will produce a scattered field, \mathbf{E}^{scat} . If the structure is assumed to be a perfect conductor, we know that the tangential component of the electric field at the surface of the structure must vanish, i.e. $(\mathbf{E}^{inc} + \mathbf{E}^{scat})_{tan} = 0$. If we want to consider a finite conductivity, the above formula becomes:

$$(\mathbf{E}^{inc} + \mathbf{E}^{scat})_{tan} = Z_s \mathbf{J} \quad (1)$$

where Z_s is the surface impedance (in Ohms) and \mathbf{J} is the induced surface current density (in A/m) on the structure.

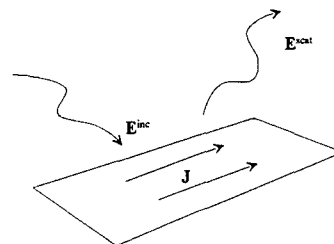


Fig. 1. Planar conducting structure subject to an incident electromagnetic field.

For the case of thin planar conducting structures, we can assume the conducting sheet to be infinitesimally thin and that the current only can flow in two orthogonal directions. Without loss of generality, we can assume the conducting sheet to be placed in the xy-plane and the two orthogonal current directions are in the x- and y-directions. From any standard textbook on electromagnetics, e.g. [6], we can find expressions for the

scattered field from a surface current density expressed in terms of a vector and a scalar potential (2).

$$E_x^{scat} = -j\omega A_x - \frac{\partial \Phi}{\partial x}, E_y^{scat} = -j\omega A_y - \frac{\partial \Phi}{\partial y} \quad (2)$$

where

$$\begin{cases} A_{x,y} = \frac{\mu}{4\pi} \iint_S J_{x,y} \frac{e^{-jkr}}{r} ds \\ \Phi = \frac{1}{4\pi\epsilon} \iint_S \sigma \frac{e^{-jkr}}{r} ds, \sigma = \frac{j}{\omega} \left(\frac{\partial J_x}{\partial x} + \frac{\partial J_y}{\partial y} \right) \end{cases} \quad (3)$$

A is the vector potential, Φ is the scalar potential and σ is the charge density which is related to the current density through the continuity equation. r is the distance between the source point (the current) and the field point. For field points on the surface of the structure, r is given as:

$$r = \sqrt{(x - x')^2 + (y - y')^2}, \text{ where } (x', y') \text{ is the}$$

source point and (x, y) the field point. In order to solve the coupled integral equations for J_x and J_y obtained by enforcing the boundary conditions in (1), we use the method of moments [1] and the same type of basis and test functions as introduced by Glisson & Wilton [2]. The first step in using the method of moments is to expand the unknowns in series of known basis functions with unknown coefficients. The choice here is to use so called pulse sub-domain basis functions. These functions are unity over a rectangular area and zero elsewhere. Thus, we express the current densities and charge density in the following way:

$$J_x = \sum_{n=1}^N J_{xn} \Pi, J_y = \sum_{m=1}^M J_{ym} \Pi, \sigma = \sum_{i=1}^I \sigma_i \Pi \quad (4)$$

where Π represents the two-dimensional pulse function. J_{xn} , J_{ym} and σ_i are the coefficients for the current and charge densities, respectively. The locations of the pulse functions for the current and charge elements are shown in Fig. 2.

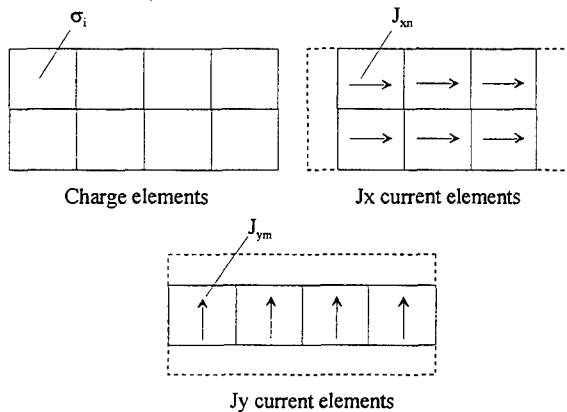


Fig. 2. Definition of current and charge elements.

Insertion of the expansions (4) in the integral equations gives:

$$E_x^{inc}(x, y) = \frac{j\omega\mu}{4\pi} \sum_{n=1}^N J_{xn} F(S_{xn}, r) + \frac{\partial}{\partial x} \left[\frac{1}{4\pi\epsilon} \sum_{i=1}^I \sigma_i F(S_{ci}, r) \right] + Z_s(x, y) J_x(x, y) \quad (5)$$

$$E_y^{inc}(x, y) = \frac{j\omega\mu}{4\pi} \sum_{m=1}^M J_{ym} F(S_{ym}, r) + \frac{\partial}{\partial y} \left[\frac{1}{4\pi\epsilon} \sum_{i=1}^I \sigma_i F(S_{ci}, r) \right] + Z_s(x, y) J_y(x, y) \quad (6)$$

where $F(S, r) = \iint_S \frac{e^{-jkr}}{r} ds$, S_{xn} represents the area of

J_x current element number n , S_{ym} the area of J_y current element number m and S_{ci} the area of charge element number i . The next step is to define two sets of testing functions, one for equation (5) and one for equation (6). The choice here is to use functions that are constants along a line in x - and y -directions, respectively, Fig. 3.

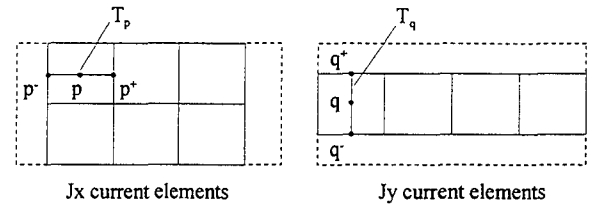


Fig. 3. Definition of test functions.

$$T_p = \begin{cases} 1, & \bar{p} \leq x \leq \bar{p}^+, y = y_p, p = 1 \dots N \\ 0, & \text{elsewhere} \end{cases} \quad (7)$$

$$T_q = \begin{cases} 1, & x = x_q, \bar{q} \leq y \leq \bar{q}^+, q = 1 \dots M \\ 0, & \text{elsewhere} \end{cases} \quad (8)$$

Multiplying equation (5) by the test functions (7) and multiplying equation (6) by the test functions (8) and integrating over each test function gives a matrix equation of the form:

$$\begin{bmatrix} E_x^{inc} \\ E_y^{inc} \end{bmatrix} = \begin{bmatrix} Z_{xx} \\ Z_{yx} \end{bmatrix} \begin{bmatrix} J_x \\ J_y \end{bmatrix} \quad (9)$$

where the sub-matrices are defined by:

$\begin{bmatrix} E_x^{inc} \end{bmatrix}$ is a column vector of dimension N and the elements: $(E_x^{inc})_p = \Delta p E_x^{inc}(p)$

$[J_x]$ is a column vector of dimension N and the elements: $(J_x)_n = J_{xn}$

$[Z_{xx}]$ is a matrix of dimension N by N and the elements:

$$(Z_{xx})_{pn} = \frac{j\omega\mu}{4\pi} \Delta p F(S_{xn}, r_p) + \Delta_{yp} Z_{sp} + \frac{j}{4\pi\omega\epsilon} \left\{ \frac{1}{\Delta_{xcn}} \left[F(S_{cn}^-, r_p^+) - F(S_{cn}^-, r_p^-) \right] - \frac{1}{\Delta_{xcn}^+} \left[F(S_{cn}^+, r_p^+) - F(S_{cn}^+, r_p^-) \right] \right\}$$

$[Z_{xy}]$ is a matrix of dimension N by M and the elements:

$$(Z_{xy})_{pm} = \frac{j}{4\pi\omega\epsilon} \left\{ \frac{1}{\Delta_{ycm}} \left[F(S_{cm}^-, r_p^+) - F(S_{cm}^-, r_p^-) \right] - \frac{1}{\Delta_{ycm}^+} \left[F(S_{cm}^+, r_p^+) - F(S_{cm}^+, r_p^-) \right] \right\}$$

and similar for the other sub-matrices. In deriving the above expressions we have used a finite-difference approximation for the derivatives of the currents in the expression for the charge density. Note that in the above expressions Z_{sp} and Z_{sq} are non-zero only for $n = p$ and $m = q$, respectively. Thus, the surface impedance effects only the diagonal elements in the matrices. They are also allowed to be complex. This means that we can model series impedances consisting of either a resistance and an inductance or a resistance and a capacitance (simulating components on a PCB). The excitation vector, $[E_x^{inc}]$, can represent either an incident field, for a radiated susceptibility analysis, or voltage sources, for a radiated emission analysis. For incident field excitation all elements of the excitation vector are non-zero and for voltage source excitation only one or a limited number of the elements are non-zero.

Equation (9) can easily be solved for the unknown current distribution by matrix inversion. However, special care must be taken when computing the matrix elements since the integrand involved in the integration of Green's function becomes singular for the self-terms (when the observation point is located within the source rectangle). Fortunately, the singularity is integrable and can be treated by changing to polar coordinates.

III. Including the ground plane

Equation (9) together with the matrix elements given above is valid for a conducting sheet (representing the conducting traces on a PCB) in the xy -plane and situated in free-space. In order to also include the case when the conducting sheet is placed over an infinitely large and perfectly conducting plane ($z=\text{constant}$) we use image theory. Since the image currents will be the opposite of the currents on the sheet we do not have to increase the size of the matrix equation, it is sufficient to modify the matrix elements according to.

$$\begin{bmatrix} E_x^{inc} + E_x^{refl} \\ E_y^{inc} + E_y^{refl} \end{bmatrix} = \begin{bmatrix} Z_{xx} - Z_{xx}^{im} & Z_{xy} - Z_{xy}^{im} \\ Z_{yx} - Z_{yx}^{im} & Z_{yy} - Z_{yy}^{im} \end{bmatrix} \begin{bmatrix} J_x \\ J_y \end{bmatrix} \quad (10)$$

where the matrices without superscript are the same as before and the matrices with the superscript "im" are computed in the same way as the corresponding matrix without the superscript but with the distance r changed

from $\sqrt{(x-x')^2 + (y-y')^2}$ to

$\sqrt{(x-x')^2 + (y-y')^2 + (2h)^2}$, when evaluating the

integrals over the Green's function. h is the distance between the conducting sheet and the ground plane (i.e. the ground plane is assumed to be defined by the plane $z=-h$). The excitation vectors will be given by:

$$E_{x,y}^{inc} + E_{x,y}^{refl} = E_{x,y}^{inc} (1 - e^{-j2kh \cos \theta}) \quad \text{for the case of}$$

incident field excitation and will remain the same as for the case without a ground plane for the case of voltage source excitation. Thus, the matrix filling time will be approximately doubled when we have a ground plane, compared to the case without a ground plane, but the matrix inversion time will remain the same.

Another case of interest is when we have one or several connections from the conducting sheet to the ground plane. In order to solve this case we have to introduce currents in the z -direction as well. Following the same procedure that was used for the case when we only had x - and y -directed currents, similar expressions for the currents can be derived. Details can be found in [7].

IV. Including the substrate

In order to extend the above theory so that also planar structures on a grounded dielectric substrate could be analysed, the natural way would be to exchange the free space Green functions to that for a grounded dielectric substrate. However, this approach requires that slowly converging integrals of Sommerfelds type have to be evaluated, see e.g. [8]-[10]. Another approach is to perform a Fourier transform of the structure along the two

uniform directions, i.e. to perform the computation in the spectral domain. This will give a spectrum of 1D field problems instead of one 3D field problem [5]. This approach will also result in slowly converging integrals, see e.g. [3], [11]. However, the convergence can be speeded up by extracting the asymptotic part of these integrals and treat this separately [12]. It can also be shown that the asymptotic part just as well can be computed in the spatial domain and in fact is equal to the impedance elements as given in Section III but computed

with a permittivity equal to $\epsilon_{eff} = (1 + \epsilon_r)/2$, [4]. Thus, in order to take the grounded dielectric substrate into account we only have to add a correction factor to the impedance elements already computed (using the permittivity $\epsilon_{eff} = (1 + \epsilon_r)/2$). The correction factors for the impedance elements in (9) are:

$$(Z_{ij})_{kl}^{diel-as} = \frac{-1}{4\pi^2} \iint_{-\infty-\infty}^{\infty} (\tilde{E}_{ij}^{diel} - \tilde{E}_{ij}^{diel,as}) \mathcal{J}_{jl} \tilde{T}_{jk}^* dk_x dk_y \quad (11)$$

where $i = x$ or y , $j = x$ or y , $k = p$ or q , $l = m$ or n . $\tilde{E}^{diel,as}$ are the asymptotic field expressions and \tilde{E}^{diel} are the exact field expressions.

$$\tilde{f}(k_x, k_y) = \iint_S f(x, y) e^{jk_x x} e^{jk_y y} dx dy$$

represent quantities in the spectral domain and $*$ denotes complex conjugate. The asymptotic field expressions in the spectral domain correspond, in the spatial domain, to the field from a single current element over a ground plane in a homogenous region. Expressions for the asymptotic part can be found in [4] and [12]. Exact field expressions can be found in e.g. [3]. The integrals (11) converge fast since the asymptotic field expressions approach the exact field expressions for large $k_x^2 + k_y^2$.

V. The user interface

The above theory has been implemented in a user-friendly computer program, PCB-MoM, that can be used on an ordinary PC running Windows 95 or NT 4.0. In using the PCB-MoM program, analysing a printed circuit board (PCB) is a three-step procedure: defining the geometry, performing a simulation and finally visualising the computed results. Each of these steps is devoted an own page in the program. Switching between these pages is done simply by clicking on the corresponding page tab, Fig. 4. In order to define the geometry the conducting segments on the PCB are simply drawn on the screen using the built-in CAD-like interface, Fig. 4.

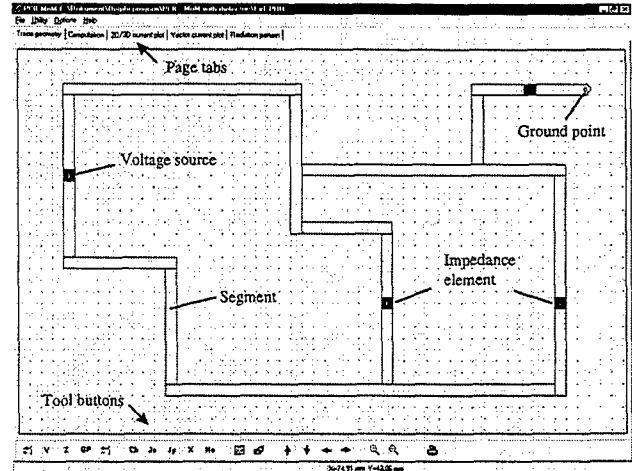


Fig. 4. The geometry definition page showing a simple structure.

The subdivision of the segments into current and charge elements is done automatically, but can also be set manually by the user. Lumped, discrete voltage sources and impedance elements can easily be defined by pointing out the locations in the layout. In the same way, ground points (i.e. metal connections to the underlying ground plane) can be defined. When the geometry is defined a simulation can be performed. All relevant parameters for the simulation is set on an own page, Fig. 5.

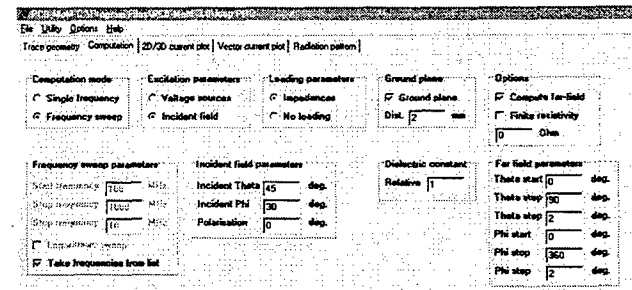


Fig. 5. Part of the computation page where parameters for the simulation are set.

On this page the excitation is either defined as voltage sources or as an incident plane wave. The existents of a ground plane and the dielectric constant for the region between the structure and the ground plane are also defined on the computation page. When a simulation is started the program will, if requested by the user, give a time estimate for how long the simulation will take. The time estimate is based upon constants saved in a file. Since the constants are dependent on the used computer they are created by the program through a calibration procedure. Before a simulation is started, the program analyses the input data and, if possible, a symmetrical matrix filling procedure will be used in order to reduce the simulation time. Fig. 6 shows the required time for

filling both a full matrix and a symmetrical matrix for a structure in free space.

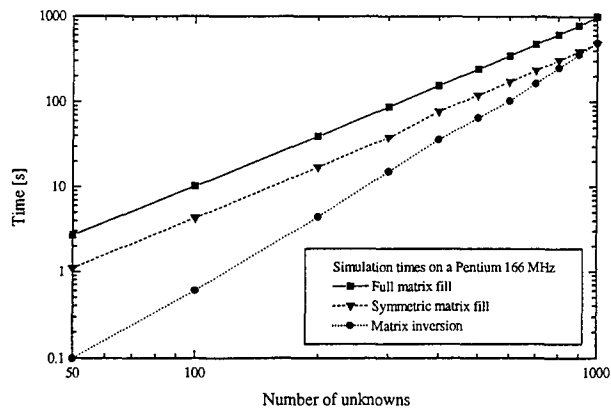


Fig. 6. Simulation times for a structure in free space on a Pentium 166 MHz.

The results from a simulation are primarily the current densities on the conducting traces. In addition the near-field in selected points and the far-field in selected angular ranges can be obtained. The computed current densities can be viewed in different ways, as a 3D plot, as a 2D plot or as a vector plot. Figures 7 and 8 show two different ways of visualisation of the current density.

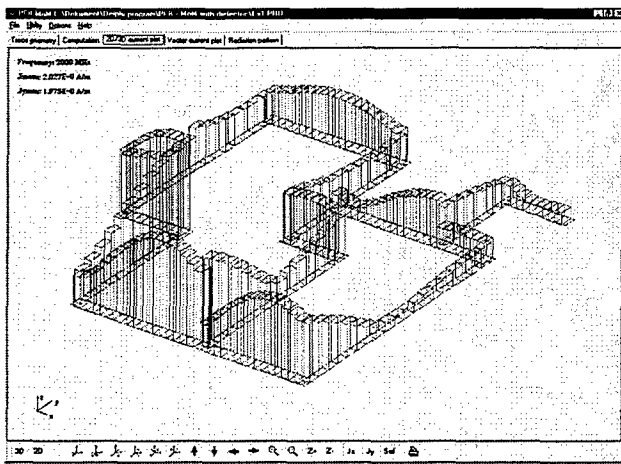


Fig. 7. Current density at 2 GHz for the structure in Fig. 4 shown as a 3D-plot.

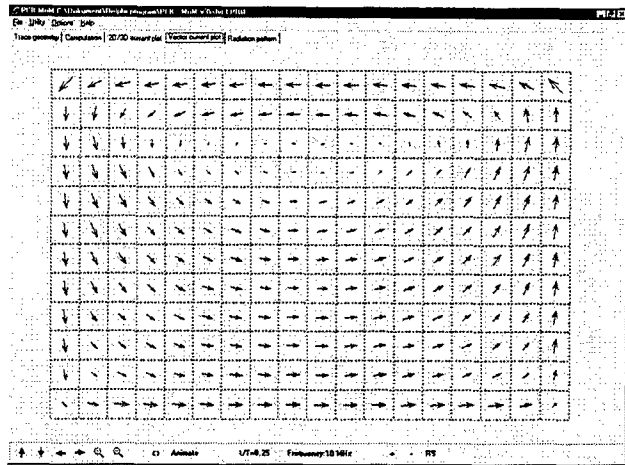


Fig. 8. Current density on a plate shown as a vector plot. Excitation is done by a current carrying straight conductor in the vicinity of the plate (not shown in the figure).

The computed radiation pattern in the far-field can be viewed as a polar plot. All computed quantities can also be listed in the program and are saved in ASCII-files. This makes it easy to perform further analysis or plotting using another program.

VI. Test cases and examples

The PCB-MoM program has been extensively tested against previously published results, against results obtained with other codes and methods, and against measurements. At low frequencies the code has been tested against results obtained with ordinary circuit theory. Results for intermediate frequencies have been tested against ordinary transmission line theory and multiconductor transmission line theory. High frequency results and problems involving dielectric material have been compared with published results obtained by other methods and also with computations done with other programs. As an example the computed and measured radiated emission from a simple PCB with a 10 MHz clock oscillator is shown in Fig. 9. For the computation it is necessary to know the output voltage from the clock oscillator at the desired frequencies. The voltage was measured with a spectrum analyzer. Since this measurement is not trivial, the uncertainty is quite high and it probably explains the disagreement between measurement and simulation. However, it is interesting to note that the overall behaviour of the radiated field is predicted well.

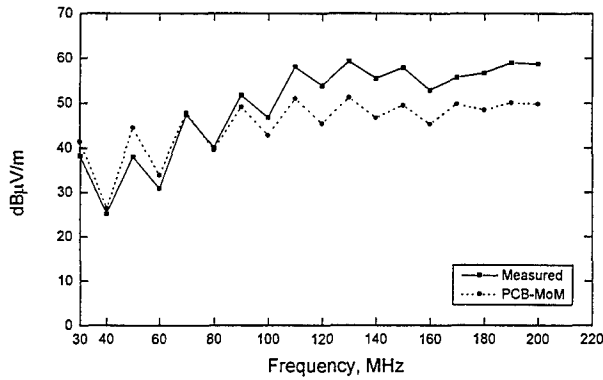


Fig. 9. Measured and computed radiated emission from a simple PCB with a 10 MHz clock oscillator.

The configuration in Fig. 10 was considered in order to verify the results against multiconductor transmission line theory. One of the lines in Fig. 10 was excited with a 1 V voltage source and the other ends of both lines were terminated with 1 k Ω resistors. The computed quantity was the current through the R_f resistor in line 2. Using the multiconductor transmission line theory the per unit length parameters, inductance matrix L and capacitance matrix C , were first computed with LC-Calc [13] which is a finite difference program. The matrices were found to be:

$$L = \begin{bmatrix} 0.383 & 0.067 \\ 0.067 & 0.383 \end{bmatrix} [\mu\text{H/m}]$$

$$C = \begin{bmatrix} 30.0 & -5.25 \\ -5.25 & 30.0 \end{bmatrix} [\text{pF/m}]$$

The per unit length parameters were then used in BMTL [14] which is a finite difference time domain program that solves the multiconductor transmission line equations. In the BMTL program the conductors were divided into 50 elements and 8192 time steps were used for the computation. This gives a frequency resolution of approximately 11.4 MHz. In the PCB-MoM program the conductors were divided into 20 current elements along the length and 4 in the transverse direction. As can be seen from the results in Fig. 10 the agreement is good.

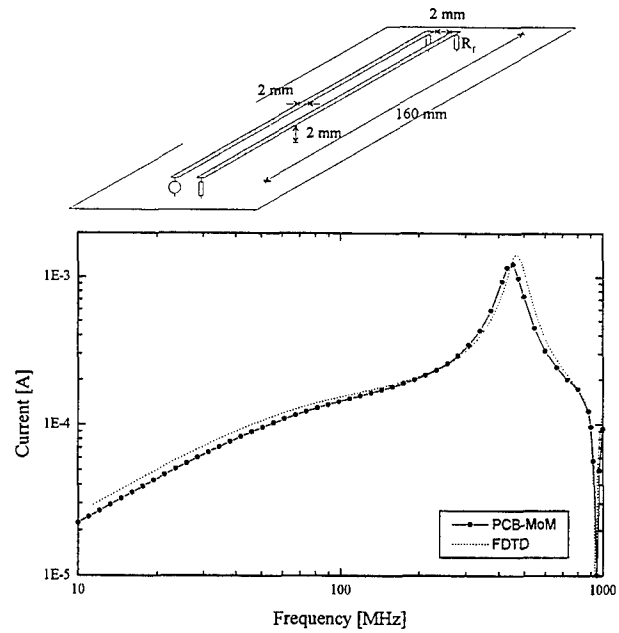


Fig. 10. Computation of crosstalk between two parallel lines that are terminated to a common ground plane. All resistors are 1 k Ω . The environment is free space. Computed quantity is current through the R_f resistor.

Computation done with PCB-MoM and with multiconductor transmission line theory implemented in a FDTD program.

As a test of the capability of computing the near field, the square plate in Fig. 11 was considered. The plate was excited with a normal incident plane wave with the E-field polarised along the x-axis. The computed quantities were the total field components E_x and E_z close to the surface of the plate. Since PCB-MoM gives the scattered field when the excitation is an incident field, the total field was computed as: $\mathbf{E}^{\text{tot}} = \mathbf{E}^{\text{scat}} + \mathbf{E}^{\text{inc}}$, where the incident field is given by: $\mathbf{E}^{\text{inc}} = \hat{x}e^{jkz}$. For the computation the plate was divided into 25 by 25 charge elements. The results in Fig. 11 agree very well with the results reported in [15] and the results obtained with the FDTD program XFDTD. In [15] two different method of moments programs and a UTD program were used. Also the E_x component, although not shown here, agrees very well with results obtained with XFDTD and results reported in [15].

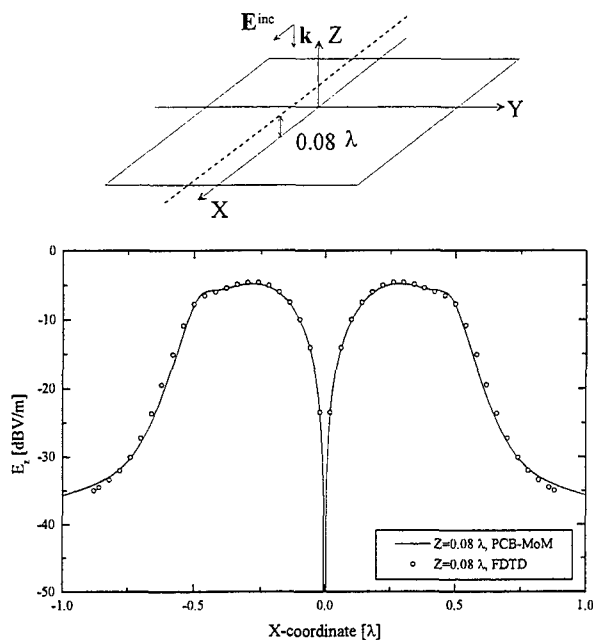


Fig. 11. Computed E_z along the line: $-\lambda < x < \lambda$, $y = 0$, $z = 0.08\lambda$ over a square plate at $z = 0$ excited with an incident plane wave. Plate dimension $\lambda \times \lambda$. Solid line represents PCB-MoM, circles the XFDTD program.

For testing the capability of treating conducting structures on a dielectric substrate the loaded rectangular loop shown in Fig. 12 was analysed. The loop was fed by a voltage generator with an amplitude of 1 Volt and an internal resistance of 50Ω . The computed quantity was the current at the feed point and the result was compared with result obtained by the commercial FDTD program XFDTD. As can be seen in Fig. 12 the agreement between the two approaches is good. However, it can be noted that the current amplitude predicted by XFDTD around 700 MHz is slightly too large. It should not be higher than 20 mA due to the internal resistance of the source.

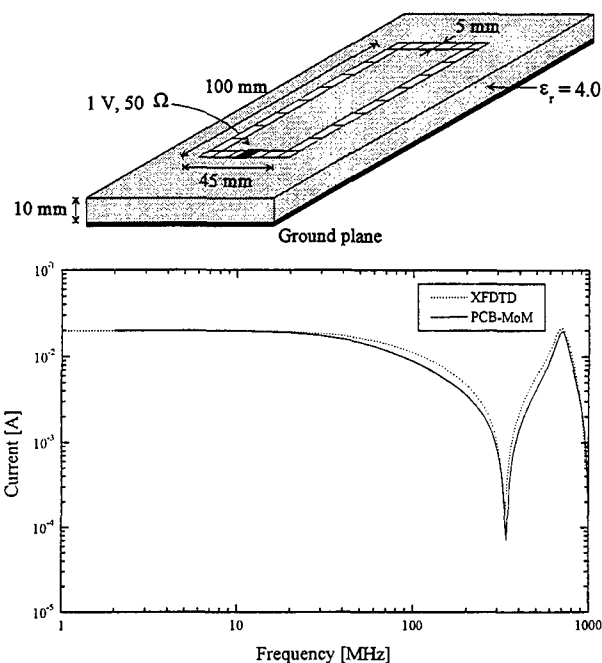


Fig. 12. Computed current amplitude at the feed point of a loaded rectangular loop on a grounded dielectric substrate with permittivity 4.0. Solid line represents PCB-MoM, dotted line the XFDTD program.

As another test of the capability of treating dielectric material the centre fed microstrip dipole in Fig. 13 was considered. The length of the dipole was varied and the input impedance at the feed point was calculated. The impedance was computed as $Z = U/I$, where U is the excitation voltage and I is the current in the current element where the voltage source is placed. Fig. 13 shows the impedance, real and imaginary parts, computed by the PCB-MoM program using 19 current elements. The agreement with results reported in [9] is found to be good. It can also be noted that the half and full wavelength resonances are predicted accurately.

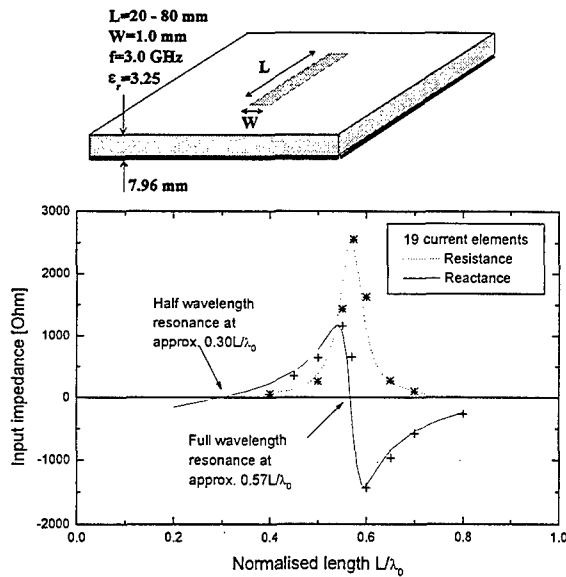


Fig. 13. Computed input impedance for a centre fed microstrip dipole with varying length. Stars and crosses represent data extracted from [9].

VII. Development history

From the beginning the program was aimed to be used for planar structures in free space and was later modified to treat also structures on a dielectric substrate. The free space routines and the user interface were all written in Delphi by Borland. Since the Pascal used in Delphi does not have support for complex numbers several routines had to be written for treating them. This also includes matrix inversion routines. The routines for treating dielectric material were written in C++, also by Borland, and added to the original program as a DLL (Dynamic Link Library).

VIII. Conclusions

We have presented a user-friendly method of moments program designed to be used in EMC applications where the interest is in determining the radiated emission and susceptibility of printed circuit boards. The intention has been to design a tool that can be of help to EMC engineers. The program has been extensively tested and the agreement with results obtained by other methods and codes has been found to be good. The code can be obtained from the first author (jan.carlsson@sp.se).

IX. References

[1] R. F. Harrington, *Field Computation by Moment Methods*. New York: Macmillan, 1968.

- [2] A. W. Glisson and D. R. Wilton, "Simple and efficient numerical methods for problems of electromagnetic radiation and scattering from surfaces," *IEEE Trans. Antennas Propagat.*, vol. AP-28, pp. 593-603, Sep. 1980.
- [3] D. M. Pozar, "Input impedance and mutual coupling of rectangular microstrip antennas," *IEEE Trans. Antennas Propagat.*, vol. AP-30, pp. 1191-1196, Nov. 1982.
- [4] J. Carlsson and P.-S. Kildal, "A physical model for the asymptotic field expression for a conducting patch on a dielectric substrate," Submitted to *IEEE Trans. Antennas Propagat.*
- [5] Z. Sipus, P.-S. Kildal, R. Leijon, and M. Johansson, "An algorithm for calculating Green's functions for planar, circular cylindrical and spherical multilayer substrates," Accepted for publication in *Applied Computational Electromagnetics Society Journal*.
- [6] C. A. Balanis, *Advanced Engineering Electromagnetics*: John Wiley & Sons inc., 1989.
- [7] J. Carlsson, "A method of moments program for radiated emission and susceptibility analysis of printed circuit boards," SP Swedish National Testing and Research Institute report 1998:03.
- [8] J. R. Mosig, "Arbitrarily shaped microstrip structures and their analysis with a mixed potential integral equation," *IEEE Trans. Microwave Theory and Tech.*, vol. 36, pp. 314-323, Feb. 1988.
- [9] M. Marin, S. Barkeshli, and P. H. Pathak, "Efficient analysis of planar microstrip geometries using a closed-form asymptotic representation of the grounded dielectric slab Green's function," *IEEE Trans. Microwave Theory and Tech.*, vol. 37, pp. 669-679, 1989.
- [10] M. I. Aksun and R. Mittra, "Spurious radiation from microstrip interconnects," *IEEE Trans. Electromagn. Compat.*, vol. 35, pp. 148-158, 1993.
- [11] E. H. Newman and D. Forrai, "Scattering from a microstrip patch," *IEEE Trans. Antennas Propagat.*, vol. AP-35, pp. 245-251, March 1987.
- [12] D. M. Pozar, "Improved computational efficiency for the moment method solution of printed dipoles and patches," *Electromagnetics*, vol. 3, pp. 299-309, Jul-Dec 1983.
- [13] J. Carlsson, "Computer code LC-Calc," (also in J. Carlsson, *Crosstalk on printed circuit boards*, SP Swedish National Testing and Research Institute report 1994:14).
- [14] J. Carlsson, "A FDTD program for computing responses on branched multi-conductor transmission lines," SP Swedish National Testing and Research Institute report 1998:16.
- [15] R. Paknys and L. R. Raschkowan, "Moment method surface patch and wire grid accuracy in the computation of near fields," *Applied Computational Electromagnetics Society Journal*, vol. 12, pp. 16-25, Nov 1997.

A Sparse Iterative Method (SIM) for Method of Moments Calculations

A.P.C. Fourie, D.C. Nitch and A.R. Clark

Department of Electrical Engineering
University of the Witwatersrand, Johannesburg
2050 South Africa
a.clark@ee.wits.ac.za

Abstract—The Sparse Iterative Method (SIM) provides a faster solution to Method of Moments (MoM) matrix equations than does LU-decomposition with forward and back substitution. The SIM produces a solution with computational time proportional to N^2 , as opposed to the N^3 time dependence associated with LU-decomposition. The SIM is implemented in an object oriented MoM program which is functionally equivalent to NEC2. In three examples, the SIM is shown to produce results as accurate as LU-decomposition. For dipoles, a flat wire grid and a generic three dimensional missile shape, the speed increase ranged from 3–30 times the speed of LU-decomposition; greater speed increases can be expected with electrically larger problems. The SIM requires no problem formulation changes, such as segment renumbering, and despite the fact that it is demonstrated for a wire MoM based on NEC2, it is general enough to be incorporated to any MoM formulation.

I. INTRODUCTION

We have investigated a stationary¹ iterative method of moments (MoM) solution technique for implementation in an object oriented method of moments program [1]. When a method of moments problem has N unknowns, and N is large, it is computationally time-consuming; most time is spent either filling the matrix and/or in the LU-decomposition of the matrix. Typical method of moment programs execute in a time, t , that is given by

$$t \propto AN^2 + BN^3 + \text{other smaller terms} \quad (1)$$

where A is the time taken to calculate a single matrix element and B is the time taken to modify a single matrix element during LU-decomposition on a specific machine.

The B coefficient in equation (1) is much smaller than the A coefficient. The A coefficient is larger because computation of an element of the interaction matrix usually involves both numerical integration and other operations. The B coefficient is smaller; modifying a matrix element during LU-decomposition involves only a few floating point operations.

Problems involving a small number of unknowns have solution times proportional to N^2 . As the problem size increases, the time associated with the BN^3 term increases more rapidly than for the AN^2 term; this latter term ultimately governs the solution time for large MoM problems.

¹A stationary method is one where the rule used to determine the next guess does not change from iteration to iteration.

Iterative methods concentrate on reducing the BN^3 component of the solution. This paper describes a method derived from the physics underlying the MoM. This Sparse Iterative Method (SIM) replaces LU-decomposition for MoM problems and results in solutions in a time proportional to N^2 , which is considerably faster than LU-decomposition. Provided a suitable number of iterations are performed, the SIM results are as accurate as those obtained by LU-decomposition. In principle, since only a small fraction of the normal interaction matrix needs to be stored, it is possible to reduce computer storage requirements using the SIM. However, a trade off in terms of computer time versus storage exists; this trade-off is discussed later.

The development and evaluation of the new method was implemented on a redesigned and rewritten version of the well known NEC2 [2] program. Nitch [1] redesigned the FORTRAN version of NEC2 using the Object Oriented Programming (OOP) paradigm and implemented it using the C++ computer language. The C++ program is functionally equivalent to NEC2, but the improved software implementation enables modifications to be easily effected. The iterative solution technique could thus be incorporated easily into NEC, allowing the SIM to be evaluated for large realistic problems. In the past, new methods have been evaluated based on simple examples and implementations, due to the programming effort required to do the evaluation for realistic cases. The use of simplified codes can result in misleading conclusions, due to the fact that the methods are only evaluated for simple cases. We believe that testing methods using realistic problems is crucial to an adequate evaluation; the implementation of the SIM in the C++ NEC made such an evaluation possible.

II. BACKGROUND TO METHOD OF MOMENTS

The detailed derivation of MoM is available from many sources, and only the features of importance to the development of the SIM will be discussed here. The method of moments for perfectly conducting wire segments, as implemented in NEC2, will be considered. In the case of point matching (equivalent to using impulse or delta weighting functions), the MoM involves finding a current distribution across all segments such that the tangential E-field at the centre of each segment is zero. Zero tangential E-Fields satisfy the boundary conditions at the interface of a perfect conductor. In order to find the currents on a structure,

the current on each segment, $I_a(n)$, is assumed to have a generic shape defined by the basis function, J_n , i.e.,

$$\mathbf{I}_a = \sum_{n=1}^N I_n J_n \quad (2)$$

where I_n are the unknown coefficients associated with the current on each segment (when subdomain basis functions are used). The value of these unknown coefficients are solved using MoM.

In the case of NEC2, the basis functions consist of the superposition of a sine, cosine and a constant term. The relative relationship between the three terms is obtained from junction boundary conditions, leaving unknown scaling factors, I_n , to be determined for each segment; MoM solves for these scaling factors.

The matrix equation formulated in a MoM solution to an electromagnetic problem can be mathematically stated as

$$\mathbf{Z}\mathbf{I} = \mathbf{V} \quad (3)$$

where \mathbf{Z} is an $N \times N$ interaction matrix, \mathbf{I} is the unknown current coefficient vector and \mathbf{V} is the specified excitation vector. The matrix equation is normally solved using LU-decomposition followed by forward and back substitution. An element of the interaction matrix, Z_{ij} , represents the tangential electric field, E_{ij}^t , induced on segment i due to radiation from the generic current density J_j on segment j .

A perhaps obvious, but important, property of the system of equations is that multiplication of the first row of \mathbf{Z} with the current vector \mathbf{I} gives E_1^t : the total tangential E-field on segment 1 due to radiation by the currents on all segments. If a segment is not excited, the tangential E-field should be zero. That is, for the general observation segment, i ,

$$E_i^t = \sum_{j=1}^N E_{ij}^t \quad (4)$$

E_{ij}^t is the tangential E-field on segment i due to a current on source segment, j . The equation for obtaining this quantity as a function of current, geometry and segment dimensions usually has the form

$$E_{ij}^t = \int_{s_j} I_j J_j G_{ij} ds \quad (5)$$

where s_j denotes integration over the surface of segment j , and G_{ij} is a function of the geometric relationship between the two segments.

The only difference between E_{ij}^t , and the matrix element Z_{ij} , is that Z_{ij} is obtained using the *normalised* form of the current ($I_j = 1$) on the source segment while the *actual* current, $I_j J_j$, is used to obtain E_{ij}^t .

The solution obtained in this manner satisfies the initial premise; i.e. the tangential E-field at the center of each segment will be zero—excluding computer rounding errors and machine precision.

The components of the total simulation time mentioned in equation (1) result from the following operations:

- N^2 elements have to be calculated in order to initialise the \mathbf{Z} -matrix. Each element is calculated by numerically solving an equation in the form of equation (5), with $I_n = 1$ for each element.
- The excitation vector, \mathbf{V} , is filled according to the excitation of each segment in the structure. Equation (3) is normally solved by factoring the \mathbf{Z} -matrix using LU-decomposition and then solving for \mathbf{I} . LU-decomposition requires N^3 operations; for large problems, matrix factoring hence comprises the largest component of the execution time.

III. PREVIOUS INVESTIGATIONS AND ATTEMPTS AT ITERATIVE METHODS

Four previous publications describe iterative methods which relate to the SIM; these are: the banded Jacobi method [3], the block Seidel technique [4], the conjugate gradient method [5] [6] and the Impedance Matrix Localization (IML) method [7].

The banded Jacobi iterative scheme described by [3] was one of the first iterative methods to be implemented in a Method of Moments EM Code. This iterative technique is implemented in the GEMACS [8] program.

In GEMACS, a banded matrix is obtained by neglecting matrix elements some distance (or band) away from the main diagonal. A second matrix, consisting of those elements that were disregarded in the banded matrix, is also generated. A first estimate of the current is found by factoring and solving the banded system. The second matrix is then used to improve the current estimate iteratively until convergence is achieved. The method is similar to the standard Jacobi iterative scheme, except that a banded, rather than a diagonal matrix is employed. Mathematically the SIM is closely related to banded Jacobi iterative scheme, except that a sparse rather than banded matrix is employed—this difference has considerable advantages however.

The following formulation of the banded Jacobi method is given in terms of equation (3). The method is initialised by breaking the \mathbf{Z} -matrix into two submatrices

$$\mathbf{Z} = \mathbf{B} + \mathbf{L}\mathbf{U} \quad (6)$$

where $\mathbf{L}\mathbf{U}$ is an upper and lower triangular matrix and \mathbf{B} is a banded diagonal matrix with upper and lower bandwidths M (number of minor diagonals). GEMACS iteratively solves the equation

$$\mathbf{B}\mathbf{I}^{k+1} = \mathbf{V} - (\mathbf{L}\mathbf{U})\mathbf{I}^k \quad (7)$$

In order to achieve convergence while using small bands, the banded Jacobi method relies on renumbering segments to ensure that the majority of the largest elements of the \mathbf{Z} -matrix lie about the main diagonal. However, with many structures, such an ordering is not always possible; when a multi-dimensional structure is electrically large, it is clearly impossible to ensure that segment numbers of adjacent

segments remain numerically close to each other—large cylinders and spherical shapes are particular examples. In such cases, the use of the banded Jacobi method invariably causes large matrix elements to lie far from the main diagonal, necessitating a wide band in the matrix for reasonable convergence rates.

A second iterative scheme was proposed by Baldwin, Boswell, Brewster and Allwright [4], who modified NEC2 to iteratively solve for a number of substructures. Their method is similar to the banded Jacobi method in that it consists of a **B**-matrix which contains all the self interaction submatrices for the substructures, and a **LU**-matrix, which contains the interaction submatrices between different substructures:

$$\mathbf{Z} = \begin{bmatrix} [\mathbf{Z}_1] & 0 & \cdots & 0 \\ 0 & [\mathbf{Z}_2] & \cdots & 0 \\ \vdots & \vdots & \ddots & \vdots \\ 0 & 0 & \cdots & [\mathbf{Z}_p] \end{bmatrix} + \begin{bmatrix} 0 & [\mathbf{Z}_{12}] & \cdots & [\mathbf{Z}_{1p}] \\ [\mathbf{Z}_{21}] & 0 & \cdots & [\mathbf{Z}_{2p}] \\ \vdots & \vdots & \ddots & \vdots \\ [\mathbf{Z}_{p1}] & [\mathbf{Z}_{p2}] & \cdots & 0 \end{bmatrix} \quad (8)$$

Each element in square brackets denotes a submatrix which contains either the self-interaction terms for a specific substructure, or the interaction between different substructures. This iterative method is akin to the banded Jacobi method, except that it uses a Seidel iteration technique. This method is a more coarsely granulated version of the banded Jacobi method and is suitable for a problem domain with unconnected substructures; good results were reported for this specific class of problems. The method is, however, not general enough for application to problems such as electrically large continuous bodies.

Conjugate gradient methods constitute the third class of iterative methods reviewed in this paper. Although Sarkar and Siarkiewicz [5] report faster convergence for this technique in comparison with stationary methods, Davidson [6], amongst others, reports slower convergence rates for the conjugate gradient method. The reason for this discrepancy possibly is a result of the fact that Sarkar investigated very simple problems (dipoles and square patches) that resulted in matrices that had only a few eigenvalues; for such matrices, the conjugate gradient method is known to converge quickly. Davidson applied the method to more realistic problems and reports that the solution times are even greater than those for LU-decomposition.

Recently, Canning [7] proposed an Impedance Matrix Localization (IML) method for MoM calculations. IML formulates sub-domain basis and weighting functions which exhibit strong directional characteristics. The radiation patterns of the basis and weighting functions are then made directional between the source and observation regions of a structure, resulting in an interaction matrix with many small elements. The small elements are set to zero, and the resulting sparse matrix is solved iteratively. The initial results presented for this technique are for simple two dimensional problems and it is difficult to compare to the SIM until results for more general three dimensional cases becomes available.

IV. DEVELOPMENT OF THE SPARSE ITERATIVE METHOD (SIM)

The SIM consists of a sparse matrix that contains only those elements that have an interaction greater than some specified value. In the first implementation of the SIM, the elements making up the sparse matrix were chosen according to the distance between interacting segments. If the source and observation segments were further apart than a distance that we called the zero interaction distance, d_0 , then their interactions were not included in the sparse matrix. An iterative scheme is then used to compensate for the couplings which were neglected. The accuracy of the solution obtained using the SIM can be forced to be as accurate as that obtained using LU-decomposition by using a sufficient number of iterations.

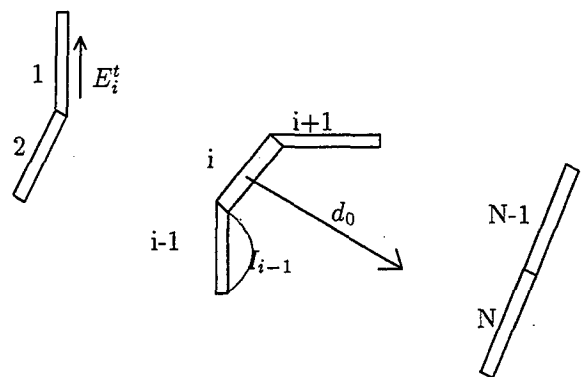


Fig. 1. Arbitrary oriented wire segments used to illustrate the development of the Sparse Iterative Method (SIM)

The following discussion concerning the development of the SIM is done with reference to figure 1. Initially, coupling between segments that are further apart than a distance, d_0 , are omitted when filling the matrix, since coupling reduces with increasing separation. Alternatively, some measure of interaction other than a distance can be used to determine which matrix elements to include. The incorporation of other parameters, such as orientation, will probably improve the performance of the method.

Omitting the coupling between segments further apart than d_0 results in a sparse matrix, **S**; the non-zero elements represent strong coupling. Thus the **Z** matrix is broken into two submatrices

$$\mathbf{Z} = \mathbf{S} + \mathbf{D} \quad (9)$$

where the **D** matrix is the dense matrix of the interactions not in the sparse matrix **S**.

The matrix equation, $\mathbf{SI} = \mathbf{V}$, is solved for the currents, **I**, on the structure where **V** is the structure excitation. The current, **I**, will not satisfy the boundary conditions at all segments, since weaker interactions were disregarded and, as a result, some segment centers will have non-zero tangential **E**-fields. A modified LU-decomposition technique[9] is

used on S to take advantage of its sparsity, and our implementation did not use specialized storage mechanisms for the sparse matrix, as it is outside the scope of this work.

The crux of our solution technique is to apply artificial sources to the structure with values that are equal and opposite to the tangential error fields on each segment. These sources compensate for the coupling that has been neglected between those segments that are further than d_0 apart. The error fields can be described by a vector of length, N , called \mathbf{E}^e . Mathematically, application of the artificial sources can be achieved by subtracting the error fields, \mathbf{E}^e from the excitation vector, \mathbf{V} . New currents are then calculated by solving $\mathbf{S}\mathbf{I} = \mathbf{V} - \mathbf{E}^e$. This procedure is performed iteratively until the solution converges.

The iterative technique described above can be expressed in concise mathematical notation as follows:

Set $\mathbf{V}_0 = \mathbf{V}$ and iterate:

$$\mathbf{S}\mathbf{I}_k = \mathbf{V}_k \quad (10)$$

$$\mathbf{E}_k^e = \mathbf{D}\mathbf{I}_k \quad (11)$$

$$\mathbf{V}_{k+1} = \mathbf{V}_k - \mathbf{E}_k^e \quad (12)$$

This procedure can be continued until the number of iterations, k , results in a converged solution for \mathbf{I}_k . Convergence is not usually easy to define without knowledge of the accurate answer. Two measures of convergence were used:

The first is the Predicted Relative Error (PRE) as defined by [8]. For the k -th iteration, the PRE is defined as

$$PRE_k = (IRE_k)^2 / IRE_{k-1} \quad (13)$$

where IRE is the Iterative Relative Error (IRE) for iteration k and is given by:

$$IRE_k = \frac{\|\mathbf{I}_k - \mathbf{I}_{k-1}\|}{\|\mathbf{I}_k\|} \quad (14)$$

- the Euclidean vector norm is implied.

The other convergence measure used was the normalised residual error, R^2 which is given by

$$R^2 = \left(\frac{\|\mathbf{E}_k^e\|}{\|\mathbf{E}_0^e\|} \right)^2 \quad (15)$$

as defined in [6]

The computer time requirements for the SIM are given by equation (16).

$$t \propto AN^2 + BN^x + kCN^2 + \text{other smaller terms} \quad (16)$$

As in equation (1), the AN^2 term is associated with calculating the interaction elements for the \mathbf{S} and \mathbf{D} matrices. The BN^x term is related to the time required to factor the sparse matrix, \mathbf{S} , where x ranges from 1–3, depending on matrix sparsity. When large sparse matrices are factored x approaches 1. The kCN^2 term is related to the time required to calculate the E-tangential errors using equation (11) for k iterations. In this case the C coefficient is quite

small since it only involves a single complex multiplication and addition.

The SIM method hence produces results in times proportional to N^2 . The SIM resulted from careful consideration of the physical mechanisms at play in the method of moments. It is interesting to note that the final method bears a similarity to the Banded Jacobi Method [8], where the updating of the RHS of equation (10) is done in exactly the same manner. The major advantage of the SIM is that a sparse, rather than a banded, matrix is employed. As such, the method is not constrained to examples which are easily renumbered. The SIM should also result in either less dense matrices to factorise, or, for similar densities, a lower number of iterations to reach convergence.

V. ILLUSTRATION OF THE OPERATION OF THE SPARSE ITERATIVE METHOD

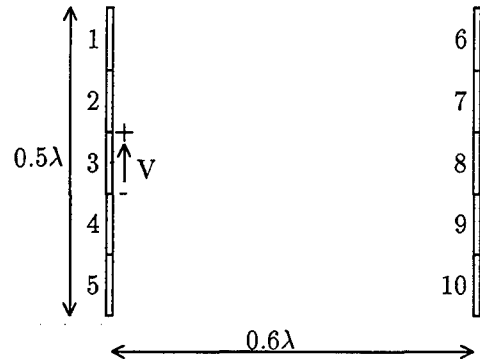


Fig. 2. Two dipole example to illustrate the operation of the Sparse Iterative Method

The SIM is best illustrated using a two dipole example (figure 2). Each dipole consists of five 0.1λ segments and are spaced 0.6λ apart. The zero interaction distance, d_0 , was set to 0.5λ , and the absolute wavelength was 10 m (29.98 MHz). The segment numbering is indicated in figure 2; the first dipole was excited with a 1 V applied E-field source in the center (segment 3). This example is hence simplified, in the sense that all the interactions on each dipole are included in the \mathbf{S} -matrix, but no interactions between the two dipoles are included, since they are spaced at more than d_0 from each other. The format of the $\mathbf{S}\mathbf{I}_0 = \mathbf{V}$ equation is shown in figure 3.

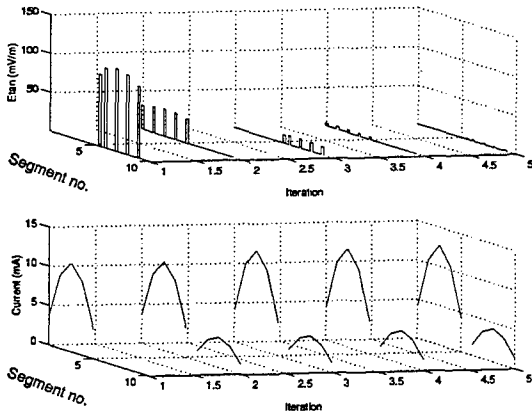
The first iteration will solve for the current on the left dipole (segments 1–5), but since interactions to the right dipole are omitted, no current will be induced on segments 6–10. Figure 4 shows this current in the bottom graph.

Figure 4 also shows the tangential E-field error, versus position on the antennas, for each iteration. After the first iteration, no E-field error is present on the left dipole—all interactions on that dipole were represented in the \mathbf{S} -matrix, and the boundary conditions satisfied by normal method of moments operation. Large E-field errors exist on the parasitic dipole, since no interactions to that antenna were taken into account. These values are then subtracted from the excitation vector for the next estimate for current,

$$\begin{bmatrix}
 Z_{1,1} & Z_{1,2} & Z_{1,3} & Z_{1,4} & Z_{1,5} & 0 & 0 & 0 & 0 & 0 \\
 Z_{2,1} & Z_{2,2} & Z_{2,3} & Z_{2,4} & Z_{2,5} & 0 & 0 & 0 & 0 & 0 \\
 Z_{3,1} & Z_{3,2} & Z_{3,3} & Z_{3,4} & Z_{3,5} & 0 & 0 & 0 & 0 & 0 \\
 Z_{4,1} & Z_{4,2} & Z_{4,3} & Z_{4,4} & Z_{4,5} & 0 & 0 & 0 & 0 & 0 \\
 Z_{5,1} & Z_{5,2} & Z_{5,3} & Z_{5,4} & Z_{5,5} & 0 & 0 & 0 & 0 & 0 \\
 0 & 0 & 0 & 0 & 0 & Z_{6,6} & Z_{6,7} & Z_{6,8} & Z_{6,9} & Z_{6,10} \\
 0 & 0 & 0 & 0 & 0 & Z_{7,6} & Z_{7,7} & Z_{7,8} & Z_{7,9} & Z_{7,10} \\
 0 & 0 & 0 & 0 & 0 & Z_{8,6} & Z_{8,7} & Z_{8,8} & Z_{8,9} & Z_{8,10} \\
 0 & 0 & 0 & 0 & 0 & Z_{9,6} & Z_{9,7} & Z_{9,8} & Z_{9,9} & Z_{9,10} \\
 0 & 0 & 0 & 0 & 0 & Z_{10,6} & Z_{10,7} & Z_{10,8} & Z_{10,9} & Z_{10,10}
 \end{bmatrix}
 \begin{bmatrix}
 I_0(1) \\
 I_0(2) \\
 I_0(3) \\
 I_0(4) \\
 I_0(5) \\
 I_0(6) \\
 I_0(7) \\
 I_0(8) \\
 I_0(9) \\
 I_0(10)
 \end{bmatrix}
 =
 \begin{bmatrix}
 0 \\
 0 \\
 1 \\
 0 \\
 0 \\
 0 \\
 0 \\
 0 \\
 0 \\
 0
 \end{bmatrix}$$

Fig. 3. Format of $\mathbf{SI}_0 = \mathbf{V}$

$$\begin{bmatrix}
 Z_{1,1} & Z_{1,2} & Z_{1,3} & Z_{1,4} & Z_{1,5} & 0 & 0 & 0 & 0 & 0 \\
 Z_{2,1} & Z_{2,2} & Z_{2,3} & Z_{2,4} & Z_{2,5} & 0 & 0 & 0 & 0 & 0 \\
 Z_{3,1} & Z_{3,2} & Z_{3,3} & Z_{3,4} & Z_{3,5} & 0 & 0 & 0 & 0 & 0 \\
 Z_{4,1} & Z_{4,2} & Z_{4,3} & Z_{4,4} & Z_{4,5} & 0 & 0 & 0 & 0 & 0 \\
 Z_{5,1} & Z_{5,2} & Z_{5,3} & Z_{5,4} & Z_{5,5} & 0 & 0 & 0 & 0 & 0 \\
 0 & 0 & 0 & 0 & 0 & Z_{6,6} & Z_{6,7} & Z_{6,8} & Z_{6,9} & Z_{6,10} \\
 0 & 0 & 0 & 0 & 0 & Z_{7,6} & Z_{7,7} & Z_{7,8} & Z_{7,9} & Z_{7,10} \\
 0 & 0 & 0 & 0 & 0 & Z_{8,6} & Z_{8,7} & Z_{8,8} & Z_{8,9} & Z_{8,10} \\
 0 & 0 & 0 & 0 & 0 & Z_{9,6} & Z_{9,7} & Z_{9,8} & Z_{9,9} & Z_{9,10} \\
 0 & 0 & 0 & 0 & 0 & Z_{10,6} & Z_{10,7} & Z_{10,8} & Z_{10,9} & Z_{10,10}
 \end{bmatrix}
 \begin{bmatrix}
 I_1(1) \\
 I_1(2) \\
 I_1(3) \\
 I_1(4) \\
 I_1(5) \\
 I_1(6) \\
 I_1(7) \\
 I_1(8) \\
 I_1(9) \\
 I_1(10)
 \end{bmatrix}
 =
 \begin{bmatrix}
 0 \\
 0 \\
 1 \\
 0 \\
 0 \\
 0 - E_0^1(1) \\
 0 - E_0^1(2) \\
 0 - E_0^1(3) \\
 0 - E_0^1(4) \\
 0 - E_0^1(5)
 \end{bmatrix}$$

Fig. 5. Format of $\mathbf{SI}_0 = \mathbf{V}$, after first iteration.Fig. 4. The current and E_{tan} error on the two dipole array example after every iteration

yielding the matrix equation shown in figure 5

Solving with this modified excitation vector yields the current and E-tangential error results for iteration 2 (see figure 4). A current is now established on the parasitic dipole with zero E-tangential errors. The reason why the tangential E-field errors are zero is because they were counter-acted by error sources that were equal and opposite to the tangential errors that were found in the previous iteration. In this iteration, the effect that the parasitic dipole current has on the source dipole is neglected, hence there will be E-tangential errors on the source dipole. A new excitation vector is formulated to negate these errors.

Figure 4 illustrates how this process results in a current distribution which satisfies the boundary conditions after a few iterations.

VI. RESULTS

This section commences with results for linear dipoles of varying electrical length. The results for this rather trivial problem demonstrate the computational advantages inherent in the SIM, compared to normal LU-decomposition. Thereafter, results for a $2\lambda^2$ square grid (544 segments) and a simple missile structure (410 segments) are presented. These more realistic examples verify the operation of the SIM for complex problems and demonstrate the computational time advantage of the SIM over LU-decomposition. The SIM computational speed advantage will increase with an increase in problem size.

All computer time results are for a Intel 486 processor running at 33 MHz and equipped with 256 kByte cache memory. The two methods both run within the same C++ NEC2 equivalent program with a software switch to select whether LU-decomposition or the SIM was to be used. The redesigned program [1] was compiled using the GCC public domain C++ compiler with optimisation. No manual effort was made to optimise either of the two routines numerically or computationally.

A. Dipoles

The dipole length was continually adjusted to ensure that segment length is maintained at $\lambda/10$. The 500 seg-

TABLE I

TABLE OF RESULTS FOR DIPOLE PROBLEMS (ALL SIMULATIONS WERE DONE WITH INTERACTION DISTANCE OF 2λ)

segments	k	S-den -sity(%)	S-factor (s)	SIM-iterate (s)	SIM Total (s)	LU-factor (s)
100	1	36	1	0.25	1.25	3
200	4	19	1	2	2	35
300	5	13	1	5	6	87
400	6	10	1	10.2	11.2	206
500	7	8	3	17.8	20.8	403
600	8	6.5	4	28.8	32.8	697
700	9	5.6	5	44.1	49.1	1106
800	9	5.0	7	58	65	1650
900	10	4.4	9	82	91	2350
1000	11	4	10	112	122	3224

ment dipole, for instance, will be 50λ in length. The dipoles were all fed on the center (or just off center) segment with an applied field voltage source. Table I gives detailed results for these simulations. The matrix fill times are not included—these are the same for LU-decomposition and the SIM. Figure 6 shows the computer time comparison between LU-decomposition and the SIM. The two components in the SIM solution, sparse matrix factoring and iteration time, are also shown in figure 6.

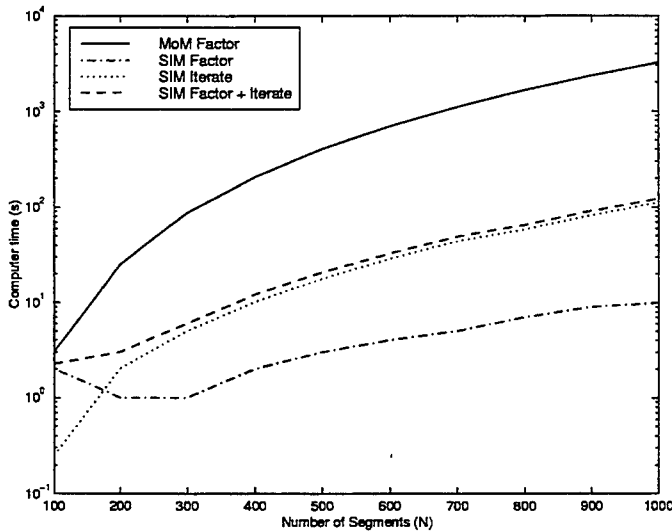


Fig. 6. Computer time comparison between the SIM and LU-decomposition solutions on a Intel 486-33 computer. SIM results are broken down in terms of the component for sparse matrix factoring and for total iteration time.

The values in figure 6 were obtained using a constant $d_0 = 2\lambda$. There is a tradeoff between the time spent on factoring the sparse matrix and the time associated with iteration to obtain the final solution. Figure 7 indicates the computer times required for factoring S , for iteration and the total solve time, all plotted versus d_0 .

Figure 7 indicates that the SIM factor time increases with increasing d_0 , since the matrix density increases. The iteration time, on the other hand, reduces with increasing

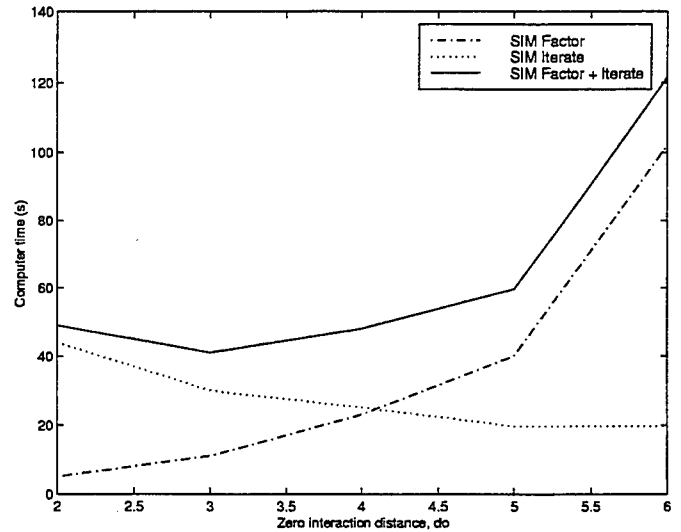


Fig. 7. Computer time versus d_0 for factoring, iteration and the combination in the SIM for a 700 segment dipole

d_0 , since more interactions are taken into account in the S -matrix and requires fewer corrections to achieve convergence. Given that the factor time increases faster than the corresponding reduction in iteration time with increasing d_0 , it is clear that the optimum is close to the minimum d_0 required for stable solutions.

For problems with a large number of unknowns, table I shows a dramatic decrease in solution time using the SIM, as opposed to LU-decomposition. The speed-up factor at 1000 segments is around 30, and this value will continue to increase for larger problems, since LU-decomposition follows a N^3 time dependence whereas the SIM is essentially limited by a N^2 time dependence. The following two sections show results for grid problems.

B. Grid Patch

A wire grid patch, with dimensions and segment numbering similar to an example presented in the GEMACS manual [8], was analysed - the geometry is shown in figure

TABLE II
TABLE OF RESULTS FOR GRID PATCH

$d_o(\lambda)$	S-density	k	PRE (%)	S-factor	SIM-iterate	SIM Total	LU-factor
0.9	39	4	0.29	458	25	483	733
0.65	24.2	3	0.64	285	20	305	733
0.4	10.6	8	0.88	170	42	212	733

8. It was hoped to compare SIM to GEMACS using other geometries, but the program is unfortunately not available due to US military restrictions.

C. Missile

A missile example drawn from [6] was used to illustrate the simulation of a more complex problem. Figures 9

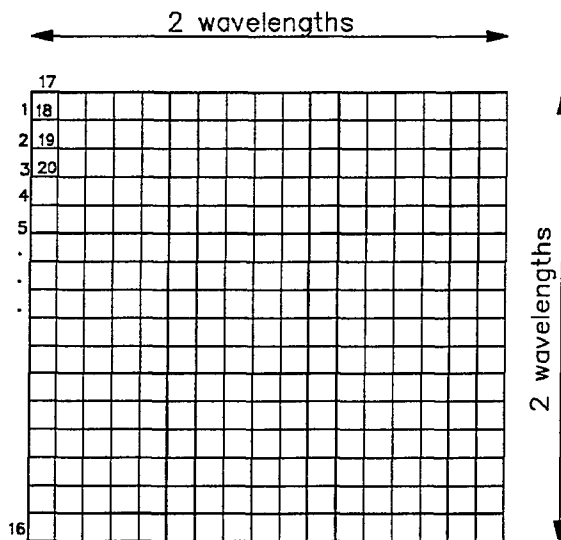


Fig. 8. The 544 segment wire grid patch problem

The grid was excited with a plane wave with a direction of propagation broadside to the patch and a polarisation of 45° relative to the patch edges. Table II shows the comparison between the SIM and LU-decomposition or various problem parameters. In this case, iterations were continued until a $PRE < 1\%$ was achieved. This value is quite accurate for most electromagnetic problems [8], but typically, values close to machine precision were obtained with 3 or 4 more iterations.

The speed increase for this problem, relative to LU-decomposition, for an interaction distance of 0.4λ , is approximately 3-4 times faster. This speed-up is much less than the approximately 20 times increase for a dipole problem with the same number of segments. Wire grid problems have a higher number of segments within the zero-interaction distance; the sparse matrix will therefore be considerably denser for a grid problem when compared to a linear dipole. As the size of the grid problems increase, so the difference between the execution time of the SIM and the LU-decomposition based techniques will become larger. The SIM is hence not inherently less successful with grid problems, but rather just requires electrically larger problems for its full potential to be achieved. Our current implementation on a 486 personal computer does not allow larger problems to be evaluated at this stage.

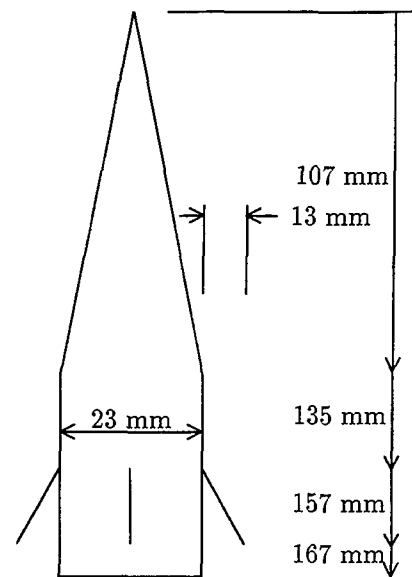


Fig. 9. The geometry of the missile geometry used as test case at a frequency of 3 GHz

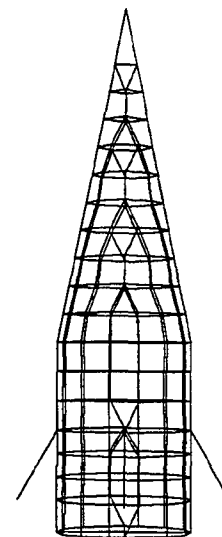


Fig. 10. The gridded 410 segment missile problem

and 10 show the actual and segmented geometry. Segments which were approximately 0.1λ in length were used, and

TABLE III
TABLE OF RESULTS FOR MISSILE EXAMPLE

$d_o(\lambda)$	S-density	k	PRE (%)	S-factor	SIM-iterate	SIM Total	LU-factor
0.35	25.7	6	0.65	42	13	55	194

wire radii were chosen to ensure a wire surface area equal to twice the actual surface area of the missile. Applied E-field voltage sources were placed on the 4 slanting wires and the 410 segment problem was analysed using both LU-decomposition and the SIM.

Table III gives the pertinent values for parameters and times for this problem. The SIM once again produced result about 4 times faster than LU-decomposition. The points raised in the previous section concerning the density of the sparse matrix also apply to this problem.

To illustrate the difference in the results produced by the two techniques, the input impedances from both methods were recorded.

LU-decomposition: 16.2458-j0.06050 Ω
SIM: 16.2432-j0.05737 Ω

VII. CONCLUSION

A sparse iterative method for replacing LU-decomposition in MoM problems has been presented; the method is based on the formulation of a sparse matrix through neglecting those matrix elements which represent coupling smaller than a predefined value.

Correction for neglecting many small couplings is then performed by calculating the tangential E-field at match points, and applying these as equal and opposite excitations to the structure. Performing this procedure iteratively results in a solution which is forced to satisfy the boundary conditions at the match points, up to any specified degree of accuracy - including that of LU-decomposition. Even when enough SIM iterations are performed such that the currents are as accurate as those obtained from LU-decomposition, the SIM still executes faster.

The convergence of the method is somewhat dependant on the particular geometry, but in all cases a 10^{-3} limit on E_{tan} guaranteed convergence. It was shown that in some cases this can be relaxed to 10^6 .

Simple comparative cases were presented to indicate computer time related aspects, and some more complex two- and three-dimensional cases were also analyzed to demonstrate the general applicability of the SIM.

REFERENCES

- [1] D. C. Nitch, *A serial and parallel design of NEC2 to demonstrate the advantages of the object-oriented paradigm in comparison with the procedural paradigm*. PhD thesis, University of the Witwatersrand, PO Box 3, Johannesburg, 2050, South Africa, 1993.
- [2] G. J. Burke and A. J. Poggio, "Numerical electromagnetics code (nec) - method of moments. parts I-III," tech. rep., Naval Ocean Systems Center (NOSC), January 1981.
- [3] T. T. Ferguson, T. H. Lehman, and R. J. Balestri, "Efficient solution of large moments problems: Theory and small problem results," *IEEE Transactions on Antennas & Propagation*, vol. AP-24, pp. 230-235, March 1976.
- [4] P. J. Baldwin, A. Boswell, D. Brewster, and J. Allwright, "Iterative calculation of ship-borne hf antenna performance," *IEE Proceedings-H*, vol. 138, pp. 151-158, April 1991.
- [5] T. K. Sarkar, K. R. Siarkiewicz, and R. F. Stratton, "Survey of numerical methods for solution of large systems of linear equations for electromagnetic field problems," *IEEE Transactions on Antennas & Propagation*, vol. AP-29, pp. 847-856, November 1981.
- [6] D. B. Davidson, *Parallel Algorithms for Electromagnetic Moment Method Formulations*. PhD thesis, University of Stellenbosch, 1991.
- [7] F. X. Canning, "The impedance matrix localization (iml) method for moment-method calculations," *Antennas and Propagation Magazine*, pp. 18-30, October 1990.
- [8] D. L. Kadlec and E. L. Coffey, "General electromagnetic model for the analysis of complex systems (GEMACS). engineering manual. (version 3)," Tech. Rep. RADC-TR-83-217, Vol II (of three), Rome Air Development Center (RBCT), 1983.
- [9] K. S. Kundert and A. Sangiovanni-Vincentelli, *Sparse User's Guide, A Sparse Linear Equation Solver, Version 1.3a*. Department of Electrical Engineering and Computer Sciences; University of California, Berkeley, April 1988.

Radiation From 3D Sources in the Presence of 2D Composite Objects of Arbitrary Cross-Sectional Shape

Ahmed A. Kishk¹, Peter Slättman² and Per-Simon Kildal³

¹ Department of Electrical Engineering, University of Mississippi
University, MS 38677, USA

² Smartwaves International
3385 Scott Boulevard, Santa Clara, CA 95054, USA

³ Electromagnetics Department, Chalmers University of Technology
S-412 96 Göteborg, SWEDEN

Abstract

A method of moment code for computing the radiation from arbitrarily oriented narrow slots or straight dipoles in the vicinity of a two dimensional (2D) multi-region composite cylinder of arbitrary cross-sectional shape and infinite extension in the z -direction is developed. The dipoles and the slots are represented by known equivalent electric and magnetic currents distributions, respectively. The finite extent of the sources are included by Fourier transforming the equivalent electric and magnetic source currents along the infinite cylinder axis. The computed radiation patterns are compared to results computed by other methods and measurements. Radiation patterns are predicted both in the elevation and azimuthal planes.

1 Introduction

Antennas consisting of three-dimensional (3D) radiating elements (sources) and two-dimensional (2D) structures (cylinders of infinite extent) can be analyzed by using a spectrum of two-dimensional solutions (S2DS), as described in [1]. Such antennas are for instance dipoles at long and narrow ground planes, or slots cut in a cylindrical surface. Generally, any antenna consisting of slots or dipoles in or in the vicinity of 2D structures of arbitrary cross-sectional shape and material combination can be analyzed by the S2DS technique. The purpose of the present paper is to present the formulation and some selected results for this general case.

The most significant part of an S2DS analysis is to solve repeatedly the special spectral domain problem obtained by Fourier-transforming the sources in the z -direction of the structure. This spectral domain problem can be interpreted as a harmonic 2D spatial

problem where the sources (and the resulting fields) have harmonic z -variation of the form $e^{-jk_z z}$ where $k_z = 0$ corresponds to the standard 2D problem. This general harmonic 2D problem must be solved for a large number of values of the spectral variable k_z in order to inverse transform to 3D spatial domain. The radiation pattern, however, can normally be found directly from the 2D harmonic solution without inverse transformation.

The harmonic 2D problem is conveniently solved for each k_z by the method of moment (MoM). Several approaches have previously been used; the field within baffles has been expanded in parallel-plate modes and solved by MoM [2], the field within a virtual circular cylinder around a triangular mast has been expanded in cylindrical sector waveguide modes and solved by MoM [3], and the induced currents on a 2D metal structure with arbitrary cross-sectional shape have been solved by MoM [4] with a decoupled electric field integral equation (EFIE) [5].

In two previous papers plane wave scattering from two-dimensional composite objects [6], and scattering from an impedance cylinder with arbitrary cross-section under oblique plane wave incidence were analyzed [7], where the equivalent electric and magnetic currents were solved for by pulse expansion and point-matching. The present paper extends that work by including equivalent electric and magnetic sources in order to model slots and dipoles in a two-dimensional structure with multiple regions of perfect electric conductors (PEC's) and homogeneous and isotropic materials. The pertaining integral equations are presented and a computer code is developed.

The computer code is verified against examples from the literature, measurements, analytic solutions and a code for coaxial multi-layer circular cylinders.

2 Statement of the Problem

We assume that we have a composite 2D object parallel to the z -axis and that 3D sources are present in its neighborhood such as dipoles, or attached to it such as slots or printed microstrip dipoles. It is very time consuming to solve the radiation problem in its present form in the spatial domain. Instead the problem will be solved in the spectral domain as a spectrum of 2D solutions as will be shown in Section 3. We will assume that the equivalent current distributions of the 3D sources are known. As in most practical applications of thin sources such as dipoles or narrow slots, the equivalent electric and magnetic current distributions, \mathbf{J} and \mathbf{M} can be assumed sinusoidal of the form

$$\mathbf{J}(u, v) = \frac{1}{W} \sin\left(\frac{\pi}{L}\left(u - \frac{L}{2}\right)\right) \delta(v) \hat{\mathbf{u}}_s, \quad (1)$$

$$-L/2 \leq u \leq L/2$$

where W is an equivalent width of the source and L is the length. The equivalent width is much smaller than both L and the wavelength. The variables u and v are the local coordinates of the source and $\hat{\mathbf{u}}_s$ is the unit vector along the current source. After transforming the source coordinates to the cylindrical coordinates (ρ, z) and using the Fourier transform defined by

$$\tilde{\mathbf{J}}(\rho, k_z) = \int_{-\infty}^{\infty} \mathbf{J}(\rho, z) e^{jk_z z} dz \quad (2)$$

and the inverse Fourier transform as

$$\mathbf{J}(\rho, z) = \frac{1}{2\pi} \int_{-\infty}^{\infty} \tilde{\mathbf{J}}(\rho, k_z) e^{-jk_z z} dk_z \quad (3)$$

where k_z is the axial wavenumber. The Fourier transform of the current in (2) with respect to z is

$$\tilde{\mathbf{J}}(t, k_z) = \begin{cases} \frac{1}{W \cos \alpha} \sin\left(\frac{\pi}{L}\left(\frac{t}{\cos \alpha} - \frac{L}{2}\right)\right) e^{jk_z t \tan \alpha}, & \text{if } \alpha \neq 90^\circ \\ -\frac{2\pi L}{W(\pi^2 - k_z^2 L^2)} \cos(k_z L/2) \delta(t) & \text{if } \alpha = 90^\circ \end{cases} \quad (4)$$

$$|t| \leq \frac{L}{2} \cos \alpha$$

where α is the angle between the source axis u and the xy -plane, and t is the projection of u in the xy -plane. The Fourier transformed current source written as $\tilde{\mathbf{J}}(t, k_z) e^{-jk_z z}$ for a particular value of k_z located in the presence of the infinitely long 2D structure, can be visualized as an infinite current sheet of width equal to the projected length of the current in the xy -plane and parallel to the z -axis with harmonic variations in the z -direction [1].

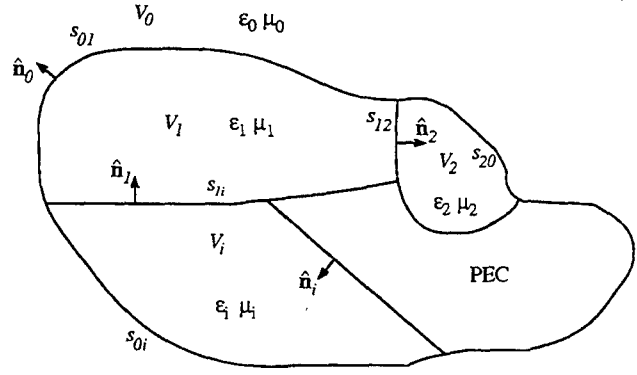


Figure 1: Cross-section of a general cylinder.

Therefore, the total fields produced by these harmonic 2D sources must be harmonic in z as well in order to satisfy the boundary conditions on the objects [1]. For each value of k_z , the problem can be considered a two dimensional problem which should be solved an infinite number of times to cover all of the k_z spectrum, and which will be summed to get the solution in the spatial domain. This process is not necessary if the primary interest is the farfield radiation patterns. For each value of $k_z \in [-k, k]$, the farfield is radiating on a cone around the z -axis with cone angle $\theta = \arccos(k_z/k)$, where k is the wave number in free space. Thus, the farfield can be computed directly from the spectral domain solution, i.e. the 2D solution [1].

In this paper, the time variation $e^{j\omega t}$ is implied and suppressed throughout.

3 Formulation of the 2D Problem

Now that we have shown that the 3D sources can be transformed to harmonic 2D sources in the spectral domain and have transformed the whole problem to a spectrum of 2D problems; let us describe the general arbitrary shape of the 2D object and derive the integral equations. The geometry and notations of such an object are given in Fig. 1. The whole space is divided into $N+1$ homogeneous regions, V_i , which may be either dielectric regions with permittivities ϵ_i and permeabilities μ_i , or closed conductor regions. These regions are numbered $i = 0, 1, 2, \dots, N$, where $i = 0$ corresponds to the exterior region, i.e. free space. Lossy materials are considered by allowing ϵ_i and μ_i , $i = 1, 2, \dots, N$ to be complex. Each region V_i is surrounded by a closed surface S_i and associated with an inward directed normal unit vector $\hat{\mathbf{n}}_i$. The surface interface between regions V_i and V_j is

denoted as $S_{ij}, i \neq j$. Thus, S_i comprises the set of all interface surfaces S_{ij} , where j represents all region numbers adjacent to region V_i . Note that S_{ij} is the same surface as S_{ji} ; however, the normal unit vectors \hat{n}_i and \hat{n}_j are in opposite directions to each other on the two surfaces. The concept of the equivalence principle is used to derive a surface integral equation (SIE) formulation for 2D objects with $N+1$ homogeneous regions. The total fields in each homogeneous region are denoted by \mathbf{E}^i and \mathbf{H}^i , $i = 0, 1, 2, \dots, N$ for the electric and magnetic fields, respectively. Any perfectly conducting region need not be considered as a region because the fields are known to be equal to zero. In the free-space region V_0 , the total fields are denoted by $(\mathbf{E}^0, \mathbf{H}^0)$. In this paper, the excitations are considered to be 3D equivalent electric or magnetic current sources with known amplitudes and current distributions. The electric sources are arbitrarily located inside any number of regions to model thin wire radiators or on the dielectric surface interfaces to model printed sources. Slots are modeled by magnetic sources on the conducting surfaces. From Maxwell's equations and the equivalence principle, one can express the fields in each region in terms of unknown electric and magnetic equivalent surface currents plus the fields due to the harmonic 2D sources present in the region.

According to the surface equivalence principle we can break the original problem into a number of auxiliary problems that are equal to the number of non-perfect conducting regions. To obtain the i th auxiliary problem the boundaries of region V_i are replaced by equivalent surface currents radiating in a homogeneous medium with the constitutive parameters of region V_i using electric currents for the conductor boundaries and equivalent electric and magnetic currents for the dielectric boundaries. The electric and magnetic currents appearing on opposite sides of a dielectric interface in different auxiliary problems are taken equal in magnitude and opposite in direction to ensure the continuity of the tangential components of the fields on these boundaries, as in the original problem. In this procedure the fields produced by the equivalent currents within the region boundaries are the same as those in the original problem, while the zero field is produced outside these boundaries. The electric and magnetic surface currents along the boundaries are

$$\mathbf{J}^i = \hat{n}_i \times \mathbf{H}^i \quad \text{and} \quad \mathbf{M}^i = -\hat{n}_i \times \mathbf{E}^i \quad \text{on } S_i \quad (5)$$

Both \mathbf{J}^i and \mathbf{M}^i have components in both the longi-

tudinal, \hat{z} , and transverse, \hat{t}_i , directions, i.e.

$$\begin{Bmatrix} \mathbf{J}^i \\ \mathbf{M}^i \end{Bmatrix} = \begin{Bmatrix} J_z^i \\ M_z^i \end{Bmatrix} \hat{z} + \begin{Bmatrix} J_t^i \\ M_t^i \end{Bmatrix} \hat{t}_i, \quad \text{on } S_i \quad (6)$$

where the transverse unit tangent is defined by

$$\hat{t}_i = \hat{z} \times \hat{n}_i \quad (7)$$

where \hat{n}_i is the unit normal to S_i . The currents on the surface S_i are the sum of the currents on all the boundaries S_{ij} , where $j \neq i$ and j represents all the region numbers adjacent to the region V_i , i.e.

$$\mathbf{J}^i = \sum_{j \neq i} \mathbf{J}^{ij}, \quad \text{on the boundaries of region } i \quad (8)$$

and similarly for \mathbf{M}^i . On the conductor boundaries the magnetic current is zero. We can now obtain the electric and magnetic fields $\mathbf{E}^i(\rho, k_z)$ and $\mathbf{H}^i(\rho, k_z)$ due to the electric current $\mathbf{J}^i(\rho', k_z)$ by using

$$\mathbf{E}^i(\rho, k_z) = -j\omega \mathbf{A}^i(\rho, k_z) \quad (9)$$

$$-j \frac{1}{\omega \epsilon_i \mu_i} \nabla \nabla \cdot \mathbf{A}^i(\rho, k_z)$$

$$\mathbf{H}^i(\rho, k_z) = \frac{1}{\mu_i} \nabla \times \mathbf{A}^i(\rho, k_z) \quad (10)$$

where the magnetic vector potential \mathbf{A} is

$$\mathbf{A}^i(\rho, k_z) = \frac{\mu_i}{j4} \int_V \mathbf{J}^i(\rho', k_z) H_0^{(2)}(k_\rho \Delta \rho) dl' \quad (11)$$

$$\Delta \rho = |\rho - \rho'|$$

The transverse wave number k_ρ is defined as $k_\rho = \sqrt{k_i^2 - k_z^2}$, $\text{Im}[k_\rho] \leq 0$, where k_i is the wave number in region i . The ∇ operator used here is defined as

$$\nabla = \nabla_t - jk_z \hat{z} \quad \text{and} \quad \nabla_t = \frac{\partial}{\partial x} \hat{x} + \frac{\partial}{\partial y} \hat{y} \quad (12)$$

After some mathematical manipulations the electric and magnetic fields due to the electric currents can be expressed in operator form as shown in [7, Appendix A]. Expressions are given for $E_t^i(J_t^i)$, $E_z^i(J_t^i)$, $E_t^i(J_z^i)$, and $E_z^i(J_z^i)$ which are each of the components of the vector operator $\mathbf{E}_{tan}^i(\mathbf{J}^i)$ for the tangential E -field at a point ρ on S_i , and in the same fashion we get $H_t^i(J_t^i)$, $H_z^i(J_t^i)$, and $H_t^i(J_z^i)$ for the tangential H -field vector operator $\mathbf{H}_{tan}^i(\mathbf{J}^i)$, i.e.

$$\mathbf{E}_{tan}^i(\mathbf{J}^i) = [E_t^i(J_t^i) + E_z^i(J_z^i)] \hat{t}_i \quad (13)$$

$$+ [E_z^i(J_t^i) + E_t^i(J_z^i)] \hat{z}$$

$$\mathbf{H}_{tan}^i(\mathbf{J}^i) = [H_t^i(J_t^i) + H_z^i(J_z^i)] \hat{t}_i + H_z^i(J_t^i) \hat{z} \quad (14)$$

The fields due to the magnetic current $\mathbf{M}^i(\rho', k_z)$ can be obtained by using duality [8, Ch.3, Sec.3-2]. The

boundary conditions must now be enforced on each boundary of the object. The boundary conditions are:

$$\begin{aligned} & -[\mathbf{E}_{tan}^i(\mathbf{J}^i) + \mathbf{E}_{tan}^j(\mathbf{J}^j) + \\ & \quad \mathbf{E}_{tan}^i(\mathbf{M}^i) + \mathbf{E}_{tan}^j(\mathbf{M}^j)] \\ & = [\mathbf{E}_{tan}^i(\mathbf{J}^{i,inc}) - \mathbf{E}_{tan}^j(\mathbf{J}^{j,inc}) + \\ & \quad \mathbf{E}_{tan}^i(\mathbf{M}^{i,inc}) - \mathbf{E}_{tan}^j(\mathbf{M}^{j,inc})] \quad \text{on } S_{ij} \end{aligned} \quad (15)$$

and

$$\begin{aligned} & -\hat{\mathbf{n}}_i \times [\mathbf{H}_{tan}^i(\mathbf{J}^i) + \mathbf{H}_{tan}^j(\mathbf{J}^j) + \\ & \quad \mathbf{H}_{tan}^i(\mathbf{M}^i) + \mathbf{H}_{tan}^j(\mathbf{M}^j)] \\ & = \hat{\mathbf{n}}_i \times [\mathbf{H}_{tan}^i(\mathbf{J}^{i,inc}) - \mathbf{H}_{tan}^j(\mathbf{J}^{j,inc}) + \\ & \quad \mathbf{H}_{tan}^i(\mathbf{M}^{i,inc}) - \mathbf{H}_{tan}^j(\mathbf{M}^{j,inc})] \\ & \quad \text{on } S_{ij}, \text{ just inside } V_j \end{aligned} \quad (16)$$

If the boundary S_{ij} is a conducting boundary and the region V_j is a conducting region equations (15) and (16) become

$$-\mathbf{E}_{tan}^i(\mathbf{J}^i) = [\mathbf{E}_{tan}^i(\mathbf{J}^{i,inc}) + \mathbf{E}_{tan}^i(\mathbf{M}^{i,inc})] \quad (17)$$

on S_{ij}

and

$$\begin{aligned} & -\hat{\mathbf{n}}_i \times \mathbf{H}_{tan}^i(\mathbf{J}^i) = \\ & \quad \hat{\mathbf{n}}_i \times [\mathbf{H}_{tan}^i(\mathbf{J}^{i,inc}) + \mathbf{H}_{tan}^i(\mathbf{M}^{i,inc})] \\ & \quad \text{on } S_{ij}, \text{ just inside } V_j \end{aligned} \quad (18)$$

Substituting operators for the fields into the expressions for the boundary conditions yields the integral equations. Only one of equations (17) and (18) is needed to solve for the unknown currents. If equation (17) is used on the perfect electric conductor (PEC) with (15) and (16) on the dielectric boundary, the formulation is called the E-PMCHW formulation. If equation (18) is used just inside the PEC boundary with (15) and (16) on the dielectric boundary, the formulation is referred to as H-PMCHW. The C-PMCHW formulation can be obtained if equations (17) and (18) are combined and used as one equation together with (15) and (16), [9]. Following the method of moments, the object contour C is divided into N linear segments with length ΔC^l , $l = 1, 2, \dots, N$

as in [9], and each current component is expanded into N pulse basis functions p^l . In equation form, the unknown currents can be expressed as

$$\mathbf{J}^i = \sum_{l=1}^N (I_t^{l,i} \hat{\mathbf{t}}_i + I_z^{l,i} \hat{\mathbf{z}}) p^l \quad \text{on all } S_{ij} \quad (19)$$

and

$$\mathbf{M}^i = \sum_{l=N+1}^{N+N_d} (M_t^{l,i} \hat{\mathbf{t}}_i + M_z^{l,i} \hat{\mathbf{z}}) p^l \quad \text{on dielectric boundaries} \quad (20)$$

where $I_t^{l,i}$, $I_z^{l,i}$, $M_t^{l,i}$, and $M_z^{l,i}$ are the unknown electric and magnetic current coefficients. The pulse functions is $p^l = 1$ on the subdomain ΔC^l and zero elsewhere. N_d is the number of segments on the dielectric boundaries. Substituting (19) and (20) into the operators defined in [7, Appendix A] and then substitute the operators in (12) to (15) and satisfy (12) to (15) at the match point (middle of the segments), the integral equations reduce to a matrix equation of order $2(N + N_d)$, which can be written in the form of a matrix equation (21).

The elements of these submatrices are given in [7, Appendix B] where $Z_{\alpha\beta}^{ij,i}$ and $Y_{\alpha\beta}^{ij,i}$ denote matrix elements obtained from the operators $E_{\alpha}^i(J_{\beta}^j)$ and $H_{\alpha}^i(J_{\beta}^j)$, respectively, on the surface S_{ij} from the region i . Therefore, the first suffix of the subscripts refers to the field component and the second suffix of the subscript refers to the current component. The first pair of the superscripts refers to the surface boundary ij and the second suffix of the superscripts refers to the region number i or j . This matrix is built assuming all the boundaries are dielectric boundaries, but on the conductor parts the columns and the rows that are corresponding to the magnetic currents and the magnetic field, respectively, which are in the third and forth columns and rows, respectively, must be removed and in the first and second columns of (21) the parts that are corresponding to conducting regions i or j must be forced to zero.

The quantities I_z^{ij} , I_t^{ij} , M_z^{ij} , and M_t^{ij} are the unknown expansion coefficients of the electric and magnetic currents, respectively. The right side columns are the excitation vectors, where $V_z^{ij,i}$, $V_t^{ij,i}$, $I_z^{ij,i}$, and $I_t^{ij,i}$ denote the incident electric and magnetic fields,

$$\begin{bmatrix} Z_{zz}^{ij,i} + Z_{zz}^{ij,j} & Z_{zt}^{ij,i} + Z_{zt}^{ij,j} & Y_{zz}^{ij,i} + Y_{zz}^{ij,j} & Y_{zt}^{ij,i} + Y_{zt}^{ij,j} \\ Z_{tz}^{ij,i} + Z_{tz}^{ij,j} & Z_{tt}^{ij,i} + Z_{tt}^{ij,j} & Y_{tz}^{ij,i} + Y_{tz}^{ij,j} & Y_{tt}^{ij,i} + Y_{tt}^{ij,j} \\ Y_{tz}^{ij,i} + Y_{tz}^{ij,j} & Y_{tt}^{ij,i} + Y_{tt}^{ij,j} & -\frac{1}{\eta_i} Z_{tz}^{ij,i} - \frac{1}{\eta_j} Z_{tz}^{ij,j} & -\frac{1}{\eta_i} Z_{tt}^{ij,i} - \frac{1}{\eta_j} Z_{tt}^{ij,j} \\ Y_{zz}^{ij,i} + Y_{zz}^{ij,j} & Y_{zt}^{ij,i} + Y_{zt}^{ij,j} & -\frac{1}{\eta_i} Z_{zz}^{ij,i} - \frac{1}{\eta_j} Z_{zz}^{ij,j} & -\frac{1}{\eta_i} Z_{zt}^{ij,i} - \frac{1}{\eta_j} Z_{zt}^{ij,j} \end{bmatrix} \begin{bmatrix} I_z^{ij} \\ I_t^{ij} \\ M_z^{ij} \\ M_t^{ij} \end{bmatrix} = \begin{bmatrix} V_z^{ij,i,inc} - V_z^{ij,j,inc} \\ V_t^{ij,i,inc} - V_t^{ij,j,inc} \\ I_z^{ij,i,inc} - I_z^{ij,j,inc} \\ I_t^{ij,i,inc} - I_t^{ij,j,inc} \end{bmatrix} \quad (21)$$

respectively, on the surface S_{ij} due to all electric and magnetic sources in region i .

4 Farfields

Once the moment method matrix equation is solved the farfields due to the currents on the outer surface boundary and the current sources in the exterior region can be computed. The field will be along a cone of half angle $\theta = \arccos(k_z/k_0)$ around the structure. The farfield operators for electric and magnetic surface currents in the (ρ, k_z) -domain are given in [1]. Our surface currents are expressed in their local coordinate system $(\hat{n}', \hat{t}', \hat{z})$ and since farfields are most conveniently expressed in a spherical coordinate system, we need to do a coordinate transformation. Using a one-point midpoint rule for the integration, the result is:

$$E_\theta = -j \frac{k}{4\pi} \frac{e^{-jk r}}{r} \quad (22)$$

$$\left[\eta_0 \sum_{l=1}^{N_0} \left(\tilde{J}_t^{l,0} \frac{k_z}{k} (\hat{t}_l' \cdot \hat{\rho}) - \tilde{J}_z^{l,0} \frac{k_\rho}{k} \right) e^{jk_\rho \tilde{\rho}_l' \cdot \hat{\rho}} \Delta C^l + \sum_{l=N_0+1}^{N_0+N_d} \tilde{M}_t^{l,0} (\hat{n}_l' \cdot \hat{\rho}) e^{jk_\rho \tilde{\rho}_l' \cdot \hat{\rho}} \Delta C^l \right]$$

$$E_\phi = -j \frac{k}{4\pi} \frac{e^{-jk r}}{r} \left[\eta_0 \sum_{l=1}^{N_0} \tilde{J}_t^{l,0} (\hat{n}_l' \cdot \hat{\rho}) e^{jk_\rho \tilde{\rho}_l' \cdot \hat{\rho}} \Delta C^l - \sum_{l=N_0+1}^{N_0+N_d} \left(\tilde{M}_t^{l,0} \frac{k_z}{k} (\hat{t}_l' \cdot \hat{\rho}) + \tilde{M}_z^{l,0} \frac{k_\rho}{k} \right) e^{jk_\rho \tilde{\rho}_l' \cdot \hat{\rho}} \Delta C^l \right] \quad (23)$$

5 Results and Discussion

The formulation presented in the previous sections has been implemented in a computer program. We have validated the code against previously published results: radiation from slot antennas [2, 3] and radiation from dipole antennas [4]. The code has also been validated against series solutions for homogeneous dielectric cylinders. In the following subsections we present validation cases involving composite dielectric/PEC structures: we compare our moment method results against a series solution for the scattered field from a dielectric cylinder under oblique plane wave illumination, measured radiation pattern from a slotted waveguide array of tilted slots in a trough partially filled with dielectric material, and calculated patterns for a four-element dipole antenna on a TV-mast covered by a thin radome.

5.1 Verification of Scattering Problems (plane wave excitation)

In order to verify the code, an exact series solution for a dielectric coated circular metal cylinder under oblique plane wave incidence with arbitrary polarization was derived in a similar way as the solution for the dielectric cylinder in [10, Ch.17, pp.144-148], and as extended in [11]. The exact and numerical solutions for the scattering widths are compared with each other in Fig. 3 for a plane wave incident from $\theta_i = 45^\circ$, $\phi_i = 180^\circ$ and $\alpha_i = 45^\circ$, α_i is the angle between the incident electric field and the plane of incidence (the $z-k$ plane). The angles are defined such that the Poynting vector \mathbf{S} of the incident wave makes an angle ϕ_i with the x -axis of the scatterer's coordinate system and an angle θ_i with the scatterer's xy -plane, where positive θ angles make the Poynting vector point below the xy -plane. The electric field makes an angle α with the plane spanned by the scatterer's z -axis and the Poynting vector, such that the projection of the electric field on $\hat{z} \times \mathbf{S}$ is positive. The radius of the PEC cylinder is $ka = 1.885$ and the outer is $ka = 3.0$. We use twenty segments per wavelength on all material interfaces, where the wavelength is the wavelength in the material. The largest difference between the two calculations is seen to be about 0.5dB for σ_ϕ around 120° , Fig. 3.

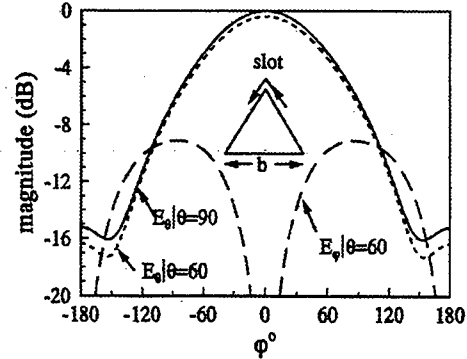


Figure 2: Radiation patterns of an edge slot on a triangular conducting post. $b = 0.4\lambda$. The horizontal pattern ($\theta = 90^\circ$) is indistinguishable from the result in [3]. The dashed curves are predicted farfield components on the cone $\theta = 60^\circ$.

5.2 Slot Excitation (equivalent magnetic current source)

Here we are going to present two different examples. The first example is the radiation from an edge slot on a triangular waveguide for base station antenna

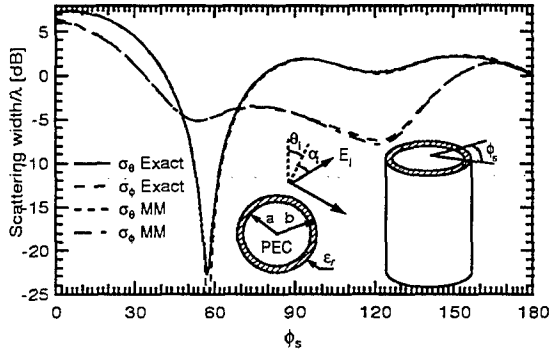


Figure 3: Scattering width from an infinitely long circular cylinder under oblique planewave incidence, $\alpha_i = \pi/4$, $\theta_i = \pi/4$, and $\phi_i = \pi$. The cylinder radii are $ka = 1.885$ and $kb = 3$, The relative dielectric constant is $\epsilon_r = 4$. Exact series solution (solid) and MM solution (dashed) using 20 basis functions per wavelength. The wavelength is taken as the wavelength in the dielectric.

application. The side of the triangle is 0.4λ long. Three slots, one on each edge of the triangle will satisfy the 360° required coverage for this base station. The geometry and the radiation patterns are shown in Fig. 2. Our computed results agrees well with the computed pattern presented in [3] for the horizontal pattern ($\theta = 90^\circ$, i.e. $k_z = 0$). Here, we also present the radiation patterns for the cone cut $\theta = 60^\circ$.

Slot antennas have been extensively used in arrays for radar applications. Normally the slot arrays are exited by a rectangular or parallel plate waveguide. Circular polarization fields of the slot antenna are normally obtained by slot pairs properly oriented to each other with a 90° phase difference between the slot aperture fields. Narrow slot apertures are also used to excite microstrip antennas. For circular polarization two perpendicular slots coupled to two microstrip lines with 90° phase shift are used to produce circular polarization. In Fig. 4 we present a single slot antenna element which radiate circular polarization. The slot is located in the broad wall of a rectangular waveguide and it is loaded by a dielectric slab and surrounded by baffles within a corrugated ground plane. The slot is rotated 18.5° with respect to the centerline of the waveguide to give the proper axial ratio for circular polarization. The thickness of the dielectric loading and the height and width of the trough are designed to provide the required quadratic phase difference between the two field components. The numerical and measured results showed a good promising performance of this element.

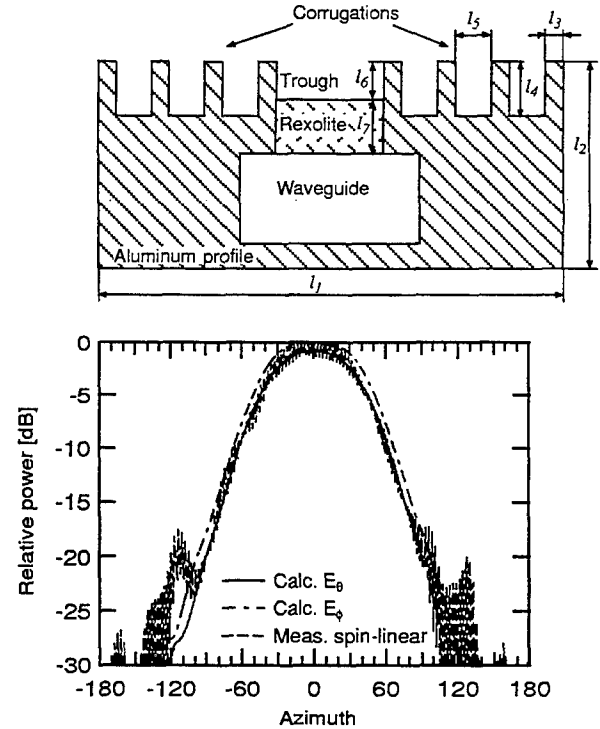


Figure 4: Cross-section of waveguide array designed for circular polarization. $l_1 = 131\text{mm}$, $l_2 = 58$, $l_3 = 5\text{mm}$, $l_4 = 15\text{mm}$, $l_5 = 10\text{mm}$, $l_6 = 10\text{mm}$, $l_7 = 15\text{mm}$, $\epsilon_r = 2.62$. Waveguide WR187, $f = 4.9\text{GHz}$. The slots are rotated 18.5° with respect to the waveguide axis and radiate into a trough partially filled with dielectric material to achieve circular polarization. The antenna is corrugated outside the trough to control the pattern in azimuth. Measured (solid) and calculated (dashed) show reasonable agreement.

5.3 Dipole Excitation (equivalent electric current source)

In this section we verify the dipole part of the computer program to previously published results and an in-house code for concentric multilayer circular cylinders. In Fig. 5 we see a circular PEC rod coated with two concentric layers of dielectric. A Hertz dipole is embedded inside the outer dielectric and tilted 45° to the z -axis. The elevation and azimuth patterns are calculated by both the present MM code and an in-house code for concentric multilayer circular cylinders where the fields are expanded in cylindrical modes [12]. In the MM solution we use 20 basis functions per wavelength and current component on all material interfaces. The wave length is taken as the shortest in the two contiguous media sharing the same boundary, i.e. the three cylindrical interfaces are divided in 64, 76, and 79 segments respectively starting with the PEC cylinder. This gives a total of 876 unknowns.

The difference in azimuth pattern for both polarizations when using only ten segments per wave length was less than 0.19dB.

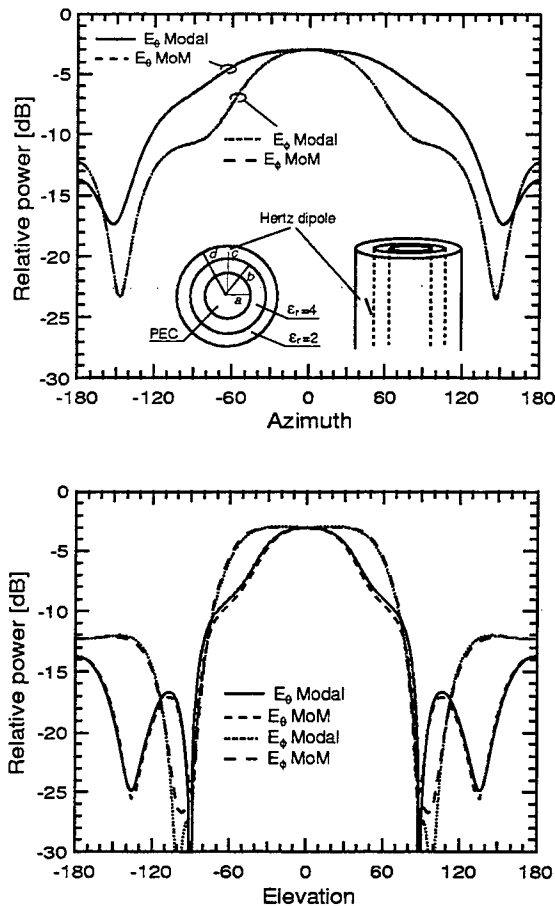


Figure 5: A circular PEC rod coated with two concentric dielectric layers with a 45° tilted electric Hertz dipole in the outer layer. The elevation and azimuth patterns are calculated by the present moment method and compared to a code for coaxial multilayer circular cylinders [12]. $a = 0.25\lambda$, $b = 0.3\lambda$, $c = 0.375\lambda$, $d = 0.45\lambda$

The other verification case consists of four horizontal half wavelength dipoles as shown in the insertion of Fig. refTVmast, one dipole on each side of the square metallic post [13]. We have calculated the horizontal radiation patterns ($k_z = 0$, $\theta = 90^\circ$) with and without a circular cylindrical thin radome enclosing the post and the dipoles, Fig. 6. The horizontal patterns agrees to within the resolutions of the graphs presented in [13]. We have also included our predicted results for an elevation angle of 30° from the horizontal plane ($k_z = 0.5k_0$, $\theta = 60^\circ$).

6 Conclusion

A computer code for analysis of radiation and scattering from 2D structures with 3D sources (and oblique plane wave incidence) has been developed. The 2D structures consists of any number of infinitely long composite cylinders, where each cylinder can have any number of dielectric and PEC regions. The sources we consider here are dipoles and slots that are arbitrarily oriented with respect to the composite cylinder and can be either inside a dielectric region or in the surrounding free space or on the interface between two regions.

The code has been verified in several different ways: analytic series solutions, other numerical results and measured data. In all cases the code performed as expected.

Acknowledgment

We would like to thank Dr. Zvonimir Šipuš for generating the validation curves for the double-layer coaxial cylinder excited by a Hertz dipole.

This work was partially supported by the National Science Foundation under Grant no. ECS-9809862, and by the Swedish National Board for Industrial and Technical Development, NUTEK.

References

- [1] P.-S. Kildal, S. Rengarajan, and A. Moldsvor, "Analysis of nearly cylindrical antennas and scattering problems using a spectrum of two-dimensional solutions," *IEEE Trans. Antennas and Propagat.*, vol. 44, pp. 1183–1192, Aug. 1996.
- [2] K. Forooghi and P.-S. Kildal, "Transverse radiation pattern of a slotted waveguide array radiating between finite height baffles in terms of a spectrum of two-dimensional solutions," *IEE Proceedings-H*, vol. 140, pp. 52–58, 1993.
- [3] J. Hirokawa, J. Wettergren, P.-S. Kildal, M. Ando, and N. Goto, "Calculation of external aperture admittance and radiation pattern of a narrow slot cut across an edge of a sectoral cylinder in terms of a spectrum of two-dimensional solutions," *IEEE Trans. Antennas and Propagat.*, vol. 42, pp. 1243–1249, 1994.
- [4] P. Slättman, J. Wettergren, and P.-S. Kildal, "Three-dimensional radiation from dipoles in the

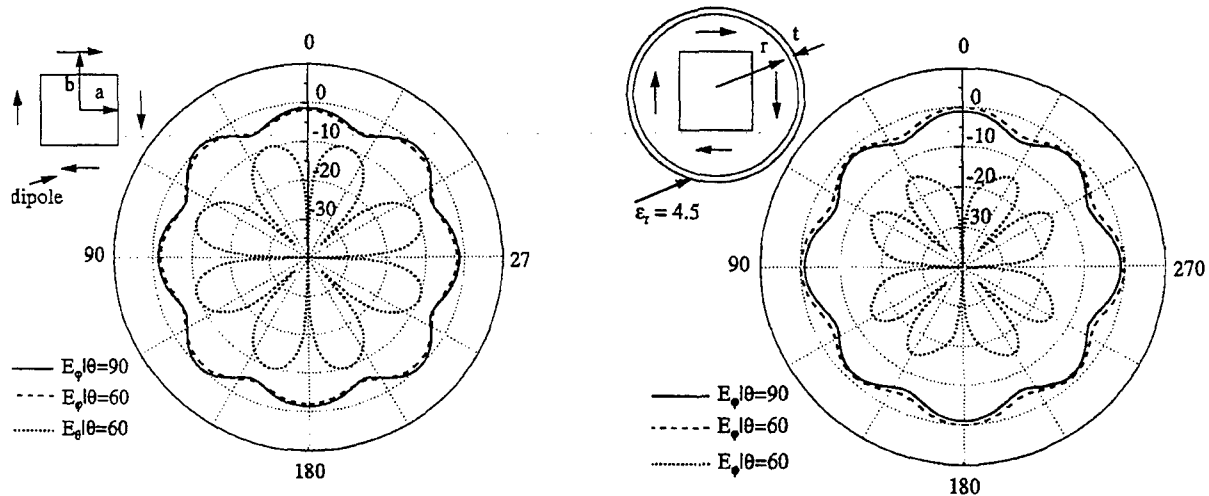


Figure 6: Radiation pattern of four dipoles around a square conducting post with $a = 35\text{cm}$, $b = 47.5\text{cm}$ and $f = 600\text{MHz}$ (left). The same antenna surrounded by a thin dielectric radome with $r = 70\text{cm}$ and $t = 1.5\text{cm}$ (right).

- presence of a conducting strip," in *IEEE AP-S Symp.*, pp. 2266–2269, June 1994.
- [5] J. Wettergren and P. Slättman, "An electric field integral equation for cylindrical structures," *IEE Proceedings-H*, vol. 143, pp. 147–151, April 1996.
 - [6] A. A. Kishk and P. M. Goggans, "Electromagnetic scattering from two-dimensional composite objects," *Applied Computational Electromagnetic Society Journal*, vol. 9, pp. 32–39, 1994.
 - [7] A. A. Kishk and P.-S. Kildal, "Electromagnetic scattering from two dimensional anisotropic impedance objects under oblique plane wave incidence," *ACES Journal*, vol. 10, no. 3, pp. 81–92, 1995.
 - [8] R. F. Harrington, *Time Harmonic Electromagnetic Fields*. McGraw-Hill, 1961.
 - [9] A. A. Kishk and L. Shafai, "Different formulations for numerical solutions of single or multibodies of revolution," *IEEE Trans. Antennas and Propagat.*, vol. AP-34, pp. 666–673, 1986.
 - [10] J. R. Wait, *Electromagnetic Radiation from Cylindrical Structures*. Peter Peregrinus Ltd., reprint ed., 1988.
 - [11] A. A. Kishk and P.-S. Kildal, "Asymptotic boundary conditions for strip loaded scatterers applied to circular dielectric cylinders under oblique incidence," *IEEE Trans. Antennas and Propagat.*, vol. 45, pp. 51–56, Jan. 1997.
 - [12] Z. Šipuš, P.-S. Kildal, R. Leijon, and M. Johansson, "An algorithm for calculating Green's functions for planar, circular cylindrical and spherical multilayer substrates." Accepted for publication in *ACES Journal*.
 - [13] A. Sadigh and E. Arvas, "Deformation of the horizontal radiation pattern of TV transmitting antennas due to a thin dielectric radome," *IEEE Trans. Antennas and Propagat.*, vol. 40, pp. 942–949, 1992.

1999 INSTITUTIONAL MEMBERS

ALLGON
Nasvagen 17
Akersberga, SWEDEN S-18425

ANDREW CORPORATION
10500 W. 153rd Street
Orland Park, IL 60462

ANSOFT EUROPE
Regal House, 9th floor
70 London Rd.
Twickenham, TW1 3QS UK

ATEA
Raleigh Road, Private Bag 12
Ascot Vale, VIC, AUSTRALIA 3032

BOEING NORTH AMERICAN SVCS
1745 Jefferson Davis Hwy
Arlington, VA 22202

BPLUS
100 University Court, PO B 1428
Blackwood, NJ 08012

BRITISH AEROSPACE
FPC 267 PO Box 5
Filton, BRISTOL, BS12 7QW UK

BRITISH BROADCASTING CO R&D
Kingswood Warren
Tadworth, SURREY, KT20 6NP UK

CHALMERS UNIV of TECHNOLOGY
Dept of Microwave Technology
Gothenburg, SWEDEN S 41296

CSIRO, CTR FOR ADV. TECH.
PO Box 883
Kenmore, QLD, 4069 AUSTRALIA

CST GMBH
Lauteschlagerstrasse 38
Darmstadt, GERMANY D-64289

CULHAM LAB
UK Atomic Energy Authority
Abingdon, OXFORD, OX14 3DB UK

DARTMOUTH COLLEGE
Feldberg Library, 6193 Murdough Ctr.
Hanover, NH 03755-3560

DAWSON UK, SUBS. DEPT.
PO Box 225
Folkestone, KENT, CT19 SEN UK

DCN INTERNATIONAL
147-24 176th Blvd..
Jamaica, NY 11434-5410

DEFENSE RESEARCH ESTAB. LIB.
3701 Carling Avenue
Ottawa, ON, K1A 0Z4 CANADA

DERA
Common Road, Funtington
Chichester, PO18 9PD UK

DEUTSCHE TELEKOM AG
PO Box 10-00-03
Darmstadt, D-64 276 GERMANY

DSTO LIBRARY
Box 1500
Salisbury, SA, 5108 AUSTRALIA

E.T.S.E. TELECOMUNICACIONES
Campus Lagoas Marcosende
Vigo, 36200 SPAIN

ELECTRONICS RESEARCH INC.
7777 Gardner Road
Chandler, IN 47610-9219

FANFIELD LTD.
Braxted Park
Witham, ESSEX, CM8 3XB UK

FGAN/FHP/AUS
Neuenahr Strasse 20
Wachtberg, Werth, 53343
GERMANY

FIRSTMARK TECHNOLOGIES
85 St. Charles Quest St.
Longueuil, PQ, J4H 1C5 CANADA

GEC MARCONI RES. CTR. LIB.
W. Hanningfield Road, Gt. Baddow
Chelmsford, ESSEX, CM2 8HN UK

HARRIS CORPORATION
1680 University Avenue
Rochester, NY 14610-9983

HKUST, UNIVERSITY LIBRARY
Clear Water Bay Road
Kowloon, HONG KONG

HUGHES RESEARCH LIBRARY
3011 Malibu Canyon Road
Malibu, CA 90265-4737

HUNTING ENGINEERING LTD.
Reddings Wood, Ampthill
Bedford, MK45 2HD UK

IABG MBH, TRM
Einsteinstrasse 20
Ottobrunn, D 85521 GERMANY

IIT RESEARCH INSTITUTE
185 Admiral Cochrane Drive
Annapolis, MD 21401-7396

INFORMATION CENTRE
A4 Bldg. Ively Road
Farnborough, HAMPS, GU14 0LK
UK

INNOVATIVE DYNAMICS
2560 N. Triphammer Road
Ithaca, NY 14850

IPS RADIO & SPACE SVC/LIBRARY
PO Box 5606
W. Chatswood, 2057 AUSTRALIA

KATHREIN-WERKE KG
Postbox 100 444
Rosenheim, D-83004 GERMANY

LICOSA LIBRARY
Via Duca Di Calabria 1/1
Florence, 50125 ITALY

LINDA HALL LIBRARY
5109 Cherry Street
Kansas City, MO 64110-2498

MISSISSIPPI STATE UNIV LIBRARY
PO Box 9570
Mississippi State, MS 39762

MITRE CORPORATION LIBRARY
202 Burlington Road
Bedford, MA 01730-1407

MOD(PE) DGSS
Abbey Wood #54, PO Box 702
Bristol, BS12 7DU UK

MOTOROLA
2001 N. Division Street
Harvard, IL 60033

MYERS ENGINEERING INTL.
PO Box 15908, 5425 NW 24th St.
Margate, FL 33063

NATIONAL AEROSPACE LAB, NLR
Anthony Fokkerweg 2
Emmeloord, 8300 NETHERLANDS

NATL RADIOLOGICAL PROT. BD.
Chilton
Didcot, OXON, OX11 0RG UK

NAVAL RESEARCH LABORATORY
C. Office
Washington, DC 20375

NGIC
220 7th Street, NE
Charlottesville, VA 22902-5396

NIKSAR
35/45 Gilbey Road
Mt. Waverley, VIC, 3149 AUSTRALIA

NNR AIR CARGO SERVICE
Hook Creed Blvd. & 145th Avenue
Valley Stream, NY 11581

NORTEL TECHNOLOGY
London Road
Harlow, ESSEX, CM17 9NA UK

PENN STATE UNIVERSITY LIB.
Pattee Library
University Park, PA 16802

PHILIPS RESEARCH LAB LIBRARY
Cross Oak Lane, Salfords
Redhill, SURREY, RH1 5HA UK

QUEEN MARY & WESTFIELD COLL
Mile End Road
London E1 4NS UK

RADIO FREQUENCY SYSTEMS
36 Garden Street
Kilsyth, VIC, 3137 AUSTRALIA

RAND AFRIKAANS UNIVERSITY
PO Box 524, Aucklandpark
Johannesburg, 2006 S AFRICA

RAYTHEON E-SYSTEMS
PO Box 6056
Greenville, TX 75403

RENTON TECH LIB/BOEING
PO Box 3707
Seattle, WA 98124-1563

ROCKWELL INTERNATIONAL
350 Collins Road
Cedar Rapids, IA 52498

SONY CORPORATION
174 Fujitsukacho, Hodogaya Ku
Yokohama MZ, 240 JAPAN

SOUTHWEST RESEARCH INST.
6220 Culebra Road
San Antonio, TX 78238

SWETS SUBSCRIPTION SERVICE
440 Creamery Way, Suite A
Exton, PA 19341

TASC - LIBRARY
55 Walkers Brook Drive
Reading, MA 01867-3297

TECHNISCHE UNIV. DELFT
Mekelweg 4, Delft
HOLLAND, 2628 CD
NETHERLANDS

TELEBRAS - CPQD, LIB.
Rod. Campinas
Campinas, SP 13088-061 BRAZIL

TELSTRA RES. LABS LIBRARY
770 Blackburn Road
Clayton, VIC, 3168 AUSTRALIA

THE UNIV OF WARWICK
Gibbet Hill Road
Coventry, CV4 7AL UK

UNIV OF CENTRAL FLORIDA LIB.
PO Box 162440
Orlando, FL 32816-2440

UNIV OF COLORADO LIBRARY
Campus Box 184
Boulder, CO 80309-0184

UNIV OF MISSOURI-ROLLA LIB.
1870 Miner Circle
Rolla, MO 65409-0001

UNIVERSITAT DER BUNDESWEHR
Werner Heisenberg Weg 39
Neubiberg, D-85577 GERMANY

US COAST GUARD ACADEMY
15 Mohegan Avenue
New London, CT 06320-4195

VECTOR FIELDS LTD.
24 Bankside Kidlington
Oxford, OX5 1JE UK

VIT, TECHNICAL RESEARCH. CTR.
PO Box 1202
Espoo, FIN-02044 FINLAND

ACES COPYRIGHT FORM

This form is intended for original, previously unpublished manuscripts submitted to ACES periodicals and conference publications. The signed form, appropriately completed, **MUST ACCOMPANY** any paper in order to be published by ACES. PLEASE READ REVERSE SIDE OF THIS FORM FOR FURTHER DETAILS.

TITLE OF PAPER:

AUTHORS(S)

PUBLICATION TITLE/DATE:

RETURN FORM TO:

Dr. Richard W. Adler
Naval Postgraduate School
Code EC/AB
833 Dyer Road, Room 437
Monterey, CA 93943-5121 USA

PART A - COPYRIGHT TRANSFER FORM

(NOTE: Company or other forms may not be substituted for this form. U.S. Government employees whose work is not subject to copyright may so certify by signing Part B below. Authors whose work is subject to Crown Copyright may sign Part C overleaf).

The undersigned, desiring to publish the above paper in a publication of ACES, hereby transfer their copyrights in the above paper to The Applied Computational Electromagnetics Society (ACES). The undersigned hereby represents and warrants that the paper is original and that he/she is the author of the paper or otherwise has the power and authority to make and execute this assignment.

Returned Rights: In return for these rights, ACES hereby grants to the above authors, and the employers for whom the work was performed, royalty-free permission to:

1. Retain all proprietary rights other than copyright, such as patent rights.
2. Reuse all or portions of the above paper in other works.
3. Reproduce, or have reproduced, the above paper for the author's personal use or for internal company use provided that (a) the source and ACES copyright are indicated, (b) the copies are not used in a way that implies ACES endorsement of a product or service of an employer, and (c) the copies per se are not offered for sale.
4. Make limited distribution of all or portions of the above paper prior to publication.
5. In the case of work performed under U.S. Government contract, ACES grants the U.S. Government royalty-free permission to reproduce all or portions of the above paper, and to authorize others to do so, for U.S. Government purposes only.

ACES Obligations: In exercising its rights under copyright, ACES will make all reasonable efforts to act in the interests of the authors and employers as well as in its own interest. In particular, ACES **REQUIRES** that:

1. The consent of the first-named author be sought as a condition in granting re-publication permission to others.
2. The consent of the undersigned employer be obtained as a condition in granting permission to others to reuse all or portions of the paper for promotion or marketing purposes.

In the event the above paper is not accepted and published by ACES or is withdrawn by the author(s) before acceptance by ACES, this agreement becomes null and void.

AUTHORIZED SIGNATURE

TITLE (IF NOT AUTHOR)

EMPLOYER FOR WHOM WORK WAS PERFORMED

DATE FORM SIGNED

PART B - U.S. GOVERNMENT EMPLOYEE CERTIFICATION

(NOTE: If your work was performed under Government contract but you are not a Government employee, sign transfer form above and see item 5 under Returned Rights).

This certifies that all authors of the above paper are employees of the U.S. Government and performed this work as part of their employment and that the paper is therefore not subject to U.S. copyright protection.

AUTHORIZED SIGNATURE

TITLE (IF NOT AUTHOR)

NAME OF GOVERNMENT ORGANIZATION

DATE FORM SIGNED

PART C - CROWN COPYRIGHT

(Note: ACES recognizes and will honor Crown Copyright as it does U.S. Copyright. It is understood that, in asserting Crown Copyright, ACES in no way diminishes its rights as publisher. Sign only if ALL authors are subject to Crown Copyright.

This certifies that all authors of the above Paper are subject to Crown Copyright. (Appropriate documentation and instructions regarding form of Crown Copyright notice may be attached).

AUTHORIZED SIGNATURE

TITLE OF SIGNEE

NAME OF GOVERNMENT BRANCH

DATE FORM SIGNED

Information to Authors

ACES POLICY

ACES distributes its technical publications throughout the world, and it may be necessary to translate and abstract its publications, and articles contained therein, for inclusion in various compendiums and similar publications, etc. When an article is submitted for publication by ACES, acceptance of the article implies that ACES has the rights to do all of the things it normally does with such an article.

In connection with its publishing activities, it is the policy of ACES to own the copyrights in its technical publications, and to the contributions contained therein, in order to protect the interests of ACES, its authors and their employers, and at the same time to facilitate the appropriate re-use of this material by others.

The new United States copyright law requires that the transfer of copyrights in each contribution from the author to ACES be confirmed in writing. It is therefore necessary that you execute either Part A-Copyright Transfer Form or Part B-U.S. Government Employee Certification or Part C-Crown Copyright on this sheet and return it to the Managing Editor (or person who supplied this sheet) as promptly as possible.

CLEARANCE OF PAPERS

ACES must of necessity assume that materials presented at its meetings or submitted to its publications is properly available for general dissemination to the audiences these activities are organized to serve. It is the responsibility of the authors, not ACES, to determine whether disclosure of their material requires the prior consent of other parties and if so, to obtain it. Furthermore, ACES must assume that, if an author uses within his/her article previously published and/or copyrighted material that permission has been obtained for such use and that any required credit lines, copyright notices, etc. are duly noted.

AUTHOR/COMPANY RIGHTS

If you are employed and you prepared your paper as a part of your job, the rights to your paper initially rest with your employer. In that case, when you sign the copyright form, we assume you are authorized to do so by your employer and that your employer has consented to all of the terms and conditions of this form. If not, it should be signed by someone so authorized.

NOTE RE RETURNED RIGHTS: Just as ACES now requires a signed copyright transfer form in order to do "business as usual", it is the intent of this form to return rights to the author and employer so that they too may do "business as usual". If further clarification is required, please contact: The Managing Editor, R.W. Adler, Naval Postgraduate School, Code EC/AB, Monterey, CA, 93943, USA (408)656-2352.

Please note that, although authors are permitted to re-use all or portions of their ACES copyrighted material in other works, this does not include granting third party requests for reprinting, republishing, or other types of re-use.

JOINT AUTHORSHIP


For jointly authored papers, only one signature is required, but we assume all authors have been advised and have consented to the terms of this form.

U.S. GOVERNMENT EMPLOYEES


Authors who are U.S. Government employees are not required to sign the Copyright Transfer Form (Part A), but any co-authors outside the Government are.

Part B of the form is to be used instead of Part A only if all authors are U.S. Government employees and prepared the paper as part of their job.


NOTE RE GOVERNMENT CONTRACT WORK: Authors whose work was performed under a U.S. Government contract but who are not Government employees are required to sign Part A-Copyright Transfer Form. However, item 5 of the form returns reproduction rights to the U.S. Government when required, even though ACES copyright policy is in effect with respect to the reuse of material by the general public.



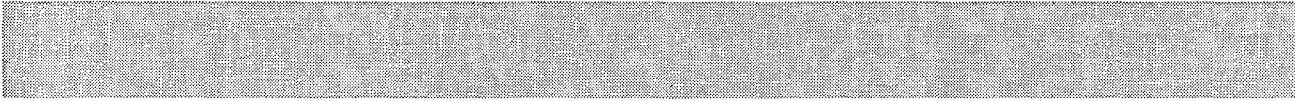
Applied Computational Electromagnetics Society



Newsletter
Volume 14 - No. 1
ISSN 1056-9170



March 1999



APPLIED COMPUTATIONAL ELECTROMAGNETICS SOCIETY (ACES)

NEWSLETTER

Vol. 14 No. 1

March 1999

TABLE OF CONTENTS

OFFICERS' REPORTS

President's Report - W. Perry Wheless, Jr	4
Annual Report - Eric Michielssen	5
Financial Report - Andreas Cangellaris	6

OFFICERS' REPORTS

ACES Committees	7
-----------------------	---

TECHNICAL FEATURE ARTICLE

"Predicting Detailed Electromagnetic Interference Rejection Requirements Using a Knowledge-Based Simulation Approach" Andrew Drozd, Jason Miller, Clifford Carroll, Jr., Andrew Blackburn Timothy Blocher, Anthony Pesta, Donald Weiner and Pramod Varshney	8
--	---

PERSPECTIVES IN CEM

"Application of the FDTD Method to Geophysical Simulations" Cynthia Furse, David Johnston, and Alan C. Tripp	12
---	----

TUTORIAL

"An Overview of the Partial Element Equivalent Circuit (PEEC) Electromagnetic Modeling Approach", Albert E. Ruehli and Andreas C. Cangellaris	17
--	----

BOOK REVIEW

"EMI/EMC Computational Modeling Handbook" Bruce Archambeault, Omar M. Ramahi, and Colin Brench	28
---	----

ANNOUNCEMENTS

2000 ACES Annual Review of Progress Call for Papers	31
1999 Annual Review of Progress Preliminary Agenda	33
1999 Registration/Short Course/Hands-on-Workshops Application	41
1999 Short Course/Hands-on-Workshops Information	43
1999 Motel Information	47
1999 NPS Campus map	48
Application for ACES Membership, Newsletter and Journal Subscription	49
ICCEA 99 International Conference on Computational Electromagnetics and its Applications	50
Advertising Rates	51
Deadlines for the Submission of Articles	51

ACES NEWSLETTER STAFF

EDITOR-IN-CHIEF, NEWSLETTER

Ray Perez
Martin Marietta Astronautics
MS 58700, PO Box 179
Denver, CO 80201, U.S.A.
Phone: 303-977-5845
Fax: 303-971-4306
email:ray.j.perez@ast.lmco.com

EDITOR-IN-CHIEF, PUBLICATIONS

W. Perry Wheless, Jr.
University of Alabama
P.O. Box 11134
Tuscaloosa, AL 35486-3008, U.S.A.
Phone: (205) 348-1757
Fax: (205) 348-6959
email:wwheless@ualvm.ua.edu

ASSOCIATE EDITOR-IN-CHIEF

David B. Davidson
Dept. Electrical and Electronic Engineering
University of Stellenbosch
Stellenbosch 7600, SOUTH AFRICA
Phone: +27 2231 77 4458 Work
Phone: +27 2231 77 6577 Home
Fax: +27 21 808 4981
email:davidson@firga.sun.ac.za

MANAGING EDITOR

Richard W. Adler
Pat Adler, Production Assistant
Naval Postgraduate School/ECE Department
Code ECAB, 833 Dyer Road, Room 437
Monterey, CA 93943-5121, U.S.A.
Phone: 408-646-1111
Fax: 408-649-0300
email:rwa@ibm.net

EDITORS

CEM NEWS FROM EUROPE

Pat R. Foster
Microwaves and Antenna Systems
16 Peachfield Road
Great Malvern, Worc, UK WR14 4AP
Phone: +44 1684 5744057
Fax: +44 1684 573509
email:prf@maasas1.demon.co.uk

TECHNICAL FEATURE ARTICLE

Andy Drozd
ANDRO Consulting Services
PO Box 543
Rome, NY 13442-0543 U.S.A.
Phone: (315) 337-4396
Fax: (314) 337-4396
email:androl@aol.com

THE PRACTICAL CEMIST

W. Perry Wheless, Jr.
University of Alabama
P.O. Box 11134
Tuscaloosa, AL 35486-3008, U.S.A.
Phone: (205) 348-1757
Fax: (205) 348-6959
email:wwheless@ualvm.ua.edu

MODELER'S NOTES

Gerald Burke
Lawrence Livermore National Labs.
Box 5504/L-156
Livermore, CA 94550, U.S.A.
Phone: (510) 422-8414
Fax: (510) 422-3013
email:burke2@llnl.gov

PERSPECTIVES IN CEM

Melinda Piket-May
University of Colorado at Boulder
ECE Dept., CB425
Boulder, CO 80309-0425
Phone: (303) 492-7448
Fax: (303) 492-2758
email:mjp@boulder.colorado.edu

TUTORIAL

Bruce Archambeault
IBM
Dept. 18DA, Bldg. 306
PO Box 12195, 3039 Cornwallis Road
Research Triangle Park, NC 27709
Phone: (919) 486-0120
Fax: (919) 543-8324
email:barch@us.ibm.com

ACES JOURNAL

EDITOR-IN-CHIEF

Ahmed Kishk
EE Department
University of Mississippi
University, MS 38677 U.S.A.
Phone: (601) 232-5385
Fax: (601) 232-7231
email:ahmed@olemiss.edu

ASSOCIATE EDITOR-IN-CHIEF

Allen Glisson
EE Department
University of Mississippi
University, MS 38677 U.S.A.
Phone: (601) 232-5353
Phone: (601) 232-7231
email:aglisson@olemiss.edu

NEWSLETTER ARTICLES AND VOLUNTEERS WELCOME

The ACES Newsletter is always looking for articles, letters, and short communications of interest to ACES members. All individuals are encouraged to write, suggest, or solicit articles either on a one-time or continuing basis. Please contact a Newsletter Editor.

AUTHORSHIP AND BERNE COPYRIGHT CONVENTION

The opinions, statements and facts contained in this Newsletter are solely the opinions of the authors and/or sources identified with each article. Articles with no author can be attributed to the editors or to the committee head in the case of committee reports. The United States recently became part of the Berne Copyright Convention. Under the Berne Convention, the copyright for an article in this newsletter is legally held by the author(s) of the article since no explicit copyright notice appears in the newsletter.

BOARD OF DIRECTORS

EXECUTIVE COMMITTEE

W. Perry Wheless, Jr. President
John Brauer, Vice President
Eric Michielssen, Secretary

Andreas Cangellaris, Treasurer
Richard W. Adler, Exec. Officer

DIRECTORS-AT-LARGE

John Brauer	1999	Andreas Cangellaris	2000	Bruce Archambeault	2001
Harold Sabbagh	1999	Ray Perez	2000	Anthony Brown	2001
Perry Wheless, Jr.	1999	Norio Takahashi	2000	Eric Michielssen	2001

NEEDED: ADVERTISING AND REPORTS EDITOR

If interested, please contact :

Ray Perez
Martin Marietta Astronautics
MS 58700, PO Box 179
Denver, CO 80201
Phone: 303-977-5845
Fax: 303-971-4306
email: ray.j.perez@ast.lmco.com

Visit us on line at: www.emclab.umn.edu/aces and
<http://aces.ee.olemiss.edu>

OFFICER'S REPORTS

PRESIDENT'S MESSAGE

Perry Wheless (wwheless@coe.eng.ua.edu)

We are already moving forward into the fog of a new year, which I trust is treating you well so far! In this report, I would like to draw your attention to several notable aspects of the upcoming ACES annual conference, ACES Publications, and service opportunities.

First, I hope you are already planning to attend our Annual Review of Progress in Applied Computational Electromagnetics symposium scheduled for the (now well-established) third week in March. Randy Haupt has been hard at work as this year's conference Chair, and everyone is looking forward to an outstanding conference event this year. Many of you will remember the early ACES conferences, which had a prominent feature of "one" parallel session of technical papers! This was a highly unusual feature in the conferences world, but one which our early members valued highly. For one thing, it afforded a common gathering place and more opportunity for both meeting and interacting with colleagues. Over the years, the ACES conference expanded to as many as four parallel sessions as our conference became an increasingly influential outlet for CEM professionals. Last year, we decided to further resist the "octopus mode" of sessions. This year, the number of papers accepted has been further reduced, toward the objective of just needing two parallel sessions. This is somewhat a calculated risk for ACES, as most conferences report the ratio of registrants to paper presenters progressively trending toward 1:1 over recent years. The argument is that acceptance of a paper is necessary for many people to obtain employer financial support for the trip. We are hoping to achieve more like a 2.5:1 ratio for ACES by making the conference well worthwhile for attendance without necessarily being involved in the technical paper program. One means for accomplishing this is a solid slate of short courses and hands-on workshops. Another is vendor exhibits, and so forth. A "comments and evaluation" form will be available to you in Monterey, and I hope you will give us some active and constructive feedback on the current structure and direction of the conference.

Regarding ACES Publications, there are three timely matters you should note. First, the ACES Journal is now in an excellent position to review manuscripts promptly, and offers you an outstanding vehicle for publishing in a recognized peer-review journal capable of quick turnaround time on your submission(s). Second, the Journal is now actively seeking Guest Editors for future Special Issue projects. Several topics have been suggested, but we are short on Guest Editors to manage these projects! This notice is directed principally to those prepared to volunteer their expertise and services, in addition to worthy S.I. topics; please directly contact either Ahmed Kishk (ahmed@olemiss.edu) or Allen Glisson (aglisson@olemiss.edu). Finally, Ray Perez (ray.j.perez@ast.lmco.com) would be pleased to work with you if you are interested in joining the ACES Newsletter team. There are many and varied ways in which you might contribute to the Newsletter; if you have aspirations along the Newsletter vein, please contact Ray at your earliest convenience.

Hear and take heed of the siren's song: "Come to Monterey in March, come to Monterey in March, come to Monterey in March." I look forward to seeing you there!

THE APPLIED COMPUTATIONAL ELECTROMAGNETICS SOCIETY, INC.

NOTICE OF THE ANNUAL BUSINESS MEETING

Notice is hereby given that the annual business meeting of the Applied Computational Electromagnetics Society, Inc. will be held on Tuesday 16 March 1999, in 102 Glasgow Hall at the Naval Postgraduate School, Monterey, CA. The meeting is scheduled to begin at 7:45 AM PST for purposes of:

1. Receiving the Financial Statement and Treasurer's Report for the time period ending 31 December 1998.
2. Announcement of the Ballot Election of the Board of Directors.

By order of the Board of Directors
Eric Michielssen, Secretary

ANNUAL REPORT 1998

As required in the Bylaws of the Applied Computational Electromagnetics Society, Inc. a California Nonprofit Public Benefit Corporation, this report is provided to the members. Additional information will be presented at the Annual Meeting and that same information will be included in the July Newsletter for the benefit of members who could not attend the Annual Meeting.

MEMBERSHIP REPORT

As of 31 December 1998, the paid-up membership totaled 430, with approximately 39 % of those from non-U.S. countries. There were 24 full time students, Unemployed and Retired; 77 industrial (organizational); and 329 individual members. The total membership has decreased by 17 % since 1 Jan 1998, with non-U.S. membership increasing by 1%.

Eric Michielssen, Secretary

MEMBERSHIP RATES EFFECTIVE 1 APRIL 1998

FULL-TIME STUDENT/RETIRED/UNEMPLOYED RATE IS \$25 FOR ALL COUNTRIES

AREA	INDIVIDUAL SURFACE	INDIVIDUAL AIRMAIL	ORGANIZATIONAL (AIRMAIL ONLY)
US & CANADA	\$65	\$65	\$115
MEXICO, CENTRAL & SOUTH AMERICA	\$68	\$70	\$115
EUROPE FORMER USSR TURKEY SCANDINAVIA	\$68	\$78	\$115
ASIA, AFRICA MID EAST, PAC RIM	\$68	\$85	\$115

1998 FINANCIAL REPORT

ASSETS

BANK ACCOUNTS	1 JAN 1998	31 DEC 1998
MAIN CHECKING	13,534	2,705
EDITOR CHECKING	3,035	2,089
SECRETARY CHECKING	2,108	2,440
SAVINGS	107	108
HIGH RATE SAVINGS	43,346	43,911
CREDIT CARD	13,202	27,003
CD #1	11,028	11,627
CD #2	11,008	11,591
CD #3	11,033	11,627
CD #4	<u>11,025</u>	<u>11,625</u>
TOTAL ASSETS	\$119,426	\$124,726

LIABILITIES: \$0

NET WORTH 31 December 1998: \$124,726

INCOME

Conference	54,570
Short Courses	14,930
Publications	2,003
Membership	26,201
Interest & misc.	<u>5,952</u>
TOTAL	\$103,656

EXPENSE

Conference	47,180
Short Courses	9,172
Publications	16,620
Services (Legal, Taxes)	4,309
Postage	13,724
Supplies & misc.	<u>5,128</u>

TOTAL **\$96,133**

NET INCREASE FOR 1998 **\$7,523**

In 1997 the net increase was \$6,527. In 1998 we enjoyed a net gain of \$7,523. Our current net worth, \$124,726 is double that of five years ago.

Andreas Cangellaris
Treasurer

PERMANENT STANDING COMMITTEES OF ACES INC.

COMMITTEE	CHAIRMAN	ADDRESS
NOMINATIONS	Adalbert Konrad	University of Toronto ECE Department 10 King's College Road Toronto, ON, CANADA M5S 1A4
ELECTIONS	Pingjuan Werner	Penn State University 321 Oakley Drive State College, PA 16803
FINANCE	Andrew Peterson	Georgia Institute of Technology School of ECE Atlanta, GA 30332-0250
WAYS & MEANS	Pat Foster	Microwaves & Antenna System 16 Peachfield Road Great Malvern, Worc, UK WR14 4AP
PUBLICATIONS	Perry Wheless	University of Alabama P.O. Box 11134 Tuscaloosa, AL 35486-3008
CONFERENCE	Robert Bevensee	BOMA Enterprises 128 Irongate Court Alamo, CA 94507-0812
AWARDS	John Brauer	Ansoft Corporation 9000 N. Deerbrook Tr., Suite 100 Milwaukee, WI 53223-2465

MEMBERSHIP ACTIVITY COMMITTEES OF ACES INC.

COMMITTEE	CHAIRMAN	ADDRESS
SOFTWARE EXCHANGE	Atef Elsherbeni	Univ of Mississippi Anderson Hall, Box #13 University, MS 38677
SOFTWARE PERFORMANCE STANDARDS	Donald Pflug	Rome Laboratory/ERST 525 Brooks Rd. Griffiss AFB, NY 13441-4505
HISTORICAL	Robert Bevensee	BOMA Enterprises PO Box 812 Alamo, CA 94507-0812

TECHNICAL FEATURE ARTICLE

PREDICTING DETAILED ELECTROMAGNETIC INTERFERENCE REJECTION REQUIREMENTS USING A KNOWLEDGE-BASED SIMULATION APPROACH

Andrew L. Drozd, Jason R. Miller, Clifford E. Carroll, Jr. & Andrew C. Blackburn¹

Timothy W. Blocher² & Anthony J. Pesta³

Donald D. Weiner⁴ & Pramod K. Varshney⁵

ABSTRACT

This paper overviews the application of a knowledge-based modeling and simulation approach for generating and analyzing a valid computational electromagnetics (CEM) structure model in order to determine detailed interference rejection requirements. An expert system is first used to generate the computational model of a complex structure comprised of co-located RF transceivers. Electromagnetic interference (EMI) analyses are performed on the model in both the frequency and time domains. This involves the use of the short-term Fourier transform (SFT) where the time scale is initially subdivided into contiguous segments in an effort to study time-dependent interactions among receptors and interferers, deduce the probability of spectral overlap, and estimate the degree of interference. Coupling is computed in the frequency domain using exact GTD theory where losses are calculated for high probability EMI cases. Frequency-domain results are ranked to determine the severity of EMI and to specify initial corrective measures with the aid of the expert system. The knowledge-base is then used to "monitor" the signal environment in the time domain and select the detailed interference rejection scheme(s) appropriate for mitigating the effects of interferers present at a victim receptor.

INTRODUCTION

Knowledge based methods using expert system technologies are extremely useful in cases where rapid decisions must be made for problems that involve a large number of parameters, variables, or "states". This can be true of the large, complex system-level EMC problem and the potentially-many electromagnetic interactions that may exist. Knowledge-based methods are one means of efficiently addressing EMC problems consisting of many co-located RF systems, and various operational and time-variant states.

The application of knowledge-based expert systems for CEM modeling and EMC analysis achieves several important objectives. First, it allows an inexperienced analyst to rapidly generate valid electromagnetic

structure models from computer-aided design data, existing CEM model information, and by employing a few basic modeling assumptions. Next, it can be used to efficiently set up the initial RF problem, and to apply the relevant system performance and EMC measures. Finally, it is useful in managing the overall computational tasks i.e., calculating EMI figures of merit and deducing corresponding cancellation requirements to mitigate predicted interferences for a large collection of RF components, operational states, and so on. The expert system approach helps to ensure that modeling, simulation, and analyses tasks are highly-productive from start to finish, and increases confidence in computed results. The heart of the approach is a robust knowledge/rule base coupled with a computational engine that provides the necessary figures of merit and recommendations to the analyst.

The knowledge base contains rules about fundamental EMC problem-solving methods and procedures. This is applied in a manner which mimics the way an experienced EMC engineer thinks and reasons out solutions. In this way, a range of alternative interference mitigation techniques is specified. The expert system can be made to "suggest" from a ranked set of solutions depending on the type of problem, the severity of predictions, and the practicality of the mitigation solution. Mitigation techniques include: relocating or swapping antenna positions, adjusting frequencies and/or power level to maintain RF links, specifying shielding requirements, modifying transmitter modulation characteristics, time blanking, adding filters, etc.

The computational engine utilizes a proven set of physics formalisms, EMC engineering models, and numerical solution methods. The engine is currently based on an enhanced version of the Intrasystem Electromagnetic Compatibility Analysis Program (IEMCAP) which has been modified to include new spectrum and coupling models, and a more accurate geodesic structure loss model based on geometrical theory of diffraction (GTD) theory.

¹ANDRO Consulting Services, P. O. Box 543, Rome, NY 13442-0543, androl@aol.com, jrmiller@borg.com, & ccarroll@borg.com

²Air Force Research Laboratory/IFSB, 525 Brooks Road, Rome, NY 13441-4505, blochert@rl.af.mil

³Air Force Research Laboratory/IFSA, 525 Brooks Road, Rome, NY 13441-4505, pestaa@rl.af.mil

⁴Syracuse University, Link Hall, Syracuse, NY 13244, (315) 443-4406, DDWEINER@neptune.syr.edu

⁵Syracuse University, Link Hall, Syracuse, NY 13244, (315) 443-4013, varshney@cat.syr.edu

The research and development to establish this capability is sponsored by the Air Force Research Laboratory Information Directorate, Rome Research Site under Contract F30602-98-C-0034. The present work adapts prior research and development findings on the application of expert systems for CEM modeling and collaborative engineering applications [1-3]. In the present research, a prototype pre/post-processor capability called the Electromagnetic Environment Effects EXpert Processor w/Embedded Reasoning Tasker (E³EXPERT) is being developed which applies an expert system to EMC problem-solving [4].

The discussions which follow do not dwell on the rigorous aspects of CEM physics formalisms, in particular, GTD theory. Rather, the "synergy" and potential benefits to be realized by combining CEM modeling techniques, EMC analysis tools, expert systems, CEM data dictionaries, data reduction methods, and visualization utilities as part of an automated EMC assessment capability are highlighted. The rigorous application of sophisticated CEM tools and techniques to EMC engineering is a topic of growing interest within both the ACES and electromagnetics community at large.

BASIS FOR A PROCEDURAL M&S SYSTEM

Figure 1 illustrates an automated, knowledge-based modeling and simulation (M&S) system that embodies a set of procedures in an EMC assessment plan. Large, complex intrasystem problems are of concern in this context. The key aspects of the procedural, knowledge-based approach are summarized below. Before describing these in more detail, consider the "core" technologies that the capability is based upon.

First, the knowledge-based simulator takes advantage of a "common database" scheme. In this way shared, reusable data resources are made available to the system's resident applications which require them. This is provided by a commercial metafile data structure (i.e., a data dictionary). This structure also supplies data to a 3-D renderer/graphical editor.

Next, "generic" objects (a basis for model abstraction) are defined. Expert system rules operate on these generic objects. The CEM modeling and EMC simulation rules are the means for incorporating knowledge about the problem domain, object behavior and inter-relationships. General and special relationships are established among classes of objects and their instances, including the specification of both inherited physical or electromagnetic properties.

The frequency- and time-domain computational engines calculate values for these objects. These values

pertain to figures of merit which are reasoned or inferred upon by the rules.

Primary communications between the user and the rest of the system are facilitated via the standard Microsoft Foundation Class (MFC) library utilities. The system is being designed to operate on a Windows 95/NT personal computer.

System Features

Commercial software packages, government codes, and customized utilities are used in the system design to provide the following:

- Windows-based control panel to process user commands and data inputs, and provide feedback.
- Man-machine interface for 3-D model rendering and graphical editing tasks.
- 3-D metafile to support object-oriented definitions and corresponding data structures.
- CAD data and CEM model input translators.
- Modeling pallet to allow canonically-based CEM models to be synthesized.
- Modeling/analysis fidelity "switch" which automatically launches the respective computational models, expert system rules to rank and classify predictions, and knowledge-based interference mitigation solutions (frequency or time domain).
- 2-D plots, analysis and transaction summaries.
- Help system and an "Assistant" capability.
- Environment to develop, test, debug, and add or modify rules, and optimize rule-firing performance.
- A self-contained capability that mimics the steps in the assessment methodology, and orchestrates the overall analysis procedures (Figure 1).

Automated EMC Assessments

Modeling & Simulation Steps. Referring to Figure 1, a CAD or existing CEM model is read in and converted to the internal 3-D metafile format. CAD and rendering formats currently supported include IGES, DXF, facet, and VRML. Alternatively, a canonical structure model (including antennas, external sources, and so on) can be synthesized using a modeling pallet. Additionally, the user must enter required system and RF or baseband port data, performance parameters, and EMC measures in order for the M&S task to proceed. After all initial data have been processed, the user invokes the expert system module to check for modeling errors or inconsistencies. Once this is completed, the user commits the model to the computational engine to perform the first stage of the analysis which involves a coarse, worst-case cull in the frequency domain.

The IEMCAP program with certain enhancements (e.g., the addition of non-average power coupling and receptor models) is being used as the basis for this engine. Data reduction techniques, based on the short-term Fourier transform (SFT) and other estimation methods, are then applied to the results to focus the analyst's attention only on the problem areas. The expert system may then be invoked again to post-process the initial results. This involves ranking predicted interferences and providing an initial range of solutions to mitigate problems. A prioritized set of solutions can be provided based on the coupling mechanism, the severity of predictions, and the practicality of the mitigation solution. These include: relocating or swapping antenna positions, adjusting frequencies and/or power level to maintain or break RF links, specifying shielding requirements, modifying transmitter modulation characteristics, time blanking, adding filters, etc. Results are output in tabular form and as 2-D plots.

If unresolved interferences persist, then the user may perform a second-stage, higher-fidelity analysis in the frequency domain where the coupling losses are computed in a similar manner as above, but this time using exact GTD ray tracing methods for only a few selected ports and "critical" frequencies. Generally, GTD is a reasonably accurate solution for frequencies which are significantly above the HF regime. This also is dependent on the physical nature of the scatterer. The advantage of using a rigorous GTD approach is that surface material properties can be taken into account and more accurate geodesic losses that include shadowing can be computed for a complex scatterer. At this point, the expert system can once again be called to assess the results, rank results, and offer solutions to mitigate predicted interferences, or to break or preserve coupling links.

If interferences cannot be totally resolved or if "grey areas" still exist in the frequency domain, the user may wish to perform a time-domain analysis where attention is now placed on the waveform propagation and losses in the transmitter and receiver front end paths. From the results of this analysis stage, detailed interference cancellation requirements are deduced. The time-domain stage applies a knowledge-based signal processing philosophy to EMC for the interference rejection problem. The environment provides an integrated environmental monitoring tool with application to EMC problem solving, and includes a capability for graphically designing communications and signal processing systems.

Knowledge-Based Interference Rejection. When complete information regarding the interference is unavailable, the expert system approach provides the receptor with a knowledge-based capability to monitor

the environment and determine the interference process along with all necessary parameters. Based on a set of expert system rules, the knowledge-base selects one or more suitable interference rejection schemes in both the frequency and time domains. The selection is made from a library of preselected techniques. In effect, the system reacts to the interference environment so as to maximize performance.

CEM/EMC Rules and Reasoning. In summary, the following reasoning-type tasks are performed by rules:

- Verify the validity and completeness of CAD and CEM model definitions (geometric reasoning).
- Assure a valid CEM model for changing frequencies and electromagnetic conditions (CEM reasoning).
- Suggest smart defaults and perform range checking (data inferencing).
- Deduce the degree of spectral overlaps to simplify the initial system culling analysis (EMC reasoning).
- Rank the severity of predicted EMI and identify an ordered set of solutions in the frequency domain.
- Apply expert system rules in the time-domain to generate detailed interference rejection requirements.

If a modeling violation is detected or an interference problem persists, the expert system provides useful information to the analyst in order to work out a solution. The expert system functions as an intelligent agent by stepping the analyst through the necessary decision points in the overall assessment methodology. The rules assure that this methodology is followed, but the user controls the final decisions.

Interference Rejection Rules. The expert system sifts through the various emitters, signals types (e.g., CW and wideband noise, transceiver nonlinearities, harmonics and spurious signals, and RF receiver front-end noise impulse responses), and receptors to arrive at the optimum interference rejection scheme(s). In the time domain stage, the received signal is analyzed by an "environmental monitor". The rules determine the nature of the interfering signals and cause associated signal parameters to be computed. A comprehensive signal analysis tool can be employed for this purpose; however, simple knowledge extraction algorithms, such as the SFT, have been successfully demonstrated.

Once the nature of the interference is known, relatively simple interference algorithms, such as notch filters, can be used. This is in lieu of complex adaptive filters which require extensive computation and are used in unknown interference environments. The interference is cancelled by nulling out those signal frequency components that do not belong to the allowable set of frequencies of the desired transmitted signal. Although this simple scheme is effective in removing the

interference at the receiver input, the input signal to the IF amplifier may still contain spurious components due to the third harmonic of the local oscillator or from other spurious harmonics. Rules are used to detect this and apply the necessary rejection.

SUMMARY

This article discussed the recent evolution of the expert system concept for interference rejection analysis as part of an EMC assessment plan for large, complex structures. Computer simulations continue to be conducted to study the effectiveness of the approach for several interference scenarios. Simulations are directed at assessing the EMC for a collection of external RF transceivers mounted on a complex airborne structure. These include fixed- and variably-tuned RF ports, spread spectrum frequency-hopped and direct sequence transceivers, and incident CW and wideband fields. The expert system approach provides a safety net around the inexperienced engineer and turns a non-expert into an expert over time. The analyst becomes more efficient in performing complex EMC analyses with increased confidence. Updates regarding the status of the capability described in this article will given in future publications.

REFERENCES

- [1] A. L. Drozd, T. W. Blocher, et. al., "Illustrating the Application of Expert Systems to Computational Electromagnetics Modeling and Simulation", Conference Proceedings of the 14th Annual Review of Progress in Applied Computational Electromagnetics, Monterey, CA, 16-20 March 1998, pp. 36-41.
- [2] A. L. Drozd, J. R. Miller, et. al., "A Knowledge-Based Modeling & Simulation Framework For CEM Applications and An Environment To Support Collaborative Engineering", Conference Proceedings of the 30th Annual Society for Computer Simulation (SCS) Summer Computer Simulation Conference, Reno, NV, 19-22 July 1998, pp. 471-476.
- [3] A. L. Drozd & T. W. Blocher, "Heuristics-Based Computational Electromagnetics: A State-of-the-Art Technique for End-to-End EMC Modeling and Analysis of Large, Complex Structures", Conference Proceedings of the 1998 IEEE International Symposium on Electromagnetic Compatibility, Denver, CO, 23-28 August 1998, pp. 1144-1149.
- [4] A. L. Drozd, A. J. Pesta, et. al. 1998. "Application and Demonstration of a Knowledge-Based Approach to Interference Rejection for EMC", Conference Proceedings of the 1998 IEEE International Symposium on Electromagnetic Compatibility, Denver, CO, 23-28 August 1998, pp. 537-542.

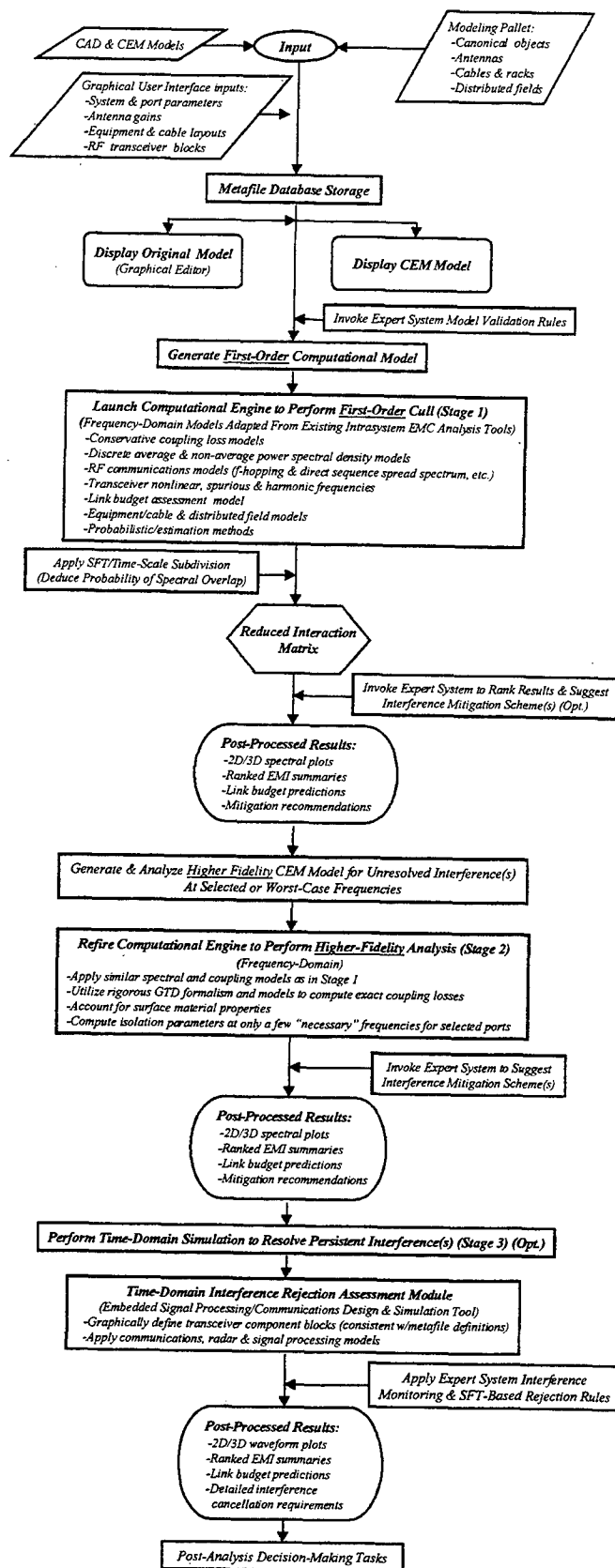


Figure 1. EMC Assessment Methodology

Application of the FDTD Method to Geophysical Simulations

By Cynthia M. Furse¹, David M. Johnson², Alan C. Tripp³

¹ Department of Electrical and Computer Engineering, UMC 4120, Utah State University, Logan, UT 84322.

² Rio Tinto Exploration, 2 Kilroe Street, Milton, QLD, 4064, Australia.

³ Department of Geology and Geophysics, 717 WBB, University of Utah, Salt Lake City, Utah 84112.

Abstract

The finite-difference time-domain (FDTD) method has been used extensively for geophysical simulations. Most of these simulations have applied quasi-static approximations to simplify the computations. This paper describes recent work applying the FDTD method without quasi-static approximations to a geophysical prospecting application. The PML boundary conditions were adapted for use in a resistive host (as opposed to air surrounding the model). The objective of this work was to determine the optimal experimental setup for a cross-borehole test to determine the size and extent of nickel sulfide deposits imbedded in resistive rock.

Introduction – FDTD Modeling in Geophysics

The FDTD method has been used for geophysical simulations for over ten years. One of the earliest applications is the work of Wang and Hohmann (1993) that models a three-dimensional layered earth in the quasi-static diffusion regime. The Du Fort-Frankel method is used for time-stepping the simplified Maxwell's equations in time on a standard FDTD staggered grid. An homogenous Dirichlet boundary condition is imposed on the fields at the subsurface boundaries of the computational mesh to truncate the computational domain. The mesh boundaries are placed far from the region of interest to ensure that the outward propagating electromagnetic fields attenuate sufficiently before reaching these perfectly reflecting surfaces. Expansion of the mesh beyond the region of interest is performed using an expanding grid, which is feasible in the diffusion regime because field variations become smoother with increasing distance. This code is limited to use at low frequencies. This code was also applied to an inversion problem using two-dimensional sources by Wang, et al. (1994), and a full-wave version of this code was applied to ground penetrating radar (GPR) (using Mur boundary conditions) by Wang and Tripp (1994a, 1994b, 1996), and the low-frequency version of the code was applied to a more computationally intensive problem using integral equations by Wang, et al. (1995). FDTD has also been applied to GPR by Livelybrooks and Fullagar (1994), Roberts and Daniels (1994), Xu and McMechan (1997), Cai et al. (1998), and Bergmann (1998).

The perfectly matched layer (PML) boundary condition was adapted for use in geophysical simulations by Chew and Weedon (1994) and applied again by Chen, et al. (1996,1997). The formulation was adapted and

simplified from the original Berenger (1994) form, and applied to geophysical simulations.

Application to Nickel Sulfide Deposits

An important class of mineral deposits have highly conductive ore zones imbedded in a resistive host. Examples include the Kambalda Basin, Sudbury Basin, and Voisey Bay nickel deposits, where the ore bodies are dominated by highly conductive pyrrhotite, giving ore conductivities of about 10^5 to 10^6 S/m. It has been suggested that cross-bore electromagnetic surveys be used to delineate these deposits. For this application multiple wells are bored in or near the deposit, and a source or line of sources is lowered down into a well. The source is commonly a loop or multiple loops excited by frequencies in the MHz range. Receiving loops are placed down other boreholes, and the transient signals they receive are analyzed to help determine the size, location, and extent of the ore mass. This can be a confusing problem, due to lack of understanding of how fields propagate in such a configuration. Recent progress in application of the FDTD method to this problem has begun to enhance this understanding, and is being used to optimize the experimental setup.

Previous modeling efforts for this application have used quasi-static or geometric optics analyses which are inappropriate for the frequency and electrical parameters encountered in these applications. To overcome these problems, Johnson (1997) and Johnson, et al. (1998 and 1999) used a traditional FDTD full-wave modeling approach without the quasi-static assumption and adapted the PML boundary conditions for use in a highly resistive rock host. A code that was used for biomedical simulations (Furse and Gandhi (1998)) was modified for this purpose. This work is described in more detail below.

Application to Geophysical Simulations

The standard finite-difference time-domain (FDTD) simulation method is thoroughly described in existing literature such as Taflov and Umashankar (1989). There are several different forms the basic algorithm can take. The one applied in Johnson (1997) and Johnson et al. (1999) uses the "total field" formulation, where all field components on the grid represent the total field component at that location (in contrast to scattered and incident fields). The geophysical prospecting tools used in cross-bore hole studies are represented by a combination of infinitesimal electric and/or magnetic dipoles, using the form of Maxwell's equations containing electric and magnetic source current terms:

$$\nabla \times \bar{E} = -\mu \frac{\partial \bar{H}}{\partial t} - \bar{M}^i$$

and

$$\nabla \times \bar{H} = \epsilon \frac{\partial \bar{E}}{\partial t} + \sigma \bar{E} + \bar{J}^i$$

where μ is the time-invariant magnetic permeability, ϵ is the time-invariant electric permittivity, σ is the time-invariant electric conductivity, and \bar{J}^i is an impressed electric current and \bar{M}^i is an impressed magnetic current. The impressed currents are zero everywhere except where the transmitter is located. Field values on the boundaries of the model region are calculated using the perfectly matched layer (PML) absorbing boundary condition as described below. Frequency-domain data from this model is derived from the time-domain data using a discrete Fourier transform (DFT).

The cross borehole experiment is shown in Figure 1. The transmitter for this experiment is a small loop (or linear array of loops), so the infinitesimal magnetic dipole is used to model the source. This is done adapting the method of Buechler et al. (1995) who simulated a Hertzian electric dipole source to the magnetic dipole source used in the crossbore study. The impressed magnetic displacement current is given by $-\Delta t \partial \bar{H}^i / \partial t$, which is evaluated using central differences in time.

PML Boundary Conditions for a Resistive Host

The frequencies used in cross borehole experiments range from a few kHz, which is in the quasi-static regime, to several MHz, which is still a low frequency application but is no longer quasi-static. The long wavelength and small attenuation of the field before it reaches the boundary presents very significant problems for the traditional absorbing boundary conditions used in

FDTD simulations. Since the PML boundary condition has been shown to be useable for low frequency applications (De Moerloose and Stuchly (1996)) when the external medium is air, it is an excellent candidate for the case at hand.

The original Berenger (1994) formulation of the PML was adapted by Chen et al. (1996) for use in non-air media. Rather than thinking of the PML as a set of layers with varying active properties, the Chen formulation is based upon a transformation of Cartesian coordinates

$$\{x, y, z\} \rightarrow \{xs_x, ys_y, zs_z\},$$

where the "coordinate stretching factors" s_x , s_y and s_z are complex numbers. The stretching factors are defined as

$$s(\mathbf{p}) = \frac{\beta(\mathbf{p})}{\omega_c \epsilon} + i \frac{\alpha(\mathbf{p})}{\omega \epsilon}$$

where ω_c is the source center frequency, and the vector \mathbf{p} can be the x , y , or z directions independently. The functions $\alpha(\mathbf{p})$ and $\beta(\mathbf{p})$ control the rate of attenuation within the PML in the direction \mathbf{p} .

The PML has been optimized in a number of ways. Lazzi and Gandhi (1997) optimized an air-host PML, and Johnson (1997) optimized the resistive host PML. Both of these methods utilize a linearized Newton method to optimize the PML coefficients. The Newton method uses least-squares minimization to determine the PML parameters that minimize the reflection at the PML boundary. This error is given by $\|d^p - d^o\|^2$ where d^p is the set of predicted field values (with no reflection from the PML boundary, found in practice using a larger FDTD grid), and d^o is the observed field values (with reflection from the PML boundary). Minimizing this function could give a PML with a large amount of variation between the stretching factors of one layer and the next. Although theoretically a good boundary, the lack of smoothness in this PML could give rise to spurious numerical errors, so it is also desirable to have a smooth transition within the PML boundary. Thus, a smoothing or regularizing function is applied, defined by $\kappa \|m - m_{apr}\|^2$, where m is the optimized model (the PML stretching factors), and m_{apr} is the a priori model (the initial guess for the PML, which should be smooth). When the regularization parameter, κ , is large, the PML region has a very smooth shape. When κ is small, there can be more deviation between the initial guess and the optimized model. Optimizing both the error and smoothness is accomplished by minimizing the regularized misfit functional

$$\Phi(m^p) = \|d^p - d^o\|^2 + \kappa \|m - m_{apr}\|^2 = A(m^p) - d^o\|^2 + k \|m - m_{apr}\|^2$$

This problem can be solved using parameter estimation techniques such as described in Portniaguine and Zhdanov (1995). In practice, this particular inverse problem is highly nonlinear, and therefore difficult to solve using this technique. Attempts to solve the inverse problem for independently varying coordinate stretching factors failed

because the forward modeling algorithm is unstable with respect to perturbations in these parameters, resulting in the Frechet derivatives being undefined. This problem was overcome by parameterizing the real and imaginary parts of the PML coordinate stretching factor profiles in terms of simple sine functions, which are desirably smooth. The PML equations should match Maxwell's equations at the interior boundary of the layer, and the stretching factors may increase towards the outer boundary. In practice, it may be necessary to introduce a DC offset (b) in the stretching factor profiles, to account for discretization of the PML. Thus the stretching factors can be written as

$$\alpha(n) = \frac{a_\alpha}{2} \left[1 + \sin \left(\frac{n\pi}{NPML} - \frac{\pi}{2} \right) \right] + b_\alpha$$

and

$$\beta(n) = \omega_c \epsilon + \frac{a_\beta}{2} \left[1 + \sin \left(\frac{n\pi}{NPML} - \frac{\pi}{2} \right) \right] + b_\beta$$

where NPML is the PML thickness expressed as a number of cells, and n is the number of cells between the given node and the interior boundary of the PML. The variables a_α , b_α , a_β and b_β are now the parameters to be optimized.

Cross-Borehole Analysis; Conductive Ore Body in a Resistive Host

The FDTD code was used to calculate the electromagnetic fields at 2 MHz for a perfectly conducting plate model. A horizontal magnetic dipole transmitter is placed at the position $(x, z) = (30\text{m}, 90\text{m})$, the conductivity of the host rock is 0.001 S/m, and the electric permittivity is $6.4\epsilon_0$. The fields are recorded in a vertical plane perpendicular to the plates and containing the transmitter. The plates extend 50 m to either side of the survey plane, and the upper edge of the plate lies at $z = 90\text{ m}$.

A conventional RIM survey collects only amplitude data, which are usually expressed in decibels relative to some arbitrarily chosen signal level. Therefore, it is useful to examine the model amplitude responses and sensitivities. For the purposes of visualization, the amplitude data are transformed as:

$$F' = 20 \log \frac{F}{F_{\max}},$$

where F is the field amplitude and F_{\max} is the maximum value. The values of the transformed field F' are clipped at a lower bound of $F' = -500\text{ dB}$. This transformation, although somewhat arbitrary, facilitates image display.

The transformed amplitudes of the horizontal magnetic field components H_x display a distinct shadow zone behind the plate, particularly in the lower portion of the target. Electromagnetic waves are diffracted by the

edges of the plate, creating a zone of partial shadow behind the upper portion of the plate. This method has been used to analyze the most accurate regions, frequencies and orientations for transmitter location in Johnson (1997).

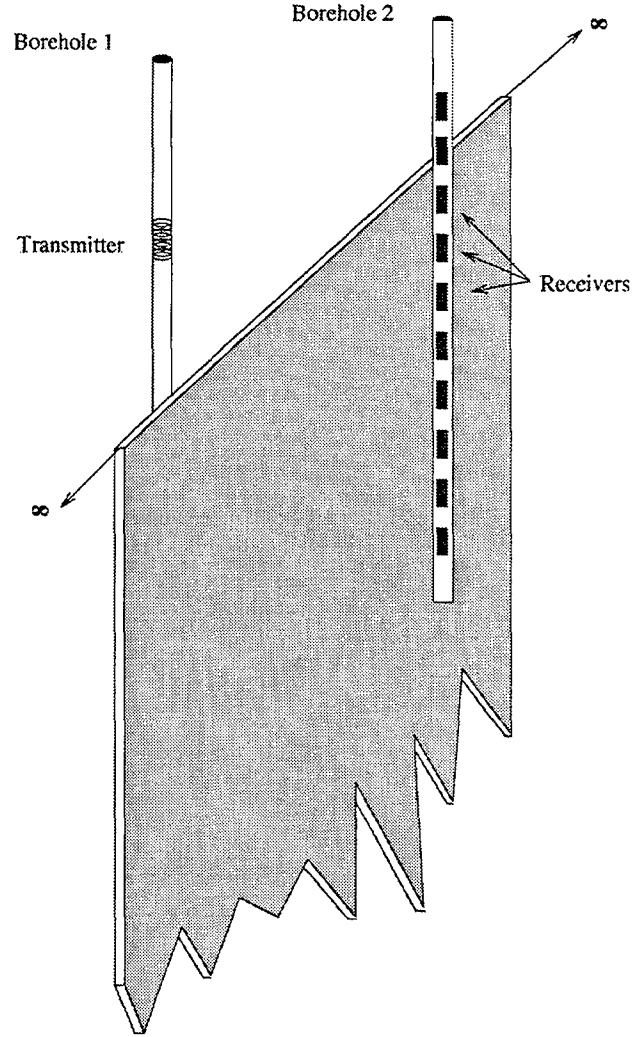


Figure 1: Cross borehole prospecting for high conductivity ore in a high resistivity rock. From Johnson et al. (1999)

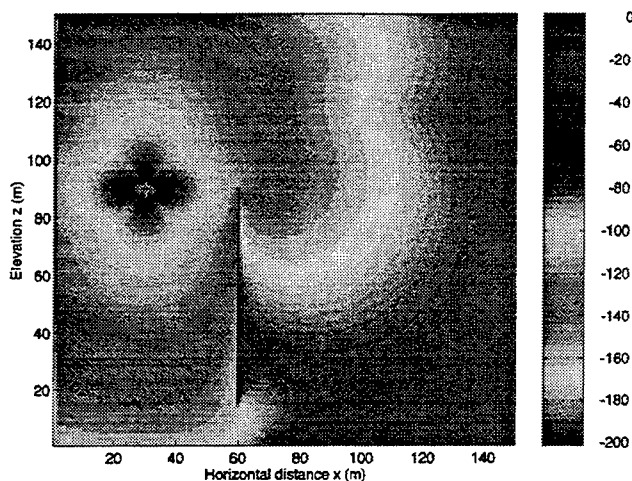


Figure 2: Horizontal magnetic field amplitudes for the conducting plate model at 2 MHz expressed in decibels relative to the maximum value. The minimum has been clipped at -500 dB. From Johnson, et al. (1999).

Conclusions

FDTD provides a valuable tool for analyzing geophysical prospecting data, experiments, tools, and methods. It has been used extensively for both forward and inverse scattering problems. The perfectly matched layer boundary conditions have been adapted for use in non-air media, and have been found to be stable and effective.

References

- Berenger, J.-P., 1994, A perfectly matched layer for the absorption of electromagnetic waves: *J. Comput. Phys.*, **114**, 185-200
- Bergmann, T., Robertson, J.O.A., and Holliger, K., 1998, Finite-difference modeling of electromagnetic wave propagation in dispersive and attenuating media, *Geophysics*, **61**(4), pp. 1007-1021
- Buechler, D.N., Roper, D.H., Durney, C.H., and Christensen, D.A., 1995, Modeling sources in the FDTD formulation and their use in quantifying source and boundary condition errors: *IEEE Trans. Microwave Theory Tech.*, **43**, 810-814.
- Chew, W.C., and Weedon, W.H., 1994, A 3-D perfectly matched medium for modified Maxwell's equations with stretched coordinates: *Micro. Opt. Tech. Lett.*, **7**, 599-604.
- Chen, Y.H., Chew, W.C., and Oristaglio, M.L., 1996, Transient modeling of subsurface EM problems using PML ABC: 66th Ann. Internat. Mtg., Soc. Expl. Geophys., Expanded Abstracts, 245-248.
- Chen, Y.H., Chew, W.C., and Oristaglio, M.L., 1997, Application of perfectly matched layers to the transient modeling of subsurface EM problems, *Geophysics*, **62**(6), pp.1730-1736
- De Moerloose J., Stuchly M.A., 1996, Reflection analysis of PML-ABCs for low frequency applications: *IEEE Microwave and Guided Wave Letters*, **6**, pp.344-346
- Furse, C. and Gandhi, O.P. Calculation of Electric Fields and Currents Induced in a Millimeter-Resolution Human Model at 60 Hz Using the FDTD Method: *Bioelectromagnetics*, **19**(5), 1998, pp.293-299
- Johnson, D.M., 1997, Finite difference time domain modeling of cross-hole electromagnetic survey data: M.Sc. Thesis, University of Utah.
- Johnson, D.M., Furse, C., and Tripp, A.C., 1999, FDTD modeling of the electromagnetic response of a conductive ore deposit in a lossy dielectric: submitted to *Geophysics*
- Lazzi, G., and Gandhi, O.P., 1997, On the optimal design of the PML absorbing boundary condition for the FDTD code: *IEEE Trans. Antennas Propagation*, **45**(5), pp.914-916
- Livelybrooks, D. and Fullagar, P.K., 1994, FDTD2D+: A finite-difference time-domain radar modeling program for two dimensional structures, 5th International Conference on Ground Penetrating Radar Expanded Abstracts, University of Waterloo, p. 87-100
- Portniaguine, O., and Zhdanov, M.S., 1995, Parameter estimation method in the solution of 3D geoelectromagnetic inverse problems: 1st Internat. Symp. on Three-Dimensional Electromagnetics, Proceedings, 397-403.
- Roberts, R.L. and Daniels, J.J., 1994, Finite-difference time-domain (FDTD) forward modeling of GPR data: 5th International Conference on Ground Penetrating Radar Expanded Abstracts, University of Waterloo, p. 185-204
- Taflove, A., and Umashankar, K.R., 1989, The finite-difference time-domain method for numerical modeling of electromagnetic interactions with arbitrary structures: in Morgan, M.A., Ed., *Progress in Electromagnetics Research*, Vol. 2, Elsevier Science Publ. Co.

Wang, T. and Hohmann, G.W. ,1993, A finite-difference time-domain solution for three-dimensional electromagnetic modeling, *Geophysics*, 58, p.797-809

Wang, T., Oristaglio, M., Tripp, A., Hohmann, G., 1994, Inversion of diffusive transient electromagnetic data by a conjugate-gradient method, *Radio Science*, v. 29, no. 4, pp. 1143-1156

Wang, T. and Tripp, A.C.,1994a, Simulation of electromagnetic wave propagation in three-dimensional structures by a finite-difference method, presented at the 7th Annual SAGEEP Meeting, Boston

Wang, T. and Tripp, A.C.,1994b, Simulation of electromagnetic wave propagation in three-dimensional structures by a finite-difference method, presented at the Ground Penetrating Radar Conference '94, Kitchener, Ontario

Wang, T. and Tripp, A.C.,1996, FDTD simulation of EM wave propagation in 3D media, *Geophysics*, 61, no.1, pp. 110-120

Wang, T., Tripp, A.C., Hohmann, G.W. ,1995, Transient electromagnetic response of a three-dimensional conductor at a geological contact with the overburden, *Geophysics*, 60, no. 4, pp. 1265-1269

Xu, T. and McMechan, G.A., 1997, GPR attenuation and its numerical simulation in 2.5 dimensions: *Geophysics*, 62(1), pp. 403-414

An Overview of the Partial Element Equivalent Circuit (PEEC) Electromagnetic Modeling Approach

Albert E. Ruehli

IBM Research Division, T. J. Watson Research Center
Yorktown Heights N.Y. 10598

and

Andreas C. Cangellaris

University of Illinois at Urbana-Champaign,
Urbana, IL 61821

Abstract

The solution of mixed or hybrid EM and electrical circuit problems is of importance for electromagnetic compatibility (EMC) as well as for electrical interconnect and package (EIP) problems. The hardware to be modeled is becoming more complex and the frequency ranges of interest are continuously increasing. This makes the electrical analysis of these problems very difficult. This paper gives an outline of the Partial Element Equivalent Circuit (PEEC) technique for the solution of such problems. This method is especially tailored for hybrid electromagnetic and circuit problems so that circuit elements can easily be accommodated. The method is also well suited for model reduction techniques which are usually based on circuit techniques. In this paper we give an outline of the PEEC approach as well as its use in conjunction with model reduction techniques for the solution of large problems. Also, a few model reduction examples are included.

1 Introduction

Today, the modeling of electromagnetic problems is of key importance in the design of new electronic systems. These systems, which usually include VLSI chips, present a real challenge to electromagnetic solvers. The geometric complexity of some of the problems, combined with orders of magnitude variation in the size of features, are very difficult to model. Specialized electromagnetic modeling techniques are

desirable for the solution of this class of problems.

The EMI analysis of interest to EIP problems tends to be quite different from the electromagnetic problems associated with the antenna and/or microwave component design. For example, instead of the well-defined and properly designed antenna structure and feed network that constitute the structure of interest in the electromagnetic analysis of a radiator, the entire interconnect structure, including the nonlinear, fast-switching digital drivers, becomes the *unintentional* radiator that must be modeled and iteratively modified to suppress radiation. Clearly, in addition to being nonlinear, the geometric complexity of the problem is overwhelming, considering that the shielding enclosure must be taken into account also in the electromagnetic analysis. In principle, the issue of geometric complexity could be overcome by the use of finer discretization in a *brute force* analysis with integral equation based and finite-element/finite-difference electromagnetic modeling approaches. However, the number of degrees of freedom (unknowns) in the resulting numerical approximation of the electromagnetic problem is prohibitively large, making such approaches unrealistic for practical applications. The inclusion of circuit elements is natural for the Partial Element Equivalent Circuit (PEEC) formulation, while it is more cumbersome to implement in some of the other techniques.

The challenges involved and the special features of the problems associated with the electromagnetic analysis of EIP problems can be summarized as follows:

- The general structure of the problems may be very heterogeneous, with linear and nonlinear circuits mixed with electromagnetic models necessary for the modeling of coupling, propagation, shielding, and radiation effects.
- The geometrical structure of the problems can be highly non-uniform, with large changes in scale and material properties.
- The feature size may vary drastically from one portion of the structure to the next, or even in different directions in space for a given structure (e.g. interconnect structures).
- The electrical size (i.e. spatial dimension measured in wavelengths) of the structure may exhibit significant variation from one portion of the system to the other, especially for very broadband (e.g. high-speed transient) simulations.
- The accuracy requirements may be more modest than what is the case for electromagnetic problems associated with antenna design and microwave passive component design.
- The current may vary rapidly with distance due to a multitude of conductors in non uniform, multi-layer arrangements. Such variations can occur within a small fraction of a millimeter.
- The current distribution inside the conductors may vary from uniform within the conductor cross section, to an almost surface current distribution (well-developed skin effect), due to the wide spectral variation associated with transient simulations.
- Solutions in both the time and the frequency domains are of importance for the same problem.

The PEEC technique represents a formulation which attempts, as much as possible, to address these challenges and modeling/simulation requirements. These requirements are in some way similar to the ones faced by the circuit simulation community in conjunction with the analysis of integrated circuits of high complexity. Depending on the level of circuit size and complexity, special techniques and solvers are used, where computational efficiency and accuracy are carefully traded off for larger circuit size. In some cases, coarse approximations are used, which for

other applications, would lead to insufficient solution accuracy.

The original PEEC model is based on an integral equation representation of Maxwell's equation [1]. A key advantage of the PEEC method is that the entire formulation is implemented in the circuit domain. Also, for the majority of applications, the Modified Nodal Analysis (MNA) formulation [2] is used which accommodates all types of circuit elements of interest. It also accommodates the very similar solution for both the time and the frequency domains which includes the electromagnetic solution. Depending on the applications and frequency bandwidth of interest, either a quasi static PEEC model or a full wave PEEC model can be developed. Recently, new enhancements have been introduced, including dielectrics [3], lossy dielectrics [4] models for non rectangular conductors [5] and incident fields [6] as well as time domain solutions [7, 8]. The MNA formulation, which is used in most circuit simulators like Spice, can be utilized for both the frequency and the time domain PEEC. An important issue exists for the time domain and for model order reduction since the basic model should be stable. Some of the recent work e.g. [9] has focused on the stability issue.

The solution of larger problems is a key issue for both EIP and EMI. Mainly, even small portions of a physical structure lead to very large electrical models. Compute time is a key limiting factor for all large EM modeling solutions. In order to tackle this problem, current research emphasis is placed on the development of reduced size *macromodels* which are tailored to specific applications. This approach addresses both the compute time and storage issues. Two such approaches for large PEEC models are *model simplification* and *model order reduction*. *Model simplification* is an approach where less important circuit elements are eliminated to obtain simplified macromodels e.g.[10]. Hence, the topology of the reduced model is related to the original circuit. This approach has been pursued by many researchers especially for quasi static models.

Model Order Reduction (MOR) is a relatively new research topic at least for the circuit simulation community. The aim of this approach is to reduce the number of eigenvalues or modes of the circuit to come up with simpler, equivalent models of a different topology than the original circuit. Mainly, only a

limited number of eigenvalues or poles are used to determine with sufficient accuracy the behavior of the circuit. The approach was first used in the circuit domain for large RC type circuits [11]. By now, it has shown promise for several interesting problems including transmission lines (e.g. [12], [13]), electromagnetic systems (e.g. [14], [15]) and PEEC models (e.g. [16], [17], [18], [19]). More details for both model simplification and model reduction will be given in Section 3.

2 Circuit-Oriented EM Models

2.1 PEEC Model

The aim of the PEEC method is to represent the EM problem in terms of circuit elements such that an equivalent circuit results. The equivalent circuit then can be used to formulate a set of circuit equations which describe the behavior of the problem. As mentioned above, they are formulated in the form of MNA equations or equivalently state equations, or

$$\sum_{i=0} \dot{\mathbf{C}}_i \mathbf{x}(t - \tau_i) + \sum_{i=0} \mathbf{G}_i \mathbf{x}(t - \tau_i) = \mathbf{B} \mathbf{u}$$

$$\mathbf{i}_N = \mathbf{B}^T \mathbf{x}_n \quad (2.1)$$

where the unknown vector $\mathbf{x} = (\mathbf{v}, \mathbf{i})^T$ consists of the nodal voltages augmented by a specific set of currents and where τ represents the delay between the circuit elements. It should be pointed out that (2.1) is in the form of a delay differential equation. These equations play a role in the study of the stability of the time domain solution of PEEC models with delays [20].

We give a very abbreviated derivation of the integral equation and the PEEC model which includes three dimensional finite dielectrics in the formulation [21]. The PEEC formulation aims at an approximations of the currents, charges and potentials (voltages) which are appropriate for an equivalent circuit representation. The displacement current due to the bound charges for the dielectrics with $\epsilon_r > 1$ is treated separately from the currents due to the free charges. At a given point inside a conductor of conductivity σ , the equation for the electric field $\bar{E} = \bar{J}/\sigma$ assumes the form

$$\bar{E}_0(\bar{r}, t) = \frac{\bar{J}(\bar{r}, t)}{\sigma} + \frac{\partial \bar{A}(\bar{r}, t)}{\partial t} + \nabla \Phi(\bar{r}, t) \quad (2.2)$$

where \bar{E}_0 is the applied electric field (if any), \bar{J} is the current density in the conductor, \bar{A} and Φ are the magnetic vector and electric scalar potentials, respectively. As indicated above, the dielectric areas are taken into account in terms of the polarization current density associated with their presence, rather than a capacitance through the scalar potential. This is accomplished by adding and subtracting $\epsilon_0 \frac{\partial \bar{E}}{\partial t}$ in the Maxwell equation for \bar{H} , or

$$\nabla \times \bar{H} = \bar{J} + \epsilon_0(\epsilon_r - 1) \frac{\partial \bar{E}}{\partial t} + \epsilon_0 \frac{\partial \bar{E}}{\partial t} \quad (2.3)$$

Here, the current in (2.3) is written as a total current

$$\bar{J}(\bar{r}, t) = \bar{J}_C(\bar{r}, t) + \epsilon_0(\epsilon_r - 1) \frac{\partial \bar{E}}{\partial t} \quad (2.4)$$

where $\bar{J}_C(\bar{r}, t)$ is the conductor current and the remaining term is the equivalent polarization current due the the dielectrics.

The vector potential \bar{A} at point \bar{r} is given by

$$\bar{A}(\bar{r}, t) = \mu \int_{v'} G(\bar{r}, \bar{r}') \bar{J}(\bar{r}', t_d) dv' \quad (2.5)$$

where the retardation time is given by

$$t_d = t - \frac{|\bar{r} - \bar{r}'|}{c} \quad (2.6)$$

which simply is the free space travel time between the points \bar{r} and \bar{r}' . It is noted that in the formulation derived here, both the retardation and the Green's functions are free space quantities where

$$G(\bar{r}, \bar{r}') = \frac{1}{4\pi |\bar{r} - \bar{r}'|} \quad (2.7)$$

The scalar potential is similarly

$$\Phi(\bar{r}, t) = \frac{1}{\epsilon_0} \int_{v'} G(\bar{r}, \bar{r}') q(\bar{r}', t_d) dv' \quad (2.8)$$

Finally, using the above we can formulate an integral equation for the electric field at a point \bar{r} which is to be located either inside a conductor or inside a dielectric region. Starting from (2.2) with the externally applied electric field set to zero, and substituting for \bar{A} and Φ from (2.5) and (2.8) respectively

$$\begin{aligned} \frac{\bar{J}(\bar{r}, t)}{\sigma} &+ \mu \int_{v'} G(\bar{r}, \bar{r}') \frac{\partial \bar{J}(\bar{r}', t_d)}{\partial t} dv' \\ &+ \epsilon_0(\epsilon_r - 1) \mu \int_{v'} G(\bar{r}, \bar{r}') \frac{\partial^2 \bar{E}(\bar{r}', t_d)}{\partial t^2} dv' \\ &+ \frac{\nabla}{\epsilon_0} \int_{v'} G(\bar{r}, \bar{r}') q(\bar{r}', t_d) dv' \\ &= \bar{E}_0(\bar{r}, t) \end{aligned} \quad (2.9)$$

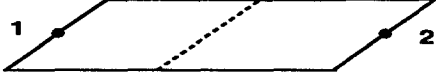


Figure 1: Flat conductor

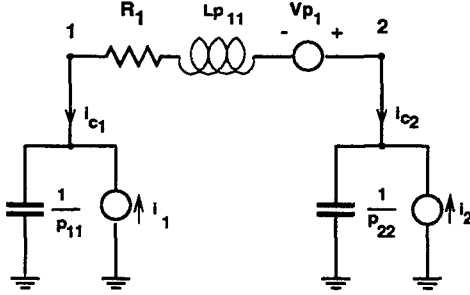


Figure 2: PEEC model with Field Source

Equation (2.4) is used for the total current in both the conductors and the dielectrics. In addition, the continuity equation

$$\nabla \cdot \bar{J} + \frac{\partial q}{\partial t} = 0 \quad (2.10)$$

is needed to solve the integral equation (2.9). The discrete version of this equation is transformed into Kirchhoff's current law.

Equation (2.9) is discretized in a special way to come up with the PEEC equivalent circuit model. We use pulse functions matching and a Galerkin solution. The inner product is formed with respect to a cell of conductor α

$$\frac{1}{a_\alpha} \int_{v_\alpha} f(\bar{r}) dv = \frac{1}{a_\alpha} \int_{a_\alpha} \int_{l_\alpha} f(\bar{r}) da dl \quad (2.11)$$

where v_α is the volume of the conductor cell α , a_α is the cross-section of the cell ($x - y$ direction) and l_α is the length (z -direction) and $f(\bar{r})$ is the integrand. This corresponds to averaging the field point \bar{r} over the cell volume v_α . From the resultant equation, we can assert what the appropriate equivalent circuit is for each term of the IE, corresponding to (2.9). It should be noted that the formulation insures that the circuit elements are indeed reciprocal. We use the very simple example of a zero thickness strip of conductor in Fig. 1 to show the PEEC circuit which corresponds to the physical structure. The conductor is represented by a single inductive cell only, while the half capacitive cells are associated which each of the end nodes 1 and 2. The nodes are chosen at the edges of the conductors so that connections to other

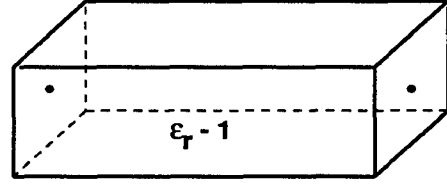
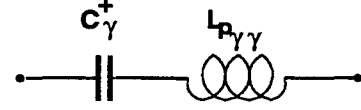


Figure 3: PEEC model for dielectric cell

elements can be established with ease for all types of circuit elements.

The contribution of each term in (2.9) is illustrated with the PEEC circuit model in Fig. 2 which corresponds to the metal strip in Fig. 1. After integration of (2.9) with the inner product (2.11) we can show that the right hand side for an external field yields the voltage source v_{p1} . This term could also represent appropriate independent sources in a circuit context. The first term on the left-hand side of the equation corresponds to the series resistance R_1 , while the second term corresponds to the partial inductance L_{p11} . The third term corresponds to the dielectric cells. The interpretation of this term is quite difficult [21]. We define the excess capacitance of a dielectric cell as

$$C_\gamma^+ := \frac{\epsilon_0(\epsilon_\gamma - 1)a_\gamma}{l_\gamma} \quad (2.12)$$

where ϵ_γ is the dielectric constant of the cell. The equivalent circuit for the dielectric bar or cell shown in Fig. 3 is given by a partial inductance $L_{p\gamma\gamma}$ in series to a capacitor C_γ^+ . This is a very important addition to the PEEC model for many problems. Finally, the forth term in (2.9) represents the free space capacitances which are represented by the capacitors and the current sources in Fig. 2.

3 Reduced Size PEEC Models

As already mentioned, the two key attributes of the PEEC formulation are its ability to model heterogeneous systems, (i.e., systems involving both lumped circuits and distributed electromagnetic components) and its suitability for hierarchical electromagnetic modeling. This second attribute is closely related

to model complexity reduction, and is of critical importance to the efficiency with which EMI analysis of packaged, high-speed structures can be effected. Model complexity reduction and macromodeling of EIP systems has been an active research topic over the last few years. In this section we consider macromodeling for PEEC circuit models. Extremely large PEEC models can be created for larger geometries. Usually, a Spice type circuit solver is used to obtain the solution waveforms of interest. In fact, *simplified macromodels* were used early on in PEEC modeling. Our view of what represents a *large* PEEC models has been upgraded several times since then. Mainly, the algorithms as well as the computer resources available to a wide users group have been drastically improved so that very large PEEC models can be solved on today's high end workstations.

3.1 Model Simplification

We first consider *model simplification* since it is a more straight forward approach. Figure 4 gives some insight into various stages of model simplification of PEEC models. As shown, different approximations can be used to eliminate circuit elements in the PEEC model. These conditions are mainly dependent on the operating conditions and the particular application. Hence, the simplified macromodel has the same basic topology but has fewer circuit elements. Engineering judgment is used in making a decision on which type of element can be discarded. Probably the simplest example is that physically very small models do not need to include retardation for moderate frequencies. In fact, we rarely used retardation in the early stages on PEEC modeling. For VLSI systems, retardation or delay has become important only recently with the decrease in system cycle time [8]. Mainly, circuit solvers like ASX [22] or SPICE [23] can be used directly to solve PEEC problems without delays. This is a very popular approach due to the extensive use of circuit solvers for VLSI designs.

Often, in model simplification the circuit elements are not completely eliminated but reduced in a clever way e.g. [10]. Further, one may eliminate circuit elements from only parts of a circuit where appropriate. Specialized solvers have been designed for the solution of the (L_p, R) PEEC case where we use the partial inductance matrix L_p and the R matrix to set up a set of circuit equations. An example of the usefulness

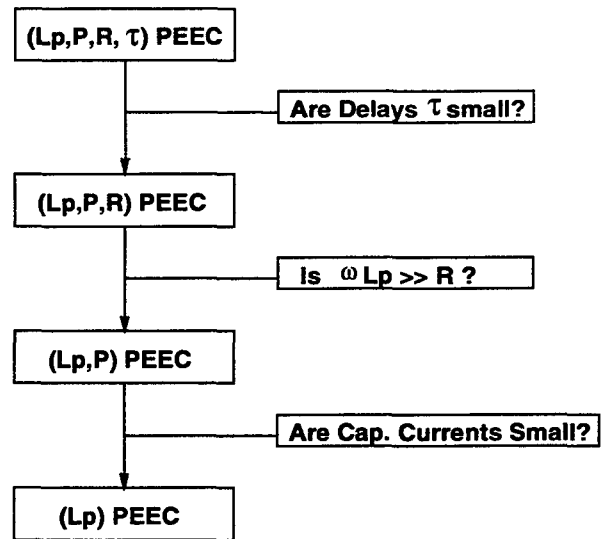


Figure 4: Example for model simplification

of the (L_p, R) PEEC model is given in [24, 25]. Very often, simplified macromodels are augmented with a limited set of *simpler* TEM mode type capacitances. The (L_p, R) PEEC model may be further reduced if the resistance is small compared to the impedances of the partial inductances for the frequencies of interest. Then a frequency independent reduction can be applied which is based on the partial inductance matrix L_p only. Again, very useful results can be obtained from these models. Similar simplified models can be constructed for the capacitances only circuits.

Model simplification is extremely important since, once properly implemented, it facilitates the simulation of very complex structures without sacrificing engineering accuracy. The unique attribute of the PEEC formulation is that physical model simplification can be effected in a very systematic, hierarchical manner, using geometric complexity and component electrical size as the guiding factors. This is illustrated clearly through an example borrowed from the area of signal integrity and interference analysis assessment in packaged electronics. PEEC starts with a rigorous, full-wave electromagnetic model for the interconnect/package structure of interest, and establishes a distributed equivalent circuit that describes explicitly the retarded inductive and capacitive coupling between the discrete electrical volume/surface currents and surface charges that constitute the unknowns in the discrete model. With this complete electromagnetic model in place, the process of model

simplification is ready to commence. Different levels of the interconnect, and different parts in the package and/or printed-circuit board of the system can be modeled for the purpose of signal integrity assessment by implementing appropriate simplifications of the full-wave discrete model. For example, if the operating bandwidth of interest is such that the characteristic dimensions of the package are a fraction of the minimum wavelength of interest, an (L_p, P, R) PEEC model suffices for the modeling of the traces, bond wires, pins, and associated ground and power planes within the single-chip package. For example, for a single-chip package of characteristic dimension of 4 cm and operating bandwidth of interest of 2 GHz, interconnect lengths do not exceed one fourth of the minimum wavelength of interest, and such a reduced PEEC model constitutes a very sound engineering approximation. Such a model results immediately from the full-wave one by setting the retardation time to zero.

With regards to the modeling of the interconnects on the integrating substrate (e.g. for MCM structures), the card, or the printed-circuit board, multi-conductor transmission line (MTL) models can be implemented. The SPICE compatibility of the PEEC formulation makes the incorporation of MTL models in it very straightforward. More specifically, the same procedures used for the incorporation of MTLs in SPICE-like simulators (e.g. [26],[27]), are used in conjunction with the PEEC formulation. An interesting demonstration of this capability has been given in [28].

In the above discussion it is assumed that the emphasis of the simulation is on the prediction of signal degradation due to crosstalk, interconnect delay, reflection, and simultaneous switching noise. If, in addition, the prediction of electromagnetic radiation from the interconnect and packaging structure is of interest, the aforementioned reduced model becomes inadequate, and retardation effects must be taken into account. Furthermore, for such radiated emissions analysis purposes, if it is possible to identify the dominant sources of radiation, the full-wave (L_p, P, R, τ) PEEC model may be used only for those portions of the structure that encompass these sources. For example, selected interconnects on printed circuit boards, which exhibit imbalances due to discontinuities or layout constraints, can be mod-

eled using the (L_p, P, R, τ) PEEC model, while the remaining of the well-balanced interconnects can be modeled using SPICE-compatible transmission line models.

While such hierarchical model simplification is a very natural alternative to brute-force electromagnetic modeling when problem model complexity becomes an issue, it has not been practiced extensively. A limited number of examples from its application have been reported thus far, with the majority of them associated with the analysis of EIP structures. A particular class of problems which can benefit significantly from the application of such a hierarchical PEEC model simplification methodology is the class of mixed-signal electronics. Fueled by the growth of portable, wireless computing and communication modules, mixed-signal integrated electronics technology has advanced very rapidly over the past few years, with sophisticated multi-functional designs involving the tight integration of high-speed digital, analog, and RF blocks on the same board. EMI/EMC assessment of such integrated systems constitutes a very challenging problem. In addition to the prediction of radiated emissions from the packaged system for the purposes of product compliance assessment, electromagnetic modeling of the interactions between the different functional blocks is required for the purposes of electrical performance assessment and design optimization. As an example, we mention the case where noise generated in the digital block of a portable computer is radiated out, and is eventually received by the antenna in the RF wireless data link block of the computer. A generic example of such an interaction was presented in [28].

3.2 Model Order Reduction

Model order reduction (MOR) techniques have become an active research topic for circuit models in general and PEEC models in particular. The beginning work for circuit MOR was based on Padé approximation [29, 30] while later work extended to the Arnoldi e.g. [25] and Lanczos' algorithms [31, 32, 33]. In fact MOR has been applied to PEEC models circuits by several researchers in recent years [34, 31, 35].

The requirement for MOR techniques stems from the fact that the complexity of the EIP structures is significant even after model simplification has been applied. For example, for a multi-pin, multi-layer

package, the conductor complexity is such that the (L_p, P, R) PEEC model may involve several thousands or even tens of thousands of unknowns. Because of the presence of the inductive and capacitive couplings, the complexity of the SPICE subcircuit that describes the PEEC model makes its direct use in non-linear circuit simulators prohibitive. The remedy to this simulation bottleneck is the application of MOR techniques.

In order to provide a brief overview of MOR, let us assume that the discrete PEEC model for an N -port EIP structure can be written in an MNA or state form as follows

$$\begin{aligned} (G + sC) \mathbf{x}_n &= \mathbf{B} \mathbf{u}_N \\ \mathbf{i}_N &= \mathbf{B}^T \mathbf{x}_n \end{aligned} \quad (3.13)$$

In the above equations, \mathbf{x}_n is the state vector of length n , with elements the unknown currents and voltages in the PEEC model. \mathbf{C} is a symmetric, nonnegative-definite, $n \times n$ matrix, describing the capacitive and inductive interactions. \mathbf{G} is an $n \times n$ matrix that incorporates the resistances as well as the constants resulting from the enforcement of the conservation of charge equation at the electric potential nodes. Finally, the vectors \mathbf{u}_N and \mathbf{i}_N denote the port voltages and currents, respectively, at the N ports of the EIP structure. The $n \times N$ matrix \mathbf{B} is a selector matrix that relates the port variables to the elements in the state vector \mathbf{x}_n . The linear dependence on s in (3.13) indicates that retardation has been neglected, and the assumed model is an (L_p, P, R) PEEC model.

From the variety of approaches available for the reduction of (3.13) we select the PRIMA methodology, proposed first in [36], because of its robustness and its ability to preserve the passivity of the circuit. Passivity of the reduced-order model is an essential requirement when several subcircuits are connected together for system-level analysis. As discussed in [37], the system resulting from the interconnection of several stable sub-circuits is not necessarily stable. However, the interconnection of passive sub-circuits results always in a stable system.

The way PRIMA effects the reduction of the system in (3.13) may be explained as follows. Consider the state-vector transformation

$$\mathbf{x}_n = \mathbf{V} \hat{\mathbf{x}}_q \quad (3.14)$$

where $\hat{\mathbf{x}}_q$ is the reduced state vector of length $q \ll n$, and \mathbf{V} is the transformation matrix of dimension

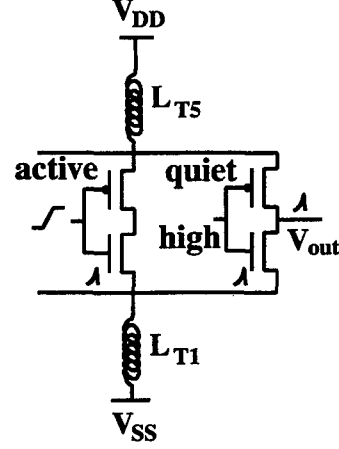


Figure 5: Electrical model of two of the output drivers connected to ground and power leads of a PQFP.

$n \times q$. Use of (3.14) in (3.13) and multiplication on the left by \mathbf{V}^T yields the reduced system

$$\begin{aligned} (\hat{\mathbf{G}} + s\hat{\mathbf{C}}) \hat{\mathbf{x}}_q &= \hat{\mathbf{B}} \mathbf{u}_N \\ \mathbf{i}_N &= \hat{\mathbf{B}}^T \hat{\mathbf{x}}_q \end{aligned} \quad (3.15)$$

where the reduced state matrices $\hat{\mathbf{G}} = \mathbf{V}^T \mathbf{G} \mathbf{V}$, $\hat{\mathbf{C}} = \mathbf{V}^T \mathbf{C} \mathbf{V}$ are of dimension $q \times q$, and the reduced selector matrix $\hat{\mathbf{B}}$ is of dimension $q \times N$. It was shown in [36] that this congruence transformation preserves passivity. In the same paper, a methodology was given for the generation of the transformation matrix \mathbf{V} from the matrices \mathbf{G} , \mathbf{C} and \mathbf{B} using a block Arnoldi algorithm.

The methodology that is used for the incorporation of the generated reduced-order model in the circuit simulator depends on the type of simulation that is of interest (e.g. transient simulation, narrow band frequency simulation, etc.), as well as the capabilities of the circuit simulator. For example, for a simulator with recursive convolution capability, a pole-residue representation of the elements of the multiport transfer function matrix of (3.15)

$$\hat{\mathbf{Y}}(s) = \hat{\mathbf{B}}^T (\hat{\mathbf{G}} + s\hat{\mathbf{C}})^{-1} \hat{\mathbf{B}} \quad (3.16)$$

is appropriate [38]. Such a pole-residue representation can be obtained in a straightforward manner following an eigendecomposition of the matrix $\hat{\mathbf{G}}^{-1} \hat{\mathbf{C}}$.

An alternative to a pole-residue representation of the multiport transfer function matrix is the direct

synthesis of a SPICE subcircuit for the equivalent reduced system. This is effected in the following fashion. Since $\hat{\mathbf{C}}$ is symmetric and real, a singular value decomposition gives $\hat{\mathbf{C}} = \mathbf{U}\mathbf{D}\mathbf{U}^T$, where $\mathbf{U}^T\mathbf{U} = \mathbf{I}$. \mathbf{I} is the identity matrix, and \mathbf{D} is diagonal, containing the singular values of $\hat{\mathbf{C}}$ (which are all positive). Insertion of this decomposition in (3.15) yields

$$\begin{aligned} (\mathbf{U}^T \hat{\mathbf{G}} \mathbf{U} + s\mathbf{D}) \hat{\mathbf{x}}'_q &= \mathbf{U}^T \hat{\mathbf{B}} \mathbf{u}_N \\ \mathbf{i}_N &= \hat{\mathbf{B}}^T \mathbf{U} \hat{\mathbf{x}}'_q \end{aligned} \quad (3.17)$$

where $\hat{\mathbf{x}}'_q = \mathbf{U}^T \hat{\mathbf{x}}_q$. The resulting state representation of the reduced equivalent circuit is compatible with the MNA formulation. Thus, it can be incorporated directly in a SPICE-like circuit simulator.

A useful application of (L_p, P, R) PEEC model order reduction is in the macromodeling of packaging structures for the purposes of simultaneous switching noise (ground bounce) calculation in SPICE. As an example, we consider the case of a Plastic Quad Flat Pack (PQFP). Because of symmetry, only one fourth of the package geometry is considered. This portion of the PQFP involves seven conducting leads. Typical lead length is 7.5 mm. The lead thickness is 10 mil, while its width varies from 0.6 mm to 1.3 mm. The spacing between adjacent leads is 100 mil. From the seven leads, five are signal, one is ground, and one is power. The five signal leads are terminated with 15 pF capacitors. The resulting five-port, with ports the lead end points on the chip side, is discretized by means of the PEEC method [17]. Despite the low density of the package, the frequency bandwidth of interest extends beyond 1 GHz. Thus, in view of the cross-sectional dimensions of the leads, skin effect must be taken into account. Consequently, the number of unknowns in the PEEC model is rather large due to the discretization of the cross sections of the leads.

Next, PRIMA is used to generate a reduced order five port macromodel of the generated (L_p, P, R) PEEC model [17]. The order of the reduced model is 20. A pole/residue representation of the macromodel is generated, which is subsequently used in conjunction with a SPICE simulator, enhanced with recursive convolution capabilities, for the purpose of simultaneous switching noise analysis. In particular, we consider the case where identical inverters with W/L ratios for the NMOS and PMOS of values 96 and 224, respectively, are connected to the five ports. With one of the drivers driven and the rest

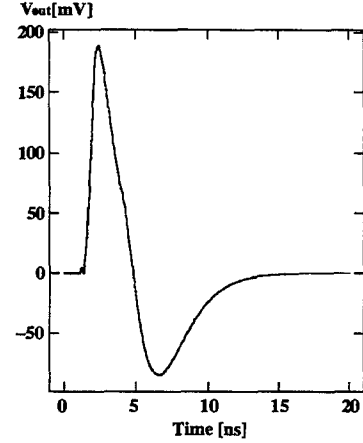


Figure 6: Simulated switching noise waveform at the quiet driver adjacent to the driven one.

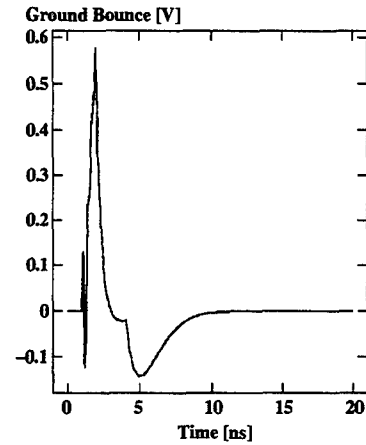


Figure 7: Recorded ground bounce at the ground lead.

kept quiet, a transient simulation is performed to calculate the switching noise (see Fig. 5). The driving signal is a 0 to 5 V transition of duration 1 ns. Fig. 6 depicts the noise recorded at the quiet driver adjacent to the driven one. Finally, Fig. 7 depicts the recorded ground bounce at the ground lead connection for all five drivers.

3.3 Model Order Reduction for PEEC Models with Retardation

Early work for retarded (L_p, P, R, τ) PEEC models started with [16] where the retardation term in the frequency domain $\exp(s\tau)$ was expanded in an infinite Taylor series. Other work for retarded PEEC models has been based on the same fundamental infinite series approach e.g. [34]. Realistic PEEC models have a

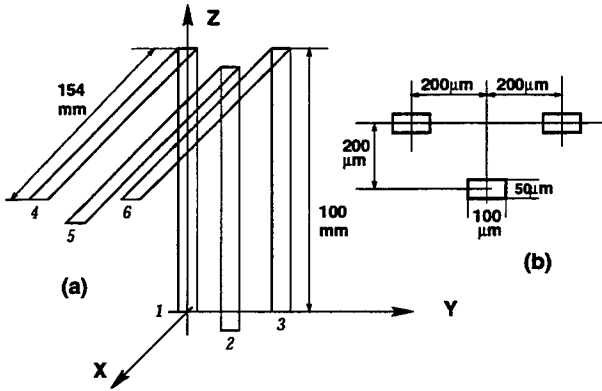


Figure 8: Tree transmission lines with bend

large number of time delays in (2.1) or, equivalently, exponentials. A local approximation is used for the exponentials in an alternate approach [19]. Briefly, the complex plane is systematically divided into local regions where each exponential is expanded about a point $s_0 + \Delta s$ with only a few terms, or

$$e^{-\tau s} = e^{-\tau s_0} (1 - \tau \Delta s + (\tau \Delta s)^2 / 2 - \dots) \quad (3.18)$$

This leads to a new system which can be approximated by a slightly larger system in each of the rectangular domains. The size of the system depends on the approximation order. The rectangular domains cover the region in the s -domain where the poles are located. The poles inside of each region are assembled into the transfer function similar to the Complex Frequency Hopping idea in [39]. In general, practical experience shows that very few subdivisions are need to be employed along the negative real axis while several subdivisions are necessary along the imaginary axis. The domain which includes the poles is systematically covered so that all the relevant poles are included. A tradeoff exists between the subdomain size and the approximation order. An Arnoldi MOR model reduction procedure is used in this work. Typically, one subdivision suffices along the real axis while up to ten divisions may be necessary along the imaginary axis. We give an example from [19] where MOR was applied to the bent three wire transmission line shown in Fig. 8. In this application, the transmission lines were modeled in terms of a port impedance matrix formulation where the port voltages relate to the port currents by an impedance matrix. The ports are chosen separately to be located at one or the other end of the transmission line. Fig. 9 gives the comparison between the PEEC model result and the MOR

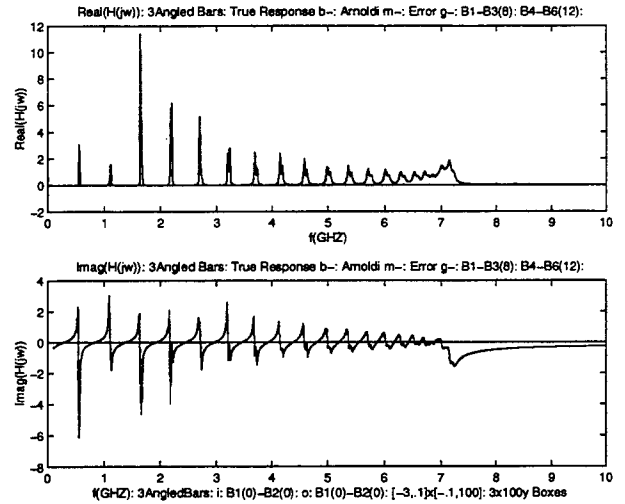


Figure 9: Impedance results from MOR

model for the input impedance Z which is between wire terminals 1 and 2. In the comparison, the exact response was obtained at 500 frequency points where a conventional *ac* analysis was used.

Figure 9 shows the real and imaginary parts of the impedance between terminals 1 and 2. The second trace which coincides with the zero axis shows the error between the analyses. It is evident that MOR provides a very good approximation. In essence, there exists a tradeoff between accuracy and compute time.

4 Conclusion

The paper summarizes the application of the PEEC method to the solution of mixed circuit and EM problems. This approach is suitable for an important class of EMC/EIP problems. This paper also includes the use of PEEC in conjunction with model reduction techniques, for the accelerated simulation of complex EIP structures, which is a very active area of research. This approach shows promise for the effective modeling of large problems which represent an important class of problems in EMI/EMC modeling of integrated packaged electronics.

References

- [1] A. E. Ruehli. Equivalent circuit models for three dimensional multiconductor systems. *IEEE Transactions on Microwave Theory and Techniques*, MTT-22(3):216-221, March 1974.

- [2] C. Ho, A. Ruehli, P. Brennan. The modified nodal appr. to netw. anal. *IEEE Transactions on Circuits and Systems*, pages 504–509, June 1975.
- [3] A. Ruehli and H. Heeb. Circuit models for three-dimensional geometries including dielectrics. *IEEE Transactions on Microwave Theory and Techniques*, 40(7):1507–1516, July 1992.
- [4] J. Garrett, A. Ruehli. PEEC-EFIE for modeling 3D geometries with lossy inhomogeneous dielectrics and incident fields. IBM Research Report RC 19245, IBM, October 1993.
- [5] R. F. Milsom, K. J. Scott, G. Clark, J. C. McEntegart, S. Ahmed and F. N. Soper. FACET – a CAE system for RF analogue simulation including layout. In *Proc. of the Design Automation Conference*, volume 26, pages 622–625, 1989.
- [6] A. E. Ruehli, J. Garrett, C. R. Paul. Circuit models for 3d structures with incident fields. In *Proc. of the IEEE Int. Symp. on Electromagnetic Compatibility*, pages 28–31, Dallas, Tx, August 1993.
- [7] W. Pinello, A. Cangellaris and A. Ruehli. Hybrid electromagnetic modeling of noise interactions in packaged electronics based on the partial element equivalent circuit formulation. *IEEE Transactions on Microwave Theory and Techniques*, 45(10):1889–1896, October 1997.
- [8] A. E. Ruehli, W.P. Pinello, A.C. Cangellaris. Comparison of differential and common mode response for short transmission line using PEEC models. In *Digest of Electr. Perf. Electronic Packaging*, volume 5, pages 169–171, Napa, Cal., November 1996.
- [9] J. E. Garrett, A. E. Ruehli, C. R. Paul. Accuracy and stability of the partial element equivalent circuit model. In *Proceedings Int. Zurich Symp. on EMC*, volume 11, pages 179–184, Zürich, Switzerland, February 1997.
- [10] G. Coen, D. De Zutter. Reduction of circuit complexity using tensor analysis of networks. In *Proceedings Int. Zurich Symp. on EMC*, volume 11, Zürich, Switzerland, February 1997.
- [11] L. T. Pillage and R. A. Rohrer. Asymptotic waveform evaluation for timing analysis. *IEEE Transactions on Computer-aided Design*, 9(4):352–366, 1990.
- [12] M. Celik and A. Cangellaris. Simulation of dispersive multiconductor transmission lines by Padé approximations via Lanczos process. *IEEE Transactions on Microwave Theory and Techniques*, 44(12):2525–2535, 1996.
- [13] S. Pasha, A. C. Cangellaris, J. L. Prince, and M. Celik. Passive model order reduction of multiconductor interconnects. In *EPEP*, pages 291–294, October 1998.
- [14] L. Zhao and A. C. Cangellaris. Reduced-order modeling of electromagnetic field interactions in unbounded domains truncated by perfectly matched layers. *Microwave and Optical Technology Letters*, 17(1):62–66, 1998.
- [15] J. E. Bracken, D.-K. Sun, and Z. J. Cendes. S-domain methods for simultaneous time and frequency characterization of electromagnetic devices. *IEEE Transactions on Microwave Theory and Techniques*, 46(9):1277–1290, 1998.
- [16] A. E. Ruehli, H. Heeb, E. Bracken and R. Rohrer. Three dimensional circuit oriented electromagnetic modeling for VLSI interconnects. In *Proceedings of the Packaging, Interconnects, Optoelectronics for the Design of Parallel Computers Workshop; Schaumburg, Illinois*, March 1992.
- [17] S. Hasan, A. Cangellaris, and J. Prince. Broadband frequency-dependent RLC equivalent circuit model extractor of microelectronic packages. In *TECHCON*, September 1998.
- [18] I. M. Elfadel and D. D. Ling. A block rational arnoldi algorithm for multipoint passive model-order reduction of multiport RLC networks. In *ICCAD*, pages 66–71, November 1997.
- [19] J. Cullum, A. Ruehli, T. Zhang. Model reduction for PEEC models including retardation. In *Digest of Electr. Perf. Electronic Packaging*, number 7, pages 287–290, West Point, NY, October 1998.

- [20] A. Bellen, N. Guglielmi, A. Ruehli. Methods for linear systems of circuit delay differential equations of neutral type. *IEEE Transactions on Circuits and Systems*, 46:212–216, January 1999.
- [21] A. Ruehli and H. Heeb. Circuit models for three-dimensional geometries including dielectrics. *IEEE Transactions on Microwave Theory and Techniques*, 40(7):1507–1516, July 1992.
- [22] W. T. Weeks, A. J. Jimenez, G. W. Mahoney, D. Mehta, H. Quasemzadeh and T. R. Scott. Algorithms for ASTAP – a network analysis program. *IEEE Transactions on Circuits Theory*, CT-20(11):628–634, November 1973.
- [23] L. W. Nagel. SPICE: A computer program to simulate semiconductor circuits. Electr. Res. Lab. Report ERL M520, University of California, Berkeley, May 1975.
- [24] P.A. Brennan, N. Raver and A.E. Ruehli. Three-dimensional inductance computations with partial element equivalent circuits. *IBM Journal of Research and Development*, 23(6):661–668, November 1979.
- [25] L. M. Silveira, M. Kamon, J. White. Direct computations of reduced-order models for circuit simulation of 3D interconnect structures. In *Digest of Electr. Perf. Electronic Packaging*, Monterey, Cal., November 1994.
- [26] V. K. Tripathi and J. B. Rettig. A spice model for multiple coupled microstrips and other transmission lines. *IEEE Transactions on Microwave Theory and Techniques*, MTT-33(12):1513–1518, 1985.
- [27] M. Celik, A. C. Cangellaris, and A. Yaghmour. An all-purpose transmission-line model for interconnect simulation in SPICE. *IEEE Transactions on Microwave Theory and Techniques*, 45(10):1857–1867, 1997.
- [28] W. P. Pinello, A. C. Cangellaris, and A. Ruehli. Prediction of differential- and common-mode noise in high-speed interconnects with the partial element equivalent circuit technique. In *ISEMC*, pages 940–945, August 1998.
- [29] L. T. Pillage and R. A. Rohrer. Asymptotic waveform evaluation for timing analysis. *IEEE Transactions on Computer-aided Design*, 9(4):352–366, 1990.
- [30] S. P. McCormick and J. Allen. Waveform moment methods for improved interconnection analysis. In *Proc. of the Design Automation Conference*, volume 27, 1990.
- [31] R. W. Freund, P. Feldmann. Efficient small-signal circuit analysis and sensitivity computations with the PVL algorithm. In *Proc. of the IEEE Int. Conf. on Computer Aided Design*, San Jose, Cal., November 1994.
- [32] R. du Cloux, W. J. de Graaf, G.P.J.F.M. Maas, R. W. van der Veen. Emc simulations and measurements. In *Proceedings Int. Zurich Symp. on EMC*, volume 10, pages 185–190, Zürich, Switzerland., March 1995.
- [33] K. Gallivan, E. Grimme, P. Van Dooren. A rational Lanczos algorithm for model reduction. *Numerical Algorithms*, 12:33–63, 1996.
- [34] E. Chiprout, H. Heeb, M.S. Nakhla and A.E. Ruehli. Simulating 3-D retarded interconnect models using complex frequency hopping (CFH). In *Proc. of the IEEE Int. Conf. on Computer Aided Design*, Santa-Clara, CA, November 1993.
- [35] P. Feldman, R.W. Freund. Efficient linear circuit analysis by Padé approximation via Lanczos process. *IEEE Transactions on Computer-aided Design*, 14:639–649, 1995.
- [36] A. Odabasioglu, M. Celik, and L. T. Pileggi. Prima: Passive reduced-order interconnect macromodeling algorithm. *IEEE Transactions on Computer-aided Design*, 17(8):645–653, 1998.
- [37] R. A. Rohrer and H. Nosrati. Passivity considerations in stability studies of numerical integration algorithms. *IEEE Transactions on Circuits and Systems*, CAS-28:857–866, 1981.
- [38] A. Semlyen and A. Dabuleanu. Fast and accurate switching transient calculations on transmission lines with ground using recursive convolution. *IEEE Transactions Power Appl. Syst.*, PAS-94:561–571, 1975.

EMI/EMC Computational Modeling Handbook

by

Bruce Archambeault, Omar M. Ramahi, and Colin Brench

reviewed by

James L. Drewnaik

Electromagnetic Compatibility Laboratory
University of Missouri-Rolla

Each of the authors of *EMI/EMC Computational Modeling Handbook* have a combination of many years of EMC (at IBM and Digital) as well as numerical electromagnetic modeling experience that results in a unique and useful presentation of this subject. As the authors remind the reader many times throughout, an EMC problem is minimally comprised of a noise source, unintended EMI antenna, and a parasitic path that couples energy from the noise source to the EMI antenna. The source is typically a high-speed digital IC, and the EMI antenna might be attached cables, or slots and apertures in a shielding enclosure. In practice, anticipating these two aspects of a potential EMI problem is much easier than the coupling path. The coupling path is related to layout features and may be parasitic inductance, capacitance, or a common impedance, and can be very difficult to anticipate at the design stage. Consequently, productively using numerical electromagnetic modeling to reduce EMI/EMC risk at the design stage can be challenging.

Numerical electromagnetic modeling is relatively mature, with many commercial codes available, and can result in good answers to *well-defined* problems. However, defining an EMI/EMC problem is in general an inexact art that typically requires both modeling as well as good EMC experience. The authors combine many years of industry EMC experience in shipping high-speed digital products, together with expertise that they have acquired in applying numerical modeling to

product EMC design to provide the reader with valuable insight into productively using numerical modeling for EMC design.

The intended audience of the book is practicing engineers that may not be experts at numerical modeling, as well as more experienced modeling people that are seeking guidance on applying modeling to product design. I think that it is also an invaluable resource for graduate students that may be focusing on fundamental numerical modeling algorithms and issues to gain exposure to a new and growing area of application for these methods. The objectives of the book are to provide a rudimentary understanding of the common numerical electromagnetic modeling methods, and more significantly insight and guidance for incorporating them into the EMC design process. As such, the authors do not intend that it will be a comprehensive treatment on any particular numerical modeling method.

The book briefly reviews the basics of the three common numerical electromagnetic modeling methods, finite-difference time-domain (FDTD), finite element (FEM), and integral equation (method of moments) formulations with some emphasis on FDTD. The critical issues in numerical modeling are determining the essential features that must be modeled, how to model them, and at what level of detail to result in a good and useful answer. In EMC design, ascertaining these very necessary details are typically difficult, and these are the issues on which the authors focus. The authors provide a good

understanding of what can reasonably be expected and achieved in practical EMC design, basic modeling concepts, and how to use numerical modeling for understanding fundamental coupling physics, as well as for layout and design.

Chapter 1 is a brief introduction to EMI/EMC modeling, and the three common modeling methods. Chapter 2 is an overview of only the essential electromagnetic theory and basic "equations of motion" that are used later in the chapters on the individual modeling methods.

The three common, full-wave numerical electromagnetic modeling approaches, FDTD, MOM, and FEM are presented in Chapters 3, 4, and 5, respectively. In each case, only the essentials for acquiring a basic understanding of these methods are given. FDTD is a logical choice to present first since it is by far the easiest to understand of the three, as well as widely useful for EMI/EMC problems, and robust. The authors give the basics of the algorithm from a differential equation perspective, meshing, time-stepping, and absorbing boundaries. An alternative approach to understanding the basic algorithm is from the integral form of Maxwell's equations that I particularly like because it gives a clear understanding of the FDTD method in terms of the underlying physics. The reader is referred to one of the references (A. Taflov, *Computational Electrodynamics: The FDTD Method*).

The MOM is presented in Chapter 4. Complete volumes are devoted to this subject, and the technical literature is vast on the MOM and applications. In the spirit of their original objectives, the authors have presented this difficult subject in a simple and straight-forward manner with Pocklington's integral equation, i.e., MOM applied to wire geometries. The treatment is brief, and more-or-less one-dimensional, but adequate for a basic understanding. A further advantage of the choice in introducing MOM in this fashion is that a

mature and commercially available MOM code (NEC) is largely wire-based.

The finite element method is presented in Chapter 5. The FEM presentation proceeds from a variational formulation and minimization of a quadratic functional, and may leave an inexperienced reader confused. An alternative path to the final algorithm is via a weak formulation (see J.N. Reddy, *An Introduction to the Finite Element Method*). I like this approach because a one-dimensional formulation is easily understandable. The 2D overview of triangular patch basis functions presented in Chapter 5 does give the reader a feeling for the solution approximation and meshing.

Chapters 6, 7, and 8 are at the heart of this book. The consistent theme emphasized in these chapters is "what and where to model" for EMI/EMC design. The reader is left with a good understanding of what is achievable in applying numerical modeling to EMC design, and how to approach and construct models that can lead to useful results. The treatment is a reflection of the authors extensive experience using modeling in their own work at IBM and Digital. Chapter 6 discusses anticipating and modeling the EMI coupling, as well as the noise source. Guidance in choosing a suitable technique, FDTD, FEM, or MOM for particular types of problems is also given.

Chapter 7 discusses creation of EMI/EMC models and details a number of examples including common-mode radiation from cables being driven against a shielding enclosure, excitation of heatsinks by an IC, and apertures in a shield. Inherent in these examples is insight into how EMI/EMC modeling can be used in developing better designs. For example, one configuration discussed, details the effects of coupling through a slot in an enclosure to an attached cable. Slots inevitably result in low-cost PC enclosures as a result of cost-effective attempts to seal unused expansion ports.

The example demonstrates developing a model to understand the coupling effects between the source, aperture, and attached cable. The result is a clear indication that the EMI problem is dominated by the source coupling to the aperture and provides direction on where attention should be focused in mitigating this problem, i.e., a ferrite sleeve on the attached cable is a waste of a good part for this particular case.

Chapter 8 is a more detailed continuation of Chapter 7, and focuses specifically on examples of multi-stage modeling for PCB level coupling to perforations in a shielding enclosure and coupling to an attached cable, antenna impedance important for I/O filter design, test site modeling, and basic PCB level modeling. The PCB level modeling example demonstrates the use of numerical modeling for developing an understanding of fundamental EMI coupling physics. The geometries can be relatively simple, but the resulting design concepts are powerful. Practicing EMC engineers commonly draw general design conclusions based on their experience with prototype or production hardware. This hardware is complex, and it is easy to draw incorrect conclusions regarding fundamental noise and coupling processes in the trial-and-error process of shipping products. Numerical EMI/EMC modeling is a powerful tool for developing an understanding of fundamental concepts, and experienced EMC engineers are well-versed in translating these to design.

Chapter 9 discusses model validation that provides good insight for engineers not experienced with modeling. Some very helpful caution is given regarding comparing radiated EMI measurements on a functioning product that are inherently not well controllable, with modeling results. Chapter 10 is a brief over-view on geometries that are representative of high-speed digital design aspects that may be suitable for numerical modeling. From the perspective of a practicing EMC engineer,

this provides direction on what can realistically be expected from numerical modeling, as well as problems on which to investigate and compare commercially available tools. From the standpoint of the numerical modeling community these problems represent some goals for which to strive, i.e., demonstrating (in particular through well-controlled measurements) modeling approaches for problems of interest to practicing EMC engineers.

Overall I found this a good book that achieves the author's stated goals very well, and I recommend it, in particular for practicing EMC engineers and numerical modelers. As I was reading the book and noting the aspects that I particularly liked or did not, I found that most of my criticisms were a matter of personal preference, and not fundamental disagreements with the treatment or presentation of topics. I would have liked to see more details in the examples that would allow the user to reproduce the author's results. While this is certainly more appropriate to research papers published in the refereed technical literature, it is important for those less experienced with modeling to initially have targets at which to shoot. Since the first author is taking a leading role in the EMC community through the IEEE EMC Society Technical Committee 9 (Computational Electromagnetics) in advancing the state of the art, and developing standard EMI/EMC modeling problems with proven results, a future addition might include this.

Application of numerical modeling in EMC design is relatively recent, and I consider this book the first stage of a "work in progress". The authors do not propose that this book is in any sense completed or concluded. I anticipate that this book will be updated and expanded periodically as the field progresses and grows.

THE APPLIED COMPUTATIONAL ELECTROMAGNETICS SOCIETY

CALL FOR PAPERS

The 16th Annual Review of Progress in Applied Computational Electromagnetics

March 20-25, 2000

Naval Postgraduate School, Monterey, California

"Share Your Knowledge and Expertise with Your Colleagues"

The Annual ACES Symposium is an ideal opportunity to participate in a large gathering of EM analysis enthusiasts. The purpose of the Symposium is to bring analysts together to share information and experience about the practical application of EM analysis using computational methods. The symposium offerings include technical presentations, demonstrations, vendor booths and short courses. All aspects of electromagnetic computational analysis are represented. Contact for details:

Technical Program Chairman

Doug H. Werner
EE Dept, Room 211, EEE
Penn State University
University Park, PA 16802
Phone: (814) 863-2946
Fax: (814) 863-8783
Email:dhw@psu.edu

Symposium Co-Chairman

Randy Haupt
EE Dept., 260
University Of Nevada
Reno, NV 89557-0153
Phone: (702) 784-6927
Fax: (702) 784-6627
Email:haupt@ee.unr.edu

Symposium Co-Chairman

PingJuan Werner
EE Dept.
Penn State Dubois Campus
Dubois, PA 15801
Phone: (814) 867-1452
Fax: (814) 863-8457
Email:dhw@psu.edu

Vendor Chair

Leo C. Kempel
Michigan State Univ.
ECE Engr.
2120 Engineering Bldg.
E. Lansing, MI 48824-1126
Phone: (517) 353 9944
Fax: (517) 353-1980
Email:l.kempel@ieee.org

Symposium Administrator

Richard W. Adler
ECE Dept, Code EC/AB
Naval Postgraduate school
833 Dyer Road, Room 437
Monterey, CA 93943-5121
Phone: (831) 646-1111
Fax: (831) 649-0300
Email:rwa@ibm.net

The ACES Symposium is a highly influential outlet for promoting awareness of recent technical contributions to the advancement of computational electromagnetics. Attendance and professional program paper participation from non-ACES members and from outside North America are encouraged and welcome.

Early Registration Fees; (approximate*)

ACES MEMBERS

\$290

NON-MEMBER

\$340

STUDENT/RETIRED/UNEMPLOYED \$130 (no proceedings)

STUDENT/RETIRED/UNEMPLOYED \$165 (includes proceedings)

*The exact fee will be announced later. Each conference registration is entitled to publish two papers in the proceedings free of charge. Excess pages over a paper limit of 8 will be charged \$15/page.

2000 ACES Symposium

Sponsored by:

ACES, NPS, U of NV, BYU, PSU

in cooperation with:

The IEEE Antennas and Propagation Society, the IEEE Electromagnetic Compatibility Society and USNC/URSI

**Visit ACES on line at: www.emclab.umn.edu/aces and
<http://aces.ee.olemiss.edu>**

THE APPLIED COMPUTATIONAL ELECTROMAGNETICS SOCIETY

CALL FOR PAPERS

The 16th Annual Review of Progress in Applied Computational Electromagnetics

March 20-25, 2000

Papers may address general issues in applied computational electromagnetics, or may focus on specific applications, techniques, codes, or computational issues of potential interest to the Applied Computational Electromagnetics Society membership. Area and topics include:

- Code validation
- Code performance analysis
- Computational studies of basic physics
- Examples of practical code application
- New codes, algorithms, code enhancements, and code fixes
- Computer Hardware Issues
- Partial list of applications:
 - antennas
 - radar imaging
 - shielding
 - EMP, EMI/EMC
 - dielectric & magnetic materials
 - microwave components
 - fiberoptics
 - communications systems
 - eddy currents
 - wave propagation
 - radar cross section
 - bioelectromagnetics
 - visualization
 - inverse scattering
 - MIMIC technology
 - remote sensing & geophysics
 - propagation through plasmas
 - non-destructive evaluation
- Partial list of techniques:
 - frequency-domain & time-domain techniques
 - integral equation & differential equation techniques
 - finite difference & finite element analysis
 - diffraction theories
 - modal expansions
 - hybrid methods
 - physical optics
 - perturbation methods
 - moment methods

INSTRUCTIONS FOR AUTHORS AND TIMETABLE

November 20, 1999: Submission deadline. Submit four copies of a full-length, camera-ready paper to the Technical Program Chairman. Please supply the following data for the corresponding author: name, address, email address, FAX, and phone numbers. See below for instructions for the format of paper.

December 21, 1999: Authors notified of acceptance.

PAPER FORMATTING REQUIREMENTS

The recommended paper length is 6 pages, with 8 pages as a maximum, including figures. The paper should be camera-ready (good resolution, clearly readable when reduced to the final print of 6 x 9 inch paper). The paper should be printed on 8-1/2 x 11 inch papers with 13/16 side margins, 1-1/16 inch top margin, and 1 inch on the bottom. On the first page, place title 1-1/2 inches from top with author and affiliation beneath the title. Single spaced type using 10 or 12 point front size, entire text should be justified (flush left and flush right). No typed page numbers, but number your pages lightly in pencil on the back of each page.

SHORT COURSES/HANDS-ON-WORKSHOP

Short courses and Hands-on-Workshops will be offered in conjunction with the Symposium covering numerical techniques, computational methods, surveys of EM analysis and code usage instruction. It is anticipated that short courses will be conducted principally on Monday and Friday. Workshops will be held Monday, Friday, and Saturday. **Short Course Fees: Half-day course \$100; Full-day course \$160. Workshop Fees: Half-day workshop \$120; Full-day workshop \$235. Fees are subject to change. Quoted fees apply only if booked before 1 March 2000.**

EXHIBITS

Vendor booths and demonstrations will feature commercial products, computer hardware and software demonstrations, and small company capabilities.

PRELIMINARY AGENDA

The Fifteenth Annual Review of Progress in Applied Computational Electromagnetics

NAVAL POSTGRADUATE SCHOOL
15-20 March 1999

Randy Haupt, Technical Program Chairman

Indira Chatterjee, Symposium Co-Chairman

James Henson, Symposium Co-Chairman

Michael Jensen, Short Course Chairman

Keith Whites, Vendor Chairman

Richard W. Adler, Symposium Administrator

MONDAY MORNING 15 MARCH 1999

0700-0730	CONTINENTAL BREAKFAST <i>(For short course and hands-on-workshop attendees only)</i>	Glasgow Courtyard
0730-0820	SHORT COURSE/HANDS-ON-WORKSHOP REGISTRATION	Glasgow 103
0830-1630	SHORT COURSE (FULL-DAY) #1 "Model-Order Reduction as a Means of Increasing the Efficiency and Effectiveness of Computational Electromagnetics" Andreas Cangellaris, University of Illinois at Urbana-Champaign, and Edmund Miller, Santa Fe, NM.	
0830-1630	SHORT COURSE (FULL-DAY) #2 "Finite-Difference Time-Domain Method" Omar Ramahi, Compaq Computer Corporation, Maynard, MA	
0830-1630	SHORT COURSE (FULL-DAY) #3 "Finite Elements for Electromagnetics", Scott Savage, Ansoft Corporation, Pittsburgh, PA.	
0830-1130	HANDS-ON-WORKSHOP (HALF-DAY) #4 "Basic MATHCAD" (Introduction for Course 9) Jovan Lebaric and Robert Vitale, Naval Postgraduate School, Monterey, CA.	
0900-1200	CONFERENCE REGISTRATION	Glasgow 103

MONDAY AFTERNOON

1330-1630	HANDS-ON-WORKSHOP (HALF-DAY) #5 "Basic MATLAB" (Introduction for Course #11) Jovan Lebaric and Robert Vitale, Naval Postgraduate School, Monterey, CA.	
1400-2000	CONFERENCE REGISTRATION	Glasgow 103

MONDAY EVENING

1900	PUBLICATIONS DINNER	
------	----------------------------	--

TUESDAY MORNING 16 MARCH 1999

0700-0745	CONTINENTAL BREAKFAST	Glasgow Courtyard
0745	ACES BUSINESS MEETING	President Perry Wheless Glasgow 102
0800	WELCOME	Randy Haupt Glasgow 102
0815	PLENARY SPEAKER:	Reinaldo Perez, JPL Glasgow 102

TUESDAY MORNING 16 MARCH 1999

SESSION 1: FDTD (Parallel with Session 2)
Chair: Atef Elsherbeni

- 0920 "A Finite-Difference Time-Domain Algorithm Based on the Recursive Convolution Approach for Propagation of Electromagnetic Waves in Nonlinear Dispersive Media" S.J. Yakura, J.T. MacGillivray, D. Dietz
- 0940 "Methods for Including Lumped Elements in FDTD Simulations" Ian Rumsey, Jason Mix, Melinda Piket-May
- 1000 "A Novel Subgridding Scheme for Refractive Index Adaptive FDTD" Fichtner T.O. Korner and W.
- 1020 **BREAK**
- 1040 "Characterizing Meander Line Antennas for RF and Wireless Communications Using the FDTD Techniques" Chun-Wen Paul Huang, Jiang-Bin James Chen, Atef Z. Elsherbeni, Charles E. Smith
- 1100 "Impulse Response of Microwave Devices by FDTD and Moment Expansion" Gaetano Marrocco, Fernando Bardati
- 1120 "The Cause of Oscillatory Dispersion Relation of Equivalent Circuit Parameters for Microstrip Components Using FDTD Method" Lee L. Liou
- 1140 "An Implicit Characteristic Based Finite Difference Method for Computational Electromagnetics" John H. Beggs, W. Roger Briley
- 1200 **LUNCH**
- 1200 **BOARD OF DIRECTORS LUNCHEON MEETING**

SESSION 2: ANTENNAS (Parallel with Session 1)
Chair: Nathan Cohen Co-Chair: Jacob Kim

- 0920 "End Fed Antennas" R.P. Haviland
- 0940 "Investigation of a Multi-Resonant Antenna for Wideband Application" P.L. Werner, N.V. Veremey, R. Mittra and D.H. Werner
- 1000 "Computation of Clustered Phased Array EM Fields Using Particle Accelerator Codes" Ross A. Speciale
- 1020 **BREAK**
- 1040 "Extended Ray-Optical Technique for Installed Performance of Large Airborne Antenna Systems" Jacob J. Kim, Kuang Wu, Sidney W. Theis, Oren B. Kesler
- 1100 "Antenna Imaging and Visualization" John Shaeffer, Brett Cooper
- 1120 "Are Fractals Naturally Frequency Invariant/Independent?" Nathan Cohen
- 1140 "The Ultimate Antenna Training Aid" Alan Nott
- 1200 **LUNCH**

TUESDAY AFTERNOON 16 MARCH 1999

INTERACTIVE POSTER SESSION
1300-1530

Ballroom, Herrmann Hall

VENDOR EXHIBITS
1300-1900

Ballroom, Herrmann Hall

WINE AND CHEESE BUFFET
1500-1700

Ballroom, Herrmann Hall

Ballroom, Herrmann Hall

N.I. Manaenkova

Reinaldo Perez

Hashim Yousif
Atef Z. Elsherbeni

Bruce Archambeault

Trevor W. Dawson

Ying Xiao and Yilong Lu

Wojciech L. Golik

Omar M. Ramahi

R.M. Bevensee

Kueichien C. Hill

John Shaeffer
Kam Horn

Ning Yuan
Changhong Liang
Xiaochun Nie

Peter J. Collins
J. Paul Skinner

Glasgow Courtyard

Feng Ling
Jianming Jin
Da-Gang Fang
Ningning Feng

Keith D. Trott
Rene D. Guidry

Yan-Chow Ma
Sunil Bindiganavale
Maurice Sancer

Leo C. Kempel

John L. Volakis
Lars S. Andersen
Thomas F. Eibert
Kubilay Sertel
Zhifang Li

WEDNESDAY MORNING 17 MARCH 1999**SESSION 4 : FINITE ELEMENTS I (cont)**

- | | | |
|------|---|------------------|
| 1120 | "A Hybrid MoM/FEM Method for Scattering from a Complex BOR with Appendages" | Andrew Greenwood |
| 1140 | "Frequency-Domain Complementary Operators for Finite Elements Simulation" | Omar M. Ramahi |

SESSION 5: MODEL-BASED PARAMETER ESTIMATION (Parallel with Session 4)
Chair: Andreas Cangellaris Co-Chair: Edmund Miller

- | | | |
|------|--|---|
| 0920 | "Model-Based Frequency Extrapolation of Antenna Radiation Characteristics on Complex Platforms" | Yanxun Wang
Hao Ling |
| 0940 | "Developing Adaptive Models and Estimating the Uncertainty of Presampled Spectral Data" | Edmund Miller |
| 1000 | "Techniques for Model-Based Parameter Estimation of Antenna Radiation Patterns" | R.J. Allard
D.H. Werner |
| 1020 | BREAK | |
| 1040 | "Full Wave Analysis of Generalized Microstrip Lines Using Model Order Reduction Techniques" | Kaladhar Radhakrishnan
Weng Cho Chew |
| 1100 | "Frequency and Angular Extrapolations in Hybrid Finite Element-Boundary Integral Systems" | Y.E. Erdemli
A.D. Brown
John L. Volakis |
| 1120 | "Reduced-Order Modeling of Three-Dimensional Electromagnetic Wave Fields" | R.F. Remis
P.M. van den Berg |
| 1140 | "Rapid Simulation of Electromagnetic Resonant Structures Using Model Order Reduction and Unstructured Finite Difference" | Li Zhao
Andreas Cangellaris |
| 1200 | LUNCH | |

WEDNESDAY AFTERNOON 17 MARCH 1999
SESSION 6: OPTIMIZATION (Parallel with Session 7)
Chair: John Volakis Co-Chair: Zach Baharav

- | | | |
|------|--|---|
| 1320 | "Recent Results in Electromagnetic Optimization of Microwave Components Including Microstrip T-Junctions" | J.W. Bandler
M.H. Bakr
N. Georgieva
M.A. Ismail
D.G. Swanson, Jr. |
| 1340 | "Extraction of Equivalent Circuits of Microwave Devices Using The Genetic Algorithm" | P.L. Werner
R. Mittra
D.H. Werner |
| 1400 | "A Comparison of Various Optimization Strategies for Yagi-Uda Antenna Design" | Eric A. Jones
William T. Jones |
| 1420 | "Broad-Banding Uniformly Excited Antenna Arrays Using a Genetic Algorithm" | Brian J. Barbisch
D.H. Werner |
| 1440 | "Optimizing Genetic Algorithm Parameters for Adaptive Nulling" | You Chung Chung
Randy Haupt |
| 1500 | BREAK | |
| 1520 | "Mutual Coupling Compensation for Circular Arrays Using a Genetic Algorithm" | Beng-Kiong Yeo
Yilong Lu |
| 1540 | "Pareto Genetic Algorithm Based Optimization of Log-Periodic Monopole Arrays Mounted on Realistic Platforms" | D.S. Weile
S.E. Fisher
E. Michielssen
W. Woody |
| 1600 | "Optimum Design of Non-Uniform Luneburg Lens Antennas: Genetic Algorithms with Adaptive Cost Function" | H. Mosallaei
Y. Rahmat-Samii |

WEDNESDAY AFTERNOON 17 MARCH 1999**SESSION 6: OPTIMIZATION (cont)**

- | | | |
|------|--|-------------------|
| 1620 | "On the Search for the Optimal Grouping of Basis Functions" | Zachi Baharav |
| 1640 | "Genetic Algorithms and their Practical Implementation Strategies for Design Optimization of Electrical Devices" | Osama A. Mohammed |

SESSION 7: WIRE MODELS (Parallel with Session 6)
Chair: Keith Lysiak Co-Chair: Chris Trueman

- | | | |
|------|---|--|
| 1320 | "Extension of a Thin-Wire Algorithm for Wires Moved Laterally within a Mesh" | Gerald J. Burke
David J. Steich |
| 1340 | "A Practical Method for Increasing the Speed and Stability of the Matrix Solve in Moment Method Simulations within a Frequency Band" | Hugh MacMillan
John M. Dunn |
| 1400 | "Modeling the Bifilar Helix Antenna Using NEC 4.1" | Steven R. Best |
| 1420 | "MMSNEC - Multiple Matrix Solver NEC" | J.V. Hagen
R. Mittra
D.H. Werner |
| 1440 | "Comparison and Results for Models of a Thick Bent-Wire Dipole Using NEC4 and WIPL" | James Stamm
Mun-Won Fenton
James K. Breakall |
| 1500 | BREAK | |
| 1520 | "MF Broadcast Antennas and Antenna Arrays: A Historic Branch of Antenna Engineering Revisited by Computer Simulation and Measurement" | John Belrose |
| 1540 | "The High Frequency Electromagnetic Environment of the U.S. Coast Guard 87-foot Coastal Patrol Boat" | Michael E. McKaughan
David Melton |
| 1600 | "Extending a MoM/PO/UTD Hybrid Method by an Automatic Selection of the Computational Methods Based on Neural Networks" | U. Jakobus
A. Buchau
F.M. Landstorfer |
| 1620 | "Umbrella Top Loaded Antennas: Base Fed, Folded, and with a Tuned Insulated Counterpoise" | John Belrose |

WEDNESDAY EVENING 17 MARCH 1999

- | | | |
|------|-----------------------|-------------------------------------|
| 1830 | NO HOST BAR | El Prado Room, Herrmann Hall |
| 1930 | AWARDS BANQUET | El Prado Room, Herrmann Hall |

THURSDAY MORNING 18 MARCH 1999

- | | | |
|---|--|--|
| 0710-0810 | CONTINENTAL BREAKFAST | Glasgow Courtyard |
| 0815 | PLENARY SPEAKER: Edmund K. Miller, Santa Fe, NM | |
| SESSION 8: CONFORMAL ANTENNAS (Parallel with Session 9)
Chair: Doug Werner Co-Chair: Ping Werner | | |
| 0920 | "Mutual Coupling Between Microstrip Antennas on a Cylindrical Surface" | Kin-Lu Wong |
| 0940 | "Simulating the Dielectric-Loaded Quadrifilar Helix Antenna Using a Brute-Force TLM Approach" | O.P. Leisten
J. C. Vardaxoglou
E. Agborow |
| 1000 | "Conformal Aperture Coupled Microstrip Patch Antennas on Cylindrical Surfaces for Radar and SDMA Applications" | D. Loffler and W. Wiesbeck |
| 1020 | BREAK | |
| 1040 | "Absorbing Boundary Conditions for Convex Object-Conformable Boundaries" | Omar M. Ramahi |
| 1100 | "Cylindrical and Conical FSS" | J.C. Vardaxoglou
G. Loukos
M. Jayawardene
R. Seager and J. Eade |

THURSDAY MORNING 18 MARCH 1999

SESSION 8: CONFORMAL ANTENNAS (cont)

- | | | |
|------|--|---|
| 1120 | "A MATLAB Code for Multi-Layered FSS:S with Generally Shaped Elements" | Anders Stjernman |
| 1140 | "A Riciprocity Approach for Calculating Radiation Patterns of Arbitrarily Shaped Patch Antennas Mounted on Circularly-Cylindrical Platforms" | Doug Werner, G.D. Mouyis
R. Mittra and J.S. Zmysto |

SESSION 9: FINITE ELEMENTS II (Parallel with Session 8) Chair: David B. Davidson

- | | | |
|------|--|--|
| 0920 | "Hierarchal 2d and 3d Vector Finite Elements for Electromagnetic Wave Eigenvalue Problems" | David B. Davidson
Riana H. Hansmann |
| 0940 | "Local Error Estimation for High-Frequency Problems Using Hierarchical Tangential Vector Finite Elements" | Scott Savage
John Manges |
| 1000 | "Time-Domain Simulation of Nonlinear Transmission Lines: Interface of Finite Elements to Circuit Analysis" | Karim N. Wassef
Andrew F. Peterson |

1020 BREAK

SESSION 10: ERRORS (Parallel with Session 8) Chair: Edmund K. Miller

- | | | |
|------|--|--|
| 1040 | "A Comparison of Solution Accuracy Resulting From Factoring and Inverting Ill-Conditioned Matrices" | Edmund K. Miller |
| 1100 | "Benchmarks for Integral Equation Solutions of Wideband Scattering: The Spherical Cap Reflector" | S.M. Booker
P.D. Smith
E.D. Vinogradova
S.S. Vinogradov |
| 1120 | "Propagation of Errors through Computer Codes via Fuzzy Logic" | R.M. Bevensee |
| 1140 | "Scalable Algorithm for Solving Boundary Value Problems Arising in Electromagnetics Based on Implicit Operator Projection" | Michal Rewienski
Michal Mrozowski |

1200 LUNCH

**SESSION 11: TIME DOMAIN METHODS (Parallel with Session 12)
Chair: John Dunn Co-Chair: Chris Holloway**

- | | | |
|------|--|--|
| 1320 | "Large Scale FD-TD--A Billion Cells" | Ulf Andersson
Gunnar Ledfelt |
| 1340 | "New High Order Time Stepping Schemes for Finite Differences" | Martin Aidam
Peter Russer |
| 1400 | "The Mismatch of Perfectly Matched Layers (PML) in Cylindrical and Spherical Coordinate System" | Li Zhao
Andreas Cangellaris |
| 1420 | "The Effect of the Binding Material Permittivity on the Input Impedance of Cthas" | Khaled M. Elsherbeni
Franz A. Pertl
Robert P.M. Craven
James E. Smith |
| 1440 | "Numerical Dispersion in Haar-Wavelet Based MRTD Scheme--Comparison Between Analytical and Numerical Results" | Masafumi Fuji
Wolfgang J.R. Hoefer |
| 1500 | BREAK | |
| 1520 | "Comparison Between Discontinuous Galerkin Method and a Finite Volume Time-Domain Method in Solving Maxwell Equations, in Heterogeneous Media" | Malika Remaki
L. Fezoui |
| 1540 | "A Controllability Method for the Calculation of the Time Periodic Solutions of the Vlasov-Maxwell System" | Mihai Bostan |
| 1600 | "Time-Domain Equivalent Edge Currents" | A. Altintas
S. Lindermeier
Peter Russer |

THURSDAY MORNING 18 MARCH 1999

SESSION 11: TIME DOMAIN METHODS (cont)

- | | | |
|------|--|---|
| 1620 | "A Numerical Study on the Accuracy of TLM-SCN Formulations for the Solution of Initial Value Problems" | Jurgen N. Rebel
Martin Aidam
Peter Russer |
| 1640 | "Multilevel, Multiresolution Analysis of Printed Antennas and Circuits: A Dual Scalar Approach" | G. Vecchi, P. Pirinoli
M. Sereno-Garino
L. Matekovits
M. Orefice |

SESSION 12: BIOELECTROMAGNETICS (Parallel with Session 11)
Chair: Cynthia Furse Co-Chair: Susan Hagness

- | | | |
|------|---|---|
| 1320 | "Computational Estimate of the Frequency Response of Metallic Implants in Biological Tissues Exposed to RF Fields" | A.H.J. Fleming
V. Anderson
J. Rowley |
| 1340 | "Towards Computational Methods for Studying Cellular Effects Due to EM Fields" | A.H.J. Fleming |
| 1400 | "Comparison of Computer Simulated and Measured SAR Values in the Head of a Human Phantom Next to a Mobile Phone" | F.J.C Meyer
U Jakobs |
| 1420 | "Validation of the FDTD Near Fields of a Portable Radio Handset and Simple Head" | C.W. Trueman
S.J. Kubina
D. Cule and W.R. Lauber. |
| 1440 | "FDTD for Bioelectromagnetics: Modeling MICS Implants in the Human Body" | Eduardo H. Villaseca |
| 1500 | BREAK | |
| 1520 | "Numerical Studies of an Ultrawideband Microwave Radar Technology for the Detection of Nonpalpable Breast Tumors" | Susan C. Hagness
Allen Taflov
Jack E. Bridges |
| 1540 | "Numerical Dosimetry for Human Occupational Exposure to Realistic 60-Hz Magnetic Fields" | Trevor W. Dawson
K. Caputa
Maria A. Stuchly |
| 1600 | "Characterization of Near Electromagnetic Fields From Hand-Held Radio Antennas" | Malcolm Packer |
| 1620 | "Application of Multigrid Method for Quick Simulation of SAR and Temperature Distribution During Hyperthermia Treatment of Cervical Malignancies" | Michal P. Debicki
Michal Mrozowski
Piotr Debicki. |

FRIDAY 19 MARCH 1999

- 0730-0830 **CONTINENTAL BREAKFAST**
(For short course and hands-on-workshop attendees only)
- 0830-1130 **SHORT COURSES (HALF-DAY) #6**
"Verification and Validation of Computational Electromagnetics Software"
Edmund K. Miller, Santa Fe, NM
- 1330-1630 **SHORT COURSES (HALF-DAY) #7**
"A Survey and Comparison of Computational Electromagnetics Options"
Edmund K. Miller, Santa Fe, NM
- 0830-1630 **SHORT COURSES (FULL-DAY) #8**
"Genetic Algorithm Optimization"
Randy L. Haupt, and J. Michael Johnson, University of Nevada, Reno, NV
- 0830-1630 **HANDS-ON-WORKSHOP (FULL-DAY) #9**
"Method of Moments (MoM) Using MATHCAD"
Jovan Lebaric and Robert Vitale, Naval Postgraduate School.
- 0830-1630 **HANDS-ON-WORKSHOP (FULL-DAY) #10**
"Introduction to Using NEC under Windows"
J.K. Breakall, Penn State University, G.J. Burke, LLNL, and R.W. Adler, Naval Postgraduate School.

PLEASE NOTE THAT A 10% DISCOUNT IS IN EFFECT FOR ALL WORKSHOPS TAKEN AFTER ATTENDING AN INITIAL WORKSHOP. THIS APPLIES TO THE GROUP OF WORKSHOPS FOR MATLAB AND MATHCAD. IT ALSO APPLIES TO THE NEC WORKSHOPS. NOTE THAT MATLAB/MATCAD DISCOUNTS DO NOT APPLY TO THE NEC WORKSHOPS, AND VICE VERSA.

SATURDAY MORNING MARCH 20, 1999

- 0730-0830 **CONTINENTAL BREAKFAST**
(For short course and hands-on-workshop attendees only)
- 0830-1630 **HANDS-ON-WORKSHOP (FULL-DAY) #11**
"Finite Difference (FD) Using MATLAB"
Jovan Lebaric and Robert Vitale, Naval Postgraduate School, Monterey, CA
- 0830-1630 **HANDS-ON-WORKSHOP (FULL-DAY) #12**
"Advanced Applications using NEC4.1 under Windows"
J.K. Breakall, Penn State University, G.J. Burke, LLNL, and R.W. Adler, Naval Postgraduate School, Monterey, CA.
-

REGISTRATION/SHORTCOURSES/HANDS-ON-WORKSHOPS

THE APPLIED COMPUTATIONAL ELECTROMAGNETICS SOCIETY
15TH ANNUAL REVIEW OF PROGRESS IN APPLIED COMPUTATIONAL ELECTROMAGNETICS
 March 15 - 20, 1999 -- Naval Postgraduate School, Monterey, CA

I. Conference Registration

Please print (Black ink) (Note: Conference Registration fee does not include ACES Membership Fee/Short Course or Workshop Fee)

 Last Name First Name Middle Initial

 Mailing Address Company/Organization/University Department/Mail Station

 City Provinces/State Country Zip/Postal Code

 Telephone Fax E-mail Amateur Radio Call Sign

	BEFORE 3/1/99	3/1/99 TO 3/14/99	At Registration
ACES MEMBER	<input type="checkbox"/> \$290	<input type="checkbox"/> \$305	<input type="checkbox"/> \$320
NON-MEMBER	<input type="checkbox"/> \$340	<input type="checkbox"/> \$355	<input type="checkbox"/> \$370
STUDENT/RETIRED/UNEMPLOYED	<input type="checkbox"/> \$130 (no proceedings)	<input type="checkbox"/> \$130	<input type="checkbox"/> \$130
STUDENT/RETIRED/UNEMPLOYED	<input type="checkbox"/> \$165 (includes proceedings)	<input type="checkbox"/> \$165	<input type="checkbox"/> \$165
BANQUET <input type="checkbox"/> Meat <input type="checkbox"/> Fish	<input type="checkbox"/> \$35	<input type="checkbox"/> \$35	<input type="checkbox"/> \$35

Total for Section I _____

II. ACES '99 Short Courses and Hands-on-Workshops

	BEFORE 3/1/99	3/1/ TO 3/14	3/15/99
1. Model-Order Reduction as a Means of Increasing the Efficiency and Effectiveness of Computational Electromagnetics. Full day: Monday, March 15	<input type="checkbox"/> \$160	<input type="checkbox"/> \$175	<input type="checkbox"/> \$190
2. Finite-Difference Time-Domain Method Full day: Monday, March 15	<input type="checkbox"/> \$160	<input type="checkbox"/> \$175	<input type="checkbox"/> \$190
3. Finite Elements for Electromagnetics Full Day: Monday March 15.	<input type="checkbox"/> \$160	<input type="checkbox"/> \$175	<input type="checkbox"/> \$190
4. Basic MATHCAD (Introduction for Course #9) Half Day, Hands-on Workshop: Monday morning, March 15	<input type="checkbox"/> \$120	<input type="checkbox"/> \$135	<input type="checkbox"/> \$150
5. Basic MATLAB (Introduction for Course #11) Half Day, Hands-on Workshop: Monday afternoon, March 15	<input type="checkbox"/> \$120	<input type="checkbox"/> \$135	<input type="checkbox"/> \$150
6. Verification and Validation of Computational Electromagnetic Software, Half Day: Friday morning, March 19	<input type="checkbox"/> \$100	<input type="checkbox"/> \$115	<input type="checkbox"/> \$130
7. A Survey and Comparison of Computational Electromagnetics Options, Half Day: Friday afternoon, March 19	<input type="checkbox"/> \$100	<input type="checkbox"/> \$115	<input type="checkbox"/> \$130

- | | | | | | | |
|--|--------------------------|-------|--------------------------|-------|--------------------------|-------|
| 8. Genetic Algorithm Optimization
Full Day: Friday, March 19 | <input type="checkbox"/> | \$160 | <input type="checkbox"/> | \$175 | <input type="checkbox"/> | \$190 |
| 9. Method of Moments (MoM) Using MATHCAD
Full Day, Hands-on Workshop: Friday, March 19 | <input type="checkbox"/> | \$235 | <input type="checkbox"/> | \$250 | <input type="checkbox"/> | \$265 |
| 10. Introduction to Using NEC Under Windows
Full-Day, Hands-on Workshop: Friday, March 20. | <input type="checkbox"/> | \$235 | <input type="checkbox"/> | \$250 | <input type="checkbox"/> | \$265 |
| 11. Finite Difference (FD) Using MATLAB
Full Day, Hands-on Workshop: Saturday, March 20. | <input type="checkbox"/> | \$235 | <input type="checkbox"/> | \$250 | <input type="checkbox"/> | \$265 |
| 12. Advanced Applications Using NEC4.1 Under Windows
Full Day, Hands-on Workshop: Saturday, March 20. | <input type="checkbox"/> | \$235 | <input type="checkbox"/> | \$250 | <input type="checkbox"/> | \$265 |

Total for Section II - _____

TOTAL PAYMENTS

Include all Applicable Fees Here

Section I _____

Section II _____

Total Remittance Submitted (U.S. Dollars Only): - _____

CREDIT CARD USERS

If you are paying by credit card & card is your own, fill out the information requested above and sign your name below.. If the card you are using is not your card, fill out the information above, and have the card holder (1) print and sign his/her name below, and (2) enter his or her complete address below.

Non-USA participants: Prices are in U.S. dollars. All currencies must be converted to U.S. dollars payable by banks with U.S. affiliates. (1) **Bank Checks**, if (a) drawn on a U.S. Bank, (b) have U.S. bank address, (c) contain series of (9) digit mandatory routing numbers; (2) **Traveler's Checks** (in U.S. \$\$); (3) **International Money Order** drawn in U.S. funds, payable in U.S.; (4) **Credit Cards**: Visa, MasterCard, Discover and AmEx.

PAYMENT SHOULD ONLY BE MADE PAYABLE TO: "ACES"

Method of payment:

- ☐ Bank Check for the total amount is enclosed (payable to ACES). ⁽¹⁾
☐ Traveler's Check for the total amount is enclosed (payable to ACES). ⁽²⁾
☐ International Money Order for the total amount is enclosed (payable to ACES). ⁽³⁾
☐ Charge to: ☐ Master Card ☐ Visa ☐ Discover ☐ AMEX. ⁽⁴⁾

Card Number

--	--	--	--	--	--	--	--	--	--	--	--	--	--	--	--	--	--	--	--

Exp. Mo. _____ Yr. _____

Print Name _____

Sign Name _____

Address _____

City/State/Country _____

Zip Code _____

Send this form to Richard W. Adler, ECE Department, Code EC/AB, Naval Postgraduate School, 833 Dyer Road, Room 437, Monterey, CA 93943-5121, telephone 831-646-1111, fax 831-649-0300, email: rwa@ibm.net

SHORT COURSE/HANDS-ON WORKSHOP INFORMATION

March 15, 19 & 20, 1999
[Monday, Friday, Saturday]

THE 15TH ANNUAL REVIEW OF PROGRESS IN APPLIED COMPUTATIONAL ELECTROMAGNETICS

GENERAL INFORMATION

The Applied Computational Electromagnetics Society (ACES) is pleased to announce twelve short courses and Hands-on-Workshops, to be offered with its annual meeting on March 15-20, 1999. The short courses will be held on Monday and Friday. Hands-on-Workshops will be held Monday, Friday, and Saturday. The fee will be \$100 for a half-day short course and \$160 for a full-day short course, if booked before Sunday, March 1, 1998. The fee for a half-day Workshop is \$120 if booked before 1 March, and for a full-day Workshop \$235 if booked before 1 March. **(See Registration/Short Course and Hands-on-Workshops Form for detailed fee and date structure).** Short Course and Hands-on-Workshops registration begins at 7:30 AM on Monday, 15th. ACES has the right to cancel a course at any time with full refund. **PREREGISTRATION BY MAIL IS SUGGESTED!** For further information contact Prof. Michael A. Jensen, Short Course Chairman, Brigham Young University, ECE Department, 459 CB, Provo, UT 84602, Phone 801-378-5736, FAX 801-378-6586, Email:jensen@ee.byu.edu, or Richard W. Adler, ECE Dept., Code EC/AB, Naval Postgraduate School, 833 Dyer Rd, Room 437, Monterey, CA 93943-5121. Phone 831-646-1111, fax 831-649-0300, email:rwa@ibm.net. **Short Course/Workshop attendance is NOT covered by the Symposium Registration Fee!** Short courses and Hands-on-Workshops can be taken without attendance at Symposium. [Note: Tuesday through Thursday will be technical sessions; Tuesday afternoon will feature vendor exhibits, Interactive Technical Session, and Wine and Cheese Buffet].

COURSE DESCRIPTIONS

1. Model-Order Reduction as a Means of Increasing the Efficiency and Effectiveness of Computational Electromagnetics

Andreas Cangellaris, University of Illinois at Urbana-Champaign and Edmund K. Miller, Santa Fe, NM - Full Day: Monday, March 15.

Hidden within first-principles solutions of Maxwell's equations, which provide what can be appropriately described as micro models of electromagnetic phenomena, is the possibility of representing various observables in simpler ways using reduced-order, or macro models, a process that is generically called 'model-order reduction' (MOR). Knowledge of such macro models, ideally that are physically based, can be helpful in ways ranging from reducing the computer cost of achieving desired solutions to developing more compact representations of observables. One specific approach to MOR is to estimate unknown parameters of macro models from sampled data, a process called 'model-based parameter estimation' (MBPE). This lecture will survey some applications of MBPE in electromagnetic modeling and demonstrate various benefits that result. It should be observed that the designation MBPE has evolved in EM primarily from application to integral-equation (IE) models, whereas the term MOR has primarily been associated with application to differential-equation (DE) models. While conceptually equivalent, it might be observed that the term MOR describes a general goal whereas MBPE describes a particular approach to achieving that goal.

The opportunities provided by MOR and MBPE are currently being explored in the context of various first-principles EM models. Examples to be discussed of MBPE applications to IEs are adaptive sampling of frequency spectra and radiation patterns, in both cases to minimize the number of samples needed to approximate a continuous response to a specified uncertainty. Other IE applications of MBPE to be illustrated are estimating the accuracy of available data and reducing the fill-time of impedance matrices. Among the most successful applications of MOR to DEs are those based on the Lanczos and Arnoldi algorithms. Examples of these will be presented with particular emphasis on how they can be incorporated directly into existing finite-difference and finite element codes, also having the goal of reducing the number of samples needed to estimate broadband frequency-responses. Direct development of reduced-order macro models for EM components and systems through the use of such algorithms will be demonstrated. Methodologies will also be presented for the incorporation of these macro models in general-purpose, network analysis-oriented simulators for system-level analysis.

2. Finite-Difference Time-Domain Method

Omar M. Ramahi, Compaq Computer Corporation, Maynard, MA - Full Day: Monday, March 15.

With the rapidly increasing complexity of today's electromagnetic applications, the Finite-Difference Time-Domain method is emerging as one of the most versatile and robust electromagnetic analysis and design tools available. The objective of this course is to introduce and provide a working knowledge of FDTD. This is intended to enable the developer to create functional FDTD-based codes, and to allow the user of FDTD codes to understand the pertinent FDTD modeling parameters which relate to the model geometry and excitation, and consequently their impact on simulation accuracy. The theoretical aspects of the FDTD method will only be addressed in as much as they impact practical applications.

The full-day course will be divided into two sessions: morning and afternoon. The first session will introduce the underlying fundamentals of second-order and fourth-order accurate FDTD method. The FDTD modeling parameters are discussed followed by a thorough coverage of the essential elements needed to create a complete FDTD model, such as primary energy sources and mesh-truncation techniques (analytical boundary conditions and perfectly matched material). Next, near and far field extension techniques are presented for scattered- and total-field formulations, and attention will be given to their practical and efficient implementation. Numerical errors are discussed with special focus on their proper interpretation in engineering applications. The first session will end with the FDTD treatment of different material, such as dispersive, magnetic and non-linear media, including distributed and lumped circuit elements.

The afternoon session will be exclusively dedicated to the application of FDTD to real-world problems in the areas of high-frequency electronic packaging, EMI/EMC, modern antenna design, and RCS prediction. In presenting these examples, emphasis is placed on correct FDTD parameters and primary energy source selection that will resemble the physical conditions of the problem. Also, we highlight the use of proper mesh-truncation techniques that will optimize the use of resources vis-a-vis the problem-specific accuracy levels. This session will discuss the proper interpretation of FDTD results, especially when extracting frequency-domain results from time-domain data.

3. Finite Elements for Electromagnetics

Scott Savage, Ansoft Corporation, Pittsburgh, PA, - Full Day: Monday, March 15.

This course will develop two-dimensional and three-dimensional finite elements for application to electromagnetic problems. Both scalar (node-based) and vector (edge-based) finite elements will be discussed in detail. Advanced topics, including adaptive refinement, mesh truncation, singular elements, and high-order basis functions will be presented. Applications will include antennas, scattering, microwave components, electronic packaging, and electromagnetic compatibility.

4. Basic MATHCAD" (Introduction for Course #9)

Jovan Lebaric and Robert Vitale, Naval Postgraduate School, Monterey, CA - Half Day, Hands-on Workshop: Monday morning, March 15.

This is a half-day hands-on workshop to introduce MATHCAD mathematical software: learn text and formula editing, numeric and symbolic calculations, and visualization and animation in MATHCAD. The workshop will be held in an 18-seat PC Lab, with one attendee per PC (enrollment limited to 18 attendees).

5. Basic MATLAB" (Introduction for Course #11)

Jovan Lebaric and Robert Vitale, Naval Postgraduate School, Monterey, CA - Half Day, Hands-on Workshop: Monday afternoon, March 15.

This is a half-day hands-on workshop to introduce MATLAB programming environment: learn basics of MATLAB syntax, matrix/vector/element-by-element operations, code vectorization, and graphics and graphical user interface (GUI) creation in MATLAB. The workshop will be held in an 18-seat PC Lab, with one attendee per PC (enrollment limited to 18 attendees).

6. Verification and Validation of Computational Electromagnetics Software

Edmund K. Miller, Santa Fe, NM - Half Day: Friday Morning, March 19.

One of the most time-consuming activities associated with developing and applying EM computer models is that of verifying code (software) performance and validating the model results. Few available computational packages offer the user any built-in assistance in resolving these important issues. This lecture will discuss the kinds of errors that most commonly occur in modeling, and present numerous examples of validation checks that can be considered. Also discussed are the kinds of information that can be realistically expected from a computer model and how and why the computed results might differ from physical reality.

7. A Survey and Comparison of Computational Electromagnetics Options

Edmund K. Miller, Santa Fe, NM - Half Day: Friday Afternoon, March 19.

The growing variety of computational electromagnetic (CEM) codes that is becoming available makes choosing a specific model for a given application increasingly confusing to the electromagneticist who is concerned with solving problems but not with becoming a software expert. This short course will compare the generic approaches on which all CEM models are based in terms of their analytical formulations, numerical implementations, and computational requirements. The relative advantages and limitations of the various model types will be summarized to identify the best modeling approach to a given problem. The goal will be to provide a basis for more informed choices when making modeling decisions for practical applications.

8. Genetic Algorithm Optimization

Randy L. Haupt and J. Michael Johnson, University of Nevada, Reno, NV - Full Day: Friday, March 19.

This course begins with the basics of genetic algorithms. The advantages and disadvantages of the genetic algorithm and comparisons with traditional numerical optimization techniques will be presented. Participants will receive enough information to code their own genetic algorithm. Selecting genetic algorithm parameters and performance measures will be discussed. Various applications to computational electromagnetics problems will be presented, such as antenna array design, MOM-genetic algorithm microstrip antenna design, and optimal wireless network layout.

9. Method of Moments (MoM) Using MATHCAD

Jovan Lebaric and Robert Vitale, Naval Postgraduate School, Monterey, CA - Full Day, Hands-on Workshop: Friday, March 19.

This is a full day hands-on workshop that requires basic MATHCAD proficiency or attendance at the BASIC MATHCAD workshop on Monday morning for MATHCAD novices. The objective of this workshop is to introduce MATHCAD implementation of MoM for static and time-harmonic EM problems. The topics are:

1. MoM for Electrostatics: Superposition, Green's Function Integrals, Potential and Field Visualization
Examples: Wire at a Known Potential, Capacitance of Parallel Wires, Microstrip Impedance
2. MoM for Radiation and Scattering for Wire Grid Models: Mixed Potential Formulation, Green's Function Integrals, Far Field Visualization
Examples: Radiation and Scattering for a Wire Dipole, Radiation for a Two Element Yagi Antenna
3. MoM Eigen Analysis: MoM Eigen-problem Formulation, Green's Function Approximations
Examples: Eigen-spectrum for a Wire Dipole, Eigen-spectrum for a "Stick" Aircraft Model
4. Code Demos: MoM code IVY and EM eigen-analysis code EIGEN The workshop will be held in an 18-seat PC Lab, with one attendee per PC (enrollment limited to 18 attendees).

10. Introduction to Using NEC under Windows

James K. Breakall, Gerry J. Burke and Richard W. Adler - Full Day, Hands-on Workshop: Friday, March 19.

During this workshop, those who are already familiar with NEC-MOM will be introduced to NEC-Win BASIC and NEC-Win PRO. The user friendly Windows interface of these codes features a powerful wire structure viewer for easy debugging of input datasets and for viewing currents on the structure, plus a set of plotters for Smith Charts, polar radiation patterns. Rectangular plots include patterns, near fields, currents, impedance and VSWR. A 3-D pattern surface plot is also available. For ease of dataset generation, the full NEC command set is supported by pop-up dialogue boxes. Each attendee will follow the instruction on a PC and will be offered a discounted price for the code.

11. Finite Difference (FD) Using MATLAB

Jovan Lebaric and Robert Vitale, Naval Postgraduate School, Monterey, CA – Full Day, Hands-on Workshop: Saturday, March 20.

This is a full day hands-on workshop that requires basic MATLAB proficiency or attendance at the BASIC MATLAB workshop on Monday afternoon for MATLAB novices. The objective of this workshop is to introduce MATLAB implementation of FD for static and transient EM problems. The topics are:

1. FD for Electrostatics and Magnetostatics: FD Formulation, Transparent Grid Termination (TGT) in Statics, Potential and Field Visualization Example: Dielectric Substrate Microstrip
2. Finite Differences in Time Domain (1-D): FD Formulation, Source Implementation, Transparent Grid Termination, Field Visualization Examples: TEM Transmission Line and Bounce Diagram Visualization, Reflection and Transmission for a Dielectric Slab
3. Finite Differences in Time Domain (2-D): FD Formulation, Source and Incident Field Implementation, Transparent Grid Termination, Field Visualization Examples: Line Source in Vicinity of a PEC Rod, Scattering for a PEC Rod. The workshop will be held in an 18-seat PC Lab, with one attendee per PC. (enrollment limited to 18 attendees).

12. Advanced Applications Using NEC4.1 under Windows

James K. Breakall, Penn State University, Gerry J. Burke, LLNL, and Richard W. Adler, Naval Postgraduate School - Full Day, Hands-on Workshop: Saturday, March 20.

This full-day hands-on workshop features the use of GNEC, containing a Windows version of NEC4.1, the latest member of the family of NEC-MOM codes. It is intended for those who are experienced NEC4 users and for those who can benefit from the same interface support of NEC-Win PRO. After a brief introduction to GNEC-specific features, the focus will be on the creation and debugging of numerical models of complex structures and the efficient use of computer memory under Windows for NEC4. The attendees will be able to interact with the instructors on a one-on-one basis and with the class during the applications portion of the workshop. Each attendee will use a PC during the instruction and will be offered a discounted price for the code, if they are a registered user of NEC4.

PLEASE NOTE THAT A 10% DISCOUNT IS IN EFFECT FOR ALL WORKSHOPS TAKEN AFTER ATTENDING AN INITIAL WORKSHOP. THIS APPLIES TO THE GROUP OF WORKSHOPS FOR MATLAB AND MATHCAD. IT ALSO APPLIES TO THE NEC WORKSHOPS. NOTE THAT MATLAB/MATCAD DISCOUNTS DO NOT APPLY TO THE NEC WORKSHOPS, AND VICE VERSA

MOTELS / HOTEL LIST FOR MARCH 1999 ACES SYMPOSIUM

15-20 MARCH 1999

**** (WITHIN WALKING DISTANCE OF NPS)**

FIRESIDE LODGE () (1 star)**
1131 10th St. Monterey, CA 93940
Phone: (831) 373-4172 FAX: (831) 655-5640
Rates: **Govt.** \$79 --- **Conf.** \$79 + tax

STAGECOACH MOTEL () (1 Star)**
1111 10th St. Monterey, CA 93940
Phone: (831) 373-3632 FAX: (831)-648-1734
Rates: **Govt.** \$85. --- **Conf.** \$85 + tax

**MONTEREY HILTON/FORMERLY
HOLIDAY INN (**) (3 Star)**
1000 Aguajito Rd. Monterey, CA 93940
(831) 373-6141 FAX: (831)375-2367
Rates: **Govt.** \$94-104 --- **Conf.** \$119-129 + tax

HYATT HOTEL & RESORT () (4 Star)**
1 Old Golf Course Rd. Monterey, CA 93940
Phone: (831) 372-1234 FAX: (831)-375-6985
Rates: **Govt.** \$94-119--- **Conf.** \$159-184 +tax.

No blocks of rooms are set aside at Monterey Bay Lodge or Super 8 Motel, but they quoted their rates below.

MONTEREY BAY LODGE () (2 Star)**
55 Camino Aguajito, Monterey, CA 93940
Phone: (831) 372-8057 FAX: (831) 655-2933
Rates: **Govt.** \$67.15 --- **Conf.** \$67.15 + tax.

SUPER 8 MOTEL (2 Star)
2050 Fremont St. Monterey, CA. 93940
Phone: (831) 373-3081 FAX: (831) 372-6730
Rates: **Govt. & Conf.** --- \$49 - \$89
Conf. \$49 - 89 + tax.

(1) MOTELS WEEKEND RATES MAY BE HIGHER THAN WEEKDAYS. (2) MENTION THAT YOU ARE ATTENDING THE "ACES" CONFERENCE AT NPS WHEN BOOKING (3) CUT OFF DATE FOR CONFERENCE RATES IS USUALLY 13 FEBRUARY 1999 (CHECK WITH THE HOTEL) (4) ATTENDEES ON GOVT ORDERS DO NOT PAY TAX. ATTENDEES PAYING CONF. RATE, PAYS TAX. THIS APPLIED TO ABOVE RATE LINE

IMPORTANT INFORMATION FOR ACES ATTENDEES, PLEASE READ.

Hotel room tax exemption requires all of the following documents: (1) Travel Orders, (2) Payment by government issued AMEX/VISA card; (3) Govt./Military identification. Regarding Govt orders: prevailing per diem lodging rate at time of arrival will be honored. Attendees on Govt. orders do NOT pay city tax; every other attendee pays city tax!

When you book a room, mention that you are attending the "ACES" Conference, at NPS, and ask for either Government, or Conference rates.

There is NO Conference PARKING at the Naval Postgraduate School or on nearby streets, so we advise you to book a room within walking distance, or plan to use a taxi.

Third Street Gate is the closest gate to the Conference Registration location. IT MAY NOT BE OPEN DURING CONFERENCE DUE TO INCREASED SECURITY. The Ninth Street gate has always been open.

AIRLINE INFORMATION

The following airlines make connections from Los Angeles and San Francisco, CA. to Monterey, CA: American & United. Delta/Sky West serves from SFO only and US Air/Express serves from LAX only. There is no airline connection directly from San Jose, CA to Monterey, CA. You can fly to San Jose, but then you must rent a car. No other ground transportation is available as of 25 January.

THINGS TO DO AND SEE IN THE MONTEREY BAY AREA

There are many activities for children and adults not attending the Conference. The colorful blue Monterey Bay is a vision of historic Monterey, rich with natural beauty and many attractions from Fisherman's Wharf, (be sure to try the seafood cocktails), to Cannery Row, the Monterey Adobes and city parks, the Monterey Bay Aquarium, Maritime Museum of Monterey, and Pacific Grove Museum of Natural History. The "Artichoke Capital of the World" is only 15 miles from Monterey, in Castroville.

Other things to do include: driving the 17-Mile Drive in Pebble Beach; Whale watching, bicycle riding, roller blading, surfing, ocean kayaking, in Pacific Grove; taking a stroll on the white sandy beach in Carmel, a visit to Mission San Carlos Borromeo Del Rio Carmelo, in Carmel, etc. The Monterey Peninsula has 20 Golf Courses. Carmel has many Art Galleries. For more information, call the Monterey Peninsula Chamber of Commerce, Visitors and Convention Bureau at (831) 649-1770.

ACES CONFERENCE

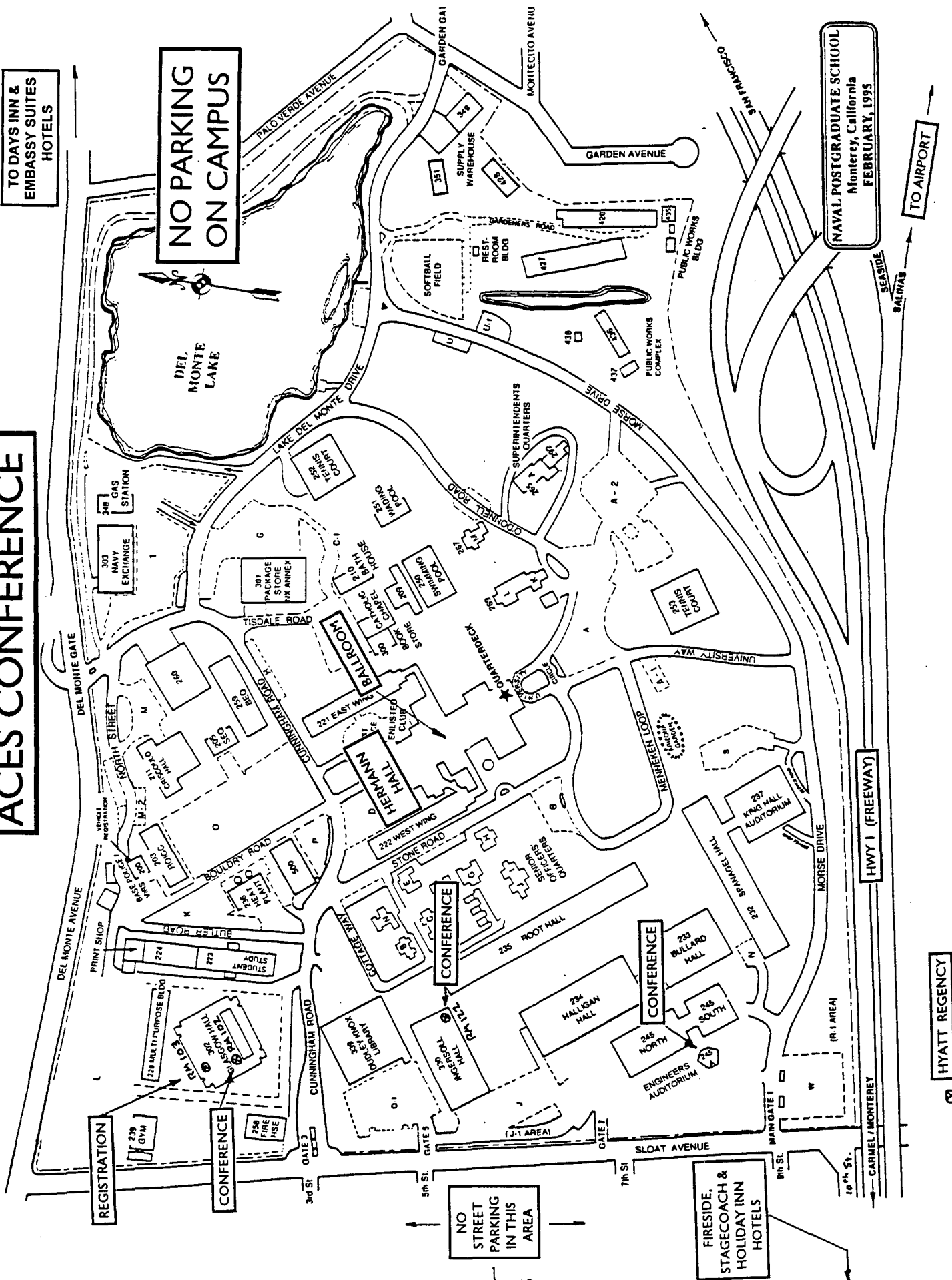
TO DAYS INN &
EMBASSY SUITES
HOTELS

NO PARKING
ON CAMPUS

NAVAL POSTGRADUATE SCHOOL
Monterey, California
FEBRUARY, 1995

TO AIRPORT

HYATT REGENCY



APPLIED COMPUTATIONAL ELECTROMAGNETICS SOCIETY

RICHARD W. ADLER, EXECUTIVE OFFICER
ECE DEPARTMENT, CODE ECAB, NAVAL POSTGRADUATE SCHOOL, 833 DYER ROAD, RM 437, MONTEREY, CA 93943-5121
PHONE: 831-646-1111 FAX: 831-649-0300 EMAIL: RWA@IBM.NET

please print

LAST NAME FIRST NAME MIDDLE INITIAL

COMPANY/ORGANIZATION/UNIVERSITY DEPARTMENT/MAIL STATION
(PLEASE LIST THE ADDRESS YOU WANT USED FOR PUBLICATIONS BELOW)

MAILING ADDRESS

CITY PROVINCE/STATE COUNTRY ZIP/POSTAL CODE

TELEPHONE FAX AMATEUR RADIO CALL SIGN

E-MAIL ADDRESS E-MAIL ADDRESS CAN BE INCLUDED IN ACES DATABASE YES ☐ NO ☐
PERMISSION IS GRANTED TO HAVE MY NAME PLACED ON MAILING LISTS WHICH MAY BE SOLD YES ☐ NO ☐**CURRENT SUBSCRIPTION PRICES**

AREA	INDIVIDUAL SURFACE MAIL	✓ INDIVIDUAL AIRMAIL	ORGANIZATIONAL (AIRMAIL ONLY)
U.S. & CANADA	() \$65	() \$65	() \$115
MEXICO, CENTRAL & SOUTH AMERICA	() \$68	() \$70	() \$115
EUROPE, FORMER USSR, TURKEY, SCANDINAVIA	() \$68	() \$78	() \$115
ASIA, AFRICA, MIDDLE EAST & PACIFIC RIM	() \$68	() \$85	() \$115

FULL-TIME STUDENT/RETIRED/UNEMPLOYED RATE IS \$25 FOR ALL COUNTRIES

Non-USA participants: Prices are in U.S. dollars. All currencies must be converted to U.S. dollars payable by banks with U.S. affiliates. (1) Bank Checks, must have U.S. address of bank; (2) Traveler's Checks (in U.S. \$\$); (3) U.S./International Money Order drawn in U.S. funds, payable in U.S., (4) Credit Cards: Visa, MasterCard, Amex and Discover.

PAYMENT METHOD: ALL CHECKS/TRAVELER'S CHECKS/MONEY ORDERS ARE PAYABLE TO "ACES"

☐ CHECK (PAYABLE TO ACES) ☐ TRAVELER'S CHECKS ☐ INTERNATIONAL MONEY ORDER
☐ CREDIT CARD ☐ VISA ☐ MASTERCARD ☐ AMEX ☐ DISCOVER

CREDIT CARD USERS

SIGNATURE AND ADDRESS OF CARD HOLDER IS MANDATORY.

IF YOU ARE PAYING VIA ANOTHER PERSONS CARD, HE/SHE MUST PRINT AND SIGN NAME AND ADDRESS.

PRINT CARD HOLDER NAME: _____

CREDIT CARD HOLDER SIGNATURE: _____

CREDIT CARD EXPIRATION DATE: ____/____

CREDIT CARD HOLDER ADDRESS: _____

CREDIT CARD ACCOUNT #

--	--	--	--	--	--	--	--	--	--	--	--	--	--	--	--	--	--	--	--

February 1999

The 1999 International Conference on Computational Electromagnetics and Its Applications(ICCEA'99) will be held in Beijing, China on Nov 1 - 4, 1999. This is the second conference on Computational Electromagnetics and Its Applications in China since the first conference was held successfully in 1994. This conference is organized and sponsored by The IEEE Beijing Section, China Committee for URSI, Chinese Institute of Electronics, in cooperation with the Applied Computational Electromagnetics Society(ACES). The working language in all documents and at the symposium is English.

Conference Topics

Suggested topics are as follows:

1. Computational Electromagnetics Theories and Techniques:

Analytical techniques(Green's function, Integral Equation, Variation, Mode Matching, etc.)
Low-frequency numerical techniques(MOM, FDTD, FEM, TLM, etc.)
High-frequency numerical techniques(PO, GO, GTD, UTD, etc.)
Approximation techniques(Perturbation Methods, Least Squares, Interactive, etc.)
Wavelet & Multi pole techniques
Genetic algorithms
Hybrid methods
Optimization

2. Applications:

Antennas and Arrays	SAR	Propagation through plasmas
Radar imaging	Stealth techniques	Temporary EMF
EMP,EMI/EMC	Wave propagation	Target identification
Dielectric & magnetic materials	Radar cross section	Remote sensing & geophysics
Microwave Chamber & shielded enclosures	Bio-electromagnetics	Communications systems
Millimeter wave & microwave components	Visualization	MIMIC technology & VLSI
Fiberoptics	Inverse scattering	
Eddy currents non-destructive evaluation		

3. Computer Software Techniques:

Code validation and code performance analysis
Examples of practical code application
New codes, algorithms, code enhancements, and code fixes
Parallel algorithms

Time Table:

The Summary or Paper Submission Deadline: **Feb.28, 1999**

Notification of Acceptance: **May.30, 1999**

Camera-Ready Manuscript Deadline: **Aug.30, 1999**

Contact Information:

For Submitting Papers:

Prof. Gao Benqing
Dept. of Electronics Engineering
Beijing Institute of Technology
P.O.Box 327, Beijing 100081, CHINA
Tel:(086)10-68912613
Fax:(086)10-68412889

For Further Information:

Mr. Dayong Liu
Chinese Institute of Electronics
P.O.Box 165, Beijing 100036, CHINA
Tel:8610-68283463
Fax:8610-68283458
E-mail:dylu@public.bta.net.cn

For the latest information on ICCEA'99, Please visit: <http://www.cie-china.org/iccea-99.htm>

✕

ICCEA-99 Reply Form

(Please Mail to Prof. Gao Benqing, Technical Program Committee, ICCEA99)

Name: Prof./Dr./Mr./Ms. _____

Mailing Address: _____

Tel: _____ Fax: _____ E-mail: _____

I wish to submit _____ paper(s) on the topic(s) _____ respectively.

ADVERTISING RATES		
	FEE	PRINTED SIZE
Full page	\$200.	7.5" x 10.0"
1/2 page	\$100.	7.5" x 4.7" or 3.5" x 10.0"
1/4 page	\$ 50	3.5" x 4.7"
<p>All ads must be camera ready copy.</p> <p>Ad deadlines are same as Newsletter copy deadlines.</p> <p>Place ads with Ray Perez, Newsletter Editor, Martin Marietta Astronautics, MS 58700, PO Box 179, Denver, CO 80201, USA. The editor reserves the right to reject ads.</p>		

DEADLINE FOR THE SUBMISSION OF ARTICLES	
<u>Issue</u>	<u>Copy Deadline</u>
March	January 13
July	May 25
November	September 25

For the **ACES NEWSLETTER** send copy to Ray Perez in the following formats:

1. A hardcopy.
2. Camera ready hardcopy of any figures.
3. If possible also send text on a floppy disk. We can read any version of MICROSOFT-WORD and ASCII files on both IBM and Macintosh disks. On IBM disks we can also read WORDPERFECT, WORDSTAR, and LATEX files. If any software other than MICROSOFT WORD has been used on Macintosh Disks, contact the Managing Editor, Richard W. Adler **before** submitting a diskette. If it is not possible to send a Macintosh disk then the hardcopy should be in Courier font **only**, for scanning purposes.

APPLIED COMPUTATIONAL ELECTROMAGNETICS SOCIETY JOURNAL

INFORMATION FOR AUTHORS

PUBLICATION CRITERIA

Each paper is required to manifest some relation to applied computational electromagnetics. **Papers may address general issues in applied computational electromagnetics, or they may focus on specific applications, techniques, codes, or computational issues.** While the following list is not exhaustive, each paper will generally relate to at least one of these areas:

1. Code validation. This is done using internal checks or experimental, analytical or other computational data. Measured data of potential utility to code validation efforts will also be considered for publication.

2. Code performance analysis. This usually involves identification of numerical accuracy or other limitations, solution convergence, numerical and physical modeling error, and parameter tradeoffs. However, it is also permissible to address issues such as ease-of-use, set-up time, run time, special outputs, or other special features.

3. Computational studies of basic physics. This involves using a code, algorithm, or computational technique to simulate reality in such a way that better or new physical insight or understanding is achieved.

4. New computational techniques, or new applications for existing computational techniques or codes.

5. "Tricks of the trade" in selecting and applying codes and techniques.

6. New codes, algorithms, code enhancement, and code fixes. This category is self-explanatory but includes significant changes to existing codes, such as applicability extensions, algorithm optimization, problem correction, limitation removal, or other performance improvement. **Note: Code (or algorithm) capability descriptions are not acceptable, unless they contain sufficient technical material to justify consideration.**

7. Code input/output issues. This normally involves innovations in input (such as input geometry standardization, automatic mesh generation, or computer-aided design) or in output (whether it be tabular, graphical, statistical, Fourier-transformed, or otherwise signal-processed). Material dealing with input/output database management, output interpretation, or other input/output issues will also be considered for publication.

8. Computer hardware issues. This is the category for analysis of hardware capabilities and limitations in meeting various types of electromagnetics computational requirements. Vector and parallel computational techniques and implementation are of particular interest.

Applications of interest include, but are not limited to, antennas (and their electromagnetic environments), networks, static fields, radar cross section, shielding, radiation hazards, biological effects, electromagnetic pulse (EMP), electromagnetic interference (EMI), electromagnetic compatibility (EMC), power transmission, charge transport, dielectric and magnetic materials, microwave components, MMIC technology, remote sensing and geophysics, communications systems, fiber optics, plasmas, particle accelerators, generators and motors, electromagnetic wave propagation, non-destructive evaluation, eddy currents, and inverse scattering.

Techniques of interest include frequency-domain and time-domain techniques, integral equation and differential equation techniques, diffraction theories, physical optics, moment methods, finite differences and finite element techniques, modal expansions, perturbation methods, and hybrid methods. This list is not exhaustive.

A unique feature of the Journal is the publication of unsuccessful efforts in applied computational electromagnetics. Publication of such material provides a means to discuss problem areas in electromagnetic modeling. Material representing an unsuccessful application or negative results in computational electromagnetics will be considered for publication only if a reasonable expectation of success (and a reasonable effort) are reflected. Moreover, such material must represent a problem area of potential interest to the ACES membership.

Where possible and appropriate, authors are required to provide statements of quantitative accuracy for measured and/or computed data. This issue is discussed in "Accuracy & Publication: Requiring quantitative accuracy statements to accompany data", by E.K. Miller, *ACES Newsletter*, Vol. 9, No. 3, pp. 23-29, 1994, ISBN 1056-9170.

EDITORIAL REVIEW

In order to ensure an appropriate level of quality control, papers are refereed. They are reviewed both for technical correctness and for adherence to the listed guidelines regarding information content. Authors should submit the initial manuscript in draft form so that any suggested changes can be made before the photo-ready copy is prepared for publication.

JOURNAL COPY INFORMATION

March issue	Copy deadline 13 January
July issue	Copy deadline 25 May
November issue	Copy deadline 25 September

STYLE FOR CAMERA-READY COPY

The ACES Journal is flexible, within reason, in regard to style. However, certain requirements are in effect:

1. The paper title should NOT be placed on a separate page. The title, author(s), abstract, and (space permitting) beginning of the paper itself should all be on the first page. The title, author(s), and author affiliations should be centered (center-justified) on the first page.
2. An abstract is REQUIRED. The abstract should state the computer codes, computational techniques, and applications discussed in the paper (as applicable) and should otherwise be usable by technical abstracting and indexing services.
3. Either British English or American English spellings may be used, provided that each word is spelled consistently throughout the paper.
4. Any commonly-accepted format for referencing is permitted, provided that internal consistency of format is maintained. As a guideline for authors who have no other preference, we recommend that references be given by author(s) name and year in the body of the paper (with alphabetical listing of all references at the end of the paper). Titles of Journals, monographs, and similar publications should be in boldface or italic font or should be underlined. Titles of papers or articles should be in quotation marks.
5. Internal consistency shall also be maintained for other elements of style, such as equation numbering. As a guideline for authors who have no other preference, we suggest that equation numbers be placed in parentheses at the right column margin.
6. The intent and meaning of all text must be clear. For authors who are NOT masters of the English language, the ACES Editorial Staff will provide assistance with grammar (subject to clarity of intent and meaning).
7. Unused space should be minimized. Sections and subsections should not normally begin on a new page.

MATERIAL, SUBMITTAL FORMAT AND PROCEDURE

The preferred format for submission and subsequent review, is 12 point font or 12 cpi, double line spacing and single column per page. Four copies of all submissions should be sent to the Editor-in-Chief (see inside front cover). Each submission must be accompanied by a covering letter. The letter should include the name, address, and telephone and/or fax number and/or e-mail address of at least one of the authors.

Only camera-ready original copies are accepted for publication. The term "**camera-ready**" means that the material is neat, legible, and reproducible. The preferred font style is Times Roman 10 point (or equivalent) such as that used in this text. A double column format similar to that used here is preferred. **No author's work will be turned down once it has been accepted because of an inability to meet the requirements concerning fonts and format.** Full details are sent to the author(s) with the letter of acceptance.

There is NO requirement for India ink or for special paper; any plain white paper may be used. However, faded lines on figures and white streaks along fold lines should be avoided. Original figures - even paste-ups - are preferred over "nth-generation" photocopies. These original figures will be returned if you so request.

While ACES reserves the right to re-type any submitted material, this is not generally done.

PUBLICATION CHARGES

ACES members are allowed 12 pages per paper without charge; non-members are allowed 8 pages per paper without charge. Mandatory page charges of \$75 a page apply to all pages in excess of 12 for members or 8 for non-members. Voluntary page charges are requested for the free (12 or 8) pages, but are NOT mandatory or required for publication. A priority courtesy guideline, which favors members, applies to paper backlogs. Full details are available from the Editor-in-Chief.

COPYRIGHTS AND RELEASES

Each primary author must sign a copyright form and obtain a release from his/her organization vesting the copyright with ACES. Forms will be provided by ACES. Both the author and his/her organization are allowed to use the copyrighted material freely for their own private purposes.

Permission is granted to quote short passages and reproduce figures and tables from an ACES Journal issue provided the source is cited. Copies of ACES Journal articles may be made in accordance with usage permitted by Sections 107 or 108 of the U.S. Copyright Law. This consent does not extend to other kinds of copying, such as for general distribution, for advertising or promotional purposes, for creating new collective works, or for resale. The reproduction of multiple copies and the use of articles or extracts for commercial purposes require the consent of the author and specific permission from ACES. Institutional members are allowed to copy any ACES Journal issue for their internal distribution only.